

POLY(URETHANE-UREA) COMPOSITE MEMBRANES WITH Ag NP/ACTIVATOR AND AgBF₄/BMImBF₄ SYSTEMS FOR LIGHT OLEFINS/PARAFFINS SEPARATIONS

Membranas compósitas de poli(uretano-
ureia) com sistemas de Ag NP/ativador e
AgBF₄/BMImBF₄ para separação de
olefinas/parafinas leves

Membranas compuestas de poli(uretano-
urea) con Ag NP/ativador y
AgBF₄/BMImBF₄ para la separación de
olefinas/parafinas ligeras

PhD Thesis in International Cotutela Regime



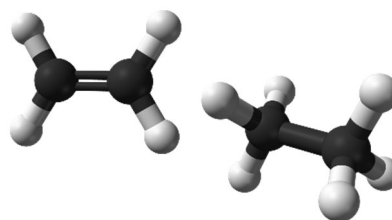
Antoniél Carlos Carolino Campos



Supervisors:

Prof. Dr. Rodrigo Azevedo dos Reis (UERJ)

Prof. Dr. Alfredo Ortiz Sainz de Aja (UC)



Tese apresentada, como requisito parcial para
obtenção do título de Doutor, ao Programa de
Pós-graduação em Engenharia Química, da
Universidade do Estado do Rio de Janeiro
UNIVERSIDADE DO ESTADO DO
RIO DE JANEIRO

Memoria de tesis doctoral presentada para optar
al título de Doctor por la Universidad de
Cantabria en el Programa de Doctorado en
Ingeniería Química, de la Energía y de Procesos
Escuela de Doctorado
UNIVERSIDAD DE CANTABRIA

Rio de Janeiro
2018

**UNIVERSIDADE DO
ESTADO DO RIO DE
JANEIRO**



**UNIVERSIDAD DE
CANTABRIA**



**ESCUELA DE DOCTORADO DE LA UNIVERSIDAD DE CANTABRIA
DOCTORADO EN INGENIERÍA QUÍMICA, DE LA ENERGÍA Y DE PROCESOS**

**PROGRAMA DE PÓS-GRADUAÇÃO EM ENGENHARIA QUÍMICA, DA UNIVERSIDADE DO
ESTADO DO RIO DE JANEIRO**

**PhD THESIS IN INTERNATIONAL COTUTELA REGIME BETWEEN THE
UNIVERSITY OF CANTABRIA AND THE RIO DE JANEIRO STATE UNIVERSITY**
**POLY(URETHANE UREA) COMPOSITE MEMBRANES WITH Ag NP/ACTIVATOR
AND AgBF₄/BMImBF₄ SYSTEMS FOR LIGHT OLEFINS/PARAFFINS SEPARATION**

**TESIS DOCTORAL EN ACUERDO INTERNACIONAL DE COTUTELA ENTRE LA UNIVERSIDAD DE
CANTABRIA Y LA UNIVERSIDAD DEL ESTADO DE RÍO DE JANEIRO**

**MEMBRANAS COMPUESTAS DE POLI(URETANO UREA) CON Ag NP/ACTIVADOR Y
AgBF₄/BMImBF₄ PARA LA SEPARACIÓN DE OLEFINAS/PARAFINAS LIGERAS**

**TESE DE DOUTORADO EM ACORDO DE COTUTELA INTERNACIONAL ENTRE A UNIVERSIDADE
DO ESTADO DO RIO DE JANEIRO E A UNIVERSIDADE DA CANTABRIA**

**MEMBRANAS COMPUESTAS DE POLI(URETANO UREA) CON Ag NP/ACTIVADOR Y
AgBF₄/BMImBF₄ PARA LA SEPARACIÓN DE OLEFINAS/PARAFINAS LIGERAS**

Presentada por: **ANTONIEL CARLOS CAROLINO CAMPOS**

Dirigida por: **PROF./DR. RODRIGO AZEVEDO DOS REIS**
PROF./DR. ALFREDO ORTIZ SAINZ DE AJA

Rio de Janeiro, June 2018

Memoria de tesis doctoral presentada para optar al título de Doctor por la
Universidad de Cantabria

Programa de Doctorado en Ingeniería Química, de la Energía y de Procesos
(BOE núm. 16, de 19 de enero de 2015. RUCT: 5601000)

Tese apresentada, como requisito parcial para obtenção do título de Doutor,
ao Programa de Pós-graduação em Engenharia Química, da Universidade
do Estado do Rio de Janeiro

Antoniél Carlos Campos thanks the Federal Agency for Support and
Evaluation of Graduate Education – CAPES (PDSE Grant -
88881.134232/2016-01) and the Spanish Ministry of Economy, Industry and
Competitiveness (CTQ2015-66078-R and CTQ2016-75158-R projects,
Spain-FEDER 2014-2020) for financial support

ABSTRACT

Light olefins are mainly produced by the naphtha steam cracking, which is among the more energy intensive processes in the petrochemical industry. To save energy, some alternatives have been proposed to partially replace or combine with cryogenic distillation, the conventional technology to separate olefins and paraffins. Within this aim, facilitated transport membranes, mainly with Ag^+ cations as selective carriers, have received great attention owing to the high selectivity and permeance provided. However, to be used industrially, the undesirable instability associated to the Ag^+ cation should be considered. Poisonous agents and polymer membrane materials are sources of Ag^+ deactivation. In recent years, great achievements on the separation performance have been reported, but the current challenge is to maintain the selectivity in long-term separation processes. Some alternatives, using dense polymeric films, have been proposed to overcome the potential causes of Ag^+ deactivation. The use of silver nanoparticles (Ag NP) as carrier; the use of ionic liquids (IL) for the stabilization of Ag^+ ; *in situ* regeneration of electrolyte polymeric membrane by using oxidizing agents; and the use of highly fluorinated polymer consist in proposing strategies to mitigate and/or overcome the problems imposed to the separation. The Chapter 1 of this Thesis presents a critical analysis of the potential causes of Ag^+ deactivation and highlights critically some perspectives of the ongoing development and application of facilitated transport membranes. Moreover, a background related to light olefins production, energy consumption involved, and theory of gas transport mechanism is introduced in this chapter.

Among alternatives to overcome Ag^+ deactivation, this Thesis focuses on the use of Ag NP as carrier and IL for Ag^+ stabilization. The polymer matrix investigated as membrane material are the waterborne poly(urethane urea)s (WPUU). The general goal of the Thesis is to prepare composite membranes with Ag NP/activator and $\text{AgBF}_4/\text{BMImBF}_4$ systems for light olefins/paraffins separation. To characterize these materials, Chapter 2 introduce some analysis techniques applied in the investigation of structure-property relationships of WPUU composites. Transmission electron microscopy (TEM), small angle scattering X-ray (SAXS), X-ray diffraction (XRD), Fourier transform infrared spectroscopy (FTIR), and thermogravimetric analysis (TGA) are presented with special attention related to the Ag NP size and the interaction between the polymer chains and silver species (Ag^0 and Ag^+).

The justification for the use of WPUU for material of gas membrane separation is found in Chapter 3. The achievement of synthesis methodology of WPUU composite with high Ag NP content, and the characterization of Ag NP/WPUU material are also found in the same chapter. All gas permeation tests are present in Chapter 4. This chapter describe the preparation of Ag NP/activator/WPUU and AgBF₄/BMImBF₄/WPUU membranes. In this work, 2 activator compounds were used for Ag NP, p-benzoquinone (p-Bq) and BMImBF₄. The discussion of paraffin and olefin mass transport trough membranes is carried out in the same chapter. The facilitated transport of olefin was not achieved in Ag NP/activator/WPUU membranes, probably caused by the low electron acceptor feature of BMImBF₄ and by the poor stability of p-Bq. On the other hand, the facilitated transport of olefins was reached in AgBF₄/BMImBF₄/WPUU membranes. However, the membrane evidenced a humidification dependence to be stable in long-term permeation experiments. Finally, Chapter 5 presents the overall conclusions of the Thesis and challenges for future researches.

Keywords: Olefin/paraffin separations; Facilitated transport membranes; Silver salts; Silver nanoparticles; Carrier poisoning; poly(urethane urea)

RESUMO

Olefinas leves são principalmente produzidas pelo craqueamento a vapor da nafta, que está entre os processos mais intensos em energia da indústria petroquímica. Para salvar energia, algumas alternativas têm sido propostas para substituir parcialmente ou combinar com a destilação criogênica, que é a tecnologia convencional para separação de parafinas e olefinas. Com esse objetivo, membranas de transporte facilitado, principalmente com cátion Ag^+ como carreador seletivo, tem recebido grande atenção devido a sua alta seletividade e permeância fornecida. Entretanto, para ser usada industrialmente, a indesejada instabilidade associada ao cátion Ag^+ deve ser considerada. Agentes contaminantes e materiais de membranas poliméricas são fonte de desativação do Ag^+ . Nos anos recentes, muitos avanços no desempenho da separação têm sido reportados, mas o desafio atual ainda é manter a seletividade em longos períodos de processo de separação. Algumas alternativas, usando filmes poliméricos densos, têm sido propostas para solucionar a potencial causa de desativação do Ag^+ . O uso de nanopartículas de prata (Ag NP) como carreador, o uso de líquidos iônicos (IL) para a estabilização do Ag^+ , regeneração *in situ* de membranas eletrólitas usando agentes oxidantes e o uso de polímeros altamente fluorados consiste em estratégias promissoras para mitigar e/ou solucionar os problemas impostos a separação. O Capítulo 1 da Tese apresenta uma análise crítica das potenciais causas de desativação do Ag^+ e destaca criteriosamente algumas perspectivas de desenvolvimento futuro a aplicações de membranas de transporte facilitado. Além disso, uma revisão bibliográfica relacionada com a produção de olefinas, consumo de energia envolvido e teoria de mecanismo de transporte de gases é introduzido neste capítulo.

Entre as alternativas para solucionar a desativação do Ag^+ , esta Tese foca no uso de Ag NP como carreador e IL para a estabilização de Ag^+ . A matriz polimérica investigada como material foram os poli(uretanos ureia)s (WPUU) sintetizado a partir de dispersão aquosa. O objetivo geral da Tese é o preparo de membranas compósitas com sistemas de Ag NP /ativador e $\text{AgBF}_4/\text{BMImBF}_4$ para a separação de olefinas e parafinas leves. Para caracterizar estes materiais, o Capítulo 2 introduz algumas técnicas de análises aplicadas em investigação da relação estrutura-propriedade de compósitos de WPUU. Microscopia eletrônica de transmissão (TEM), espalhamento a baixo ângulo de raios X (SAXS), difração de raios X (XDR), espectroscopia de absorção na região do infravermelho por transformada de Fourier (FTIR) e análise termogravimétrica (TGA) são apresentadas com especial atenção relacionada ao

tamanho das Ag NP e a interação entre as cadeias poliméricas e as espécies de prata (Ag^0 e Ag^+).

A justificativa para o uso de WPUU para material de membrana de separação de gás é encontrada no Capítulo 3. Os avanços da metodologia de síntese dos compósitos de WPUU com elevado conteúdo de Ag NP e a caracterização do material de Ag NP/WPUU são também encontrados no mesmo capítulo. Todos os experimentos de testes de permeação de gás são apresentados no Capítulo 4. Este capítulo descreve a preparação de membranas de Ag NP/ativador/WPUU e $\text{AgBF}_4/\text{BMImBF}_4/\text{WPUU}$. Neste trabalho, foram utilizados 2 compostos ativadores para as Ag NP, p-benzoquinona (p-Bq) e BMImBF_4 . A discussão de transporte de massa de parafina e olefina através das membranas é realizado no mesmo capítulo. O transporte facilitado de olefinas não foi alcançado nas membranas de Ag NP/ativador/WPUU, provavelmente causado pela baixa característica aceptora de elétrons do BMImBF_4 e pela fraca estabilidade da p-Bq. Por outro lado, o transporte facilitado de olefinas foi alcançado nas membranas de $\text{AgBF}_4/\text{BMImBF}_4/\text{WPUU}$. Entretanto, a membrana evidenciou uma dependência de umidificação para ser estável em experimentos de permeação de longa duração. Finalmente, o Capítulo 5 apresenta as conclusões gerais da Tese e os desafios para futuras pesquisas.

Palavras-chave: Separação olefina/parafina; membrana de transporte facilitado, sais de prata, nanopartículas de prata, desativação de carreador, poli(uretano-urea)

RESUMEN

Las olefinas ligeras son producidas principalmente mediante el craqueo a vapor de las naftas, siendo este uno de los procesos más intensivos en energía de la industria petroquímica. Con el objetivo de disminuir el consumo energético, en los últimos años se han propuesto diferentes alternativas para sustituir parcialmente o combinar con la destilación criogénica, tecnología convencional para la separación de mezclas olefina/parafina. En este sentido, destacan las membranas de transporte facilitado, que contienen el catión Ag^+ como carrier selectivo, proporcionando a estos materiales una alta selectividad y permeabilidad. Sin embargo, para ser empleada industrialmente, se debe considerar la inestabilidad asociada al cation Ag^+ . Diferentes agentes contaminantes, así como algunos elementos en la composición de las membranas poliméricas son fuente de desactivación de la Ag^+ . En los últimos años, se han reportado muchos avances en el desempeño de esta separación, pero el desafío actual sigue siendo mantener la selectividad en largos períodos de tiempo. Algunas alternativas, usando películas poliméricas densas, han sido propuestas para solucionar la potencial causa de desactivación del catión Ag^+ . El uso de nanopartículas de plata (Ag NP) como transportador, el uso de líquidos iónicos (IL) para la estabilización de los cationes Ag^+ , la regeneración *in situ* de las membranas electrolíticas usando agentes oxidantes y el uso de polímeros altamente fluorados forman parte de las principales estrategias prometedoras para mitigar y/o solucionar los problemas impuestos a la separación. El Capítulo 1 de la Tesis presenta un análisis crítico de las potenciales causas de desactivación del catión Ag^+ y destaca cuidadosamente algunas perspectivas de desarrollo futuro a aplicaciones de membranas de transporte facilitado. Además, una revisión bibliográfica relacionada con la producción de olefinas, el consumo de energía involucrado y la teoría del mecanismo de transporte de gases se introduce en este capítulo.

Entre las alternativas para solucionar la desactivación del catión Ag^+ , esta tesis se centra en el uso de Ag NP como transportador y el uso de IL para la estabilización de Ag^+ . La matriz polimérica investigada como material fue los poli(uretanos urea)s (WPUU) sintetizados a partir de dispersiones acuosas. El objetivo general de la Tesis es la preparación de membranas compuestas con sistemas de Ag NP /activador y $\text{AgBF}_4/\text{BMImBF}_4$ para la separación de olefinas y parafinas ligeras. Para caracterizar estos materiales, el Capítulo 2 introduce algunas técnicas de análisis aplicadas a la investigación de las relaciones estructura-propiedad de compuestos de WPUU. La microscopía electrónica de transmisión (TEM), dispersión a bajo

ángulo de rayos X (SAXS), difracción de rayos X (XDR), espectroscopia de absorción en la región del infrarrojo por transformada de Fourier (FTIR) y análisis termogravimétrico (TGA) se presentan con especial atención relacionada al tamaño de las Ag NP y la interacción entre las cadenas poliméricas y las especies de plata (Ag^0 y Ag^+).

La justificación en el uso de WPUU como material en la membrana de separación de gases se encuentra en el Capítulo 3. Los avances de la metodología de síntesis de los compuestos de WPUU con alto contenido de Ag NP y la caracterización del material de Ag NP/WPUU también se encuentran en el mismo capítulo. Todos los experimentos de pruebas de permeación de gases se presentan en el Capítulo 4. En este capítulo se describe la preparación de las membranas de Ag NP/activador/WPUU y $\text{AgBF}_4/\text{BMImBF}_4/\text{WPUU}$. En este trabajo, se utilizaron 2 compuestos activadores para las Ag NP, p-benzoquinona (p-Bq) y BMImBF_4 . La discusión de transporte de masa de parafina y olefina a través de las membranas se realiza en el mismo capítulo. El transporte facilitado de olefinas no fue alcanzado en las membranas de Ag NP/activador/WPUU, probablemente causado por la baja capacidad aceptora de electrones del BMImBF_4 y por la débil estabilidad de la p-Bq. Por otro lado, el transporte facilitado de olefinas se alcanzó en las membranas de $\text{AgBF}_4/\text{BMImBF}_4/\text{WPUU}$. Sin embargo, la membrana evidenció una dependencia con su humidificación para ser estable en experimentos de permeación de larga duración. Finalmente, el Capítulo 5 presenta las conclusiones generales de la Tesis y los desafíos para futuras investigaciones.

Palabras clave: Separación olefina/parafina; membrana de transporte facilitado, sales de plata, nanopartículas de plata, desactivación de cargador, poli (uretano-urea)

LIST OF FIGURES

Figure 1. Production of propylene by process. ^{4,8,11}	3
Figure 2. Representation of solution-diffusion mechanism. ⁶⁸	8
Figure 3. Representation of the facilitated transport mechanism in membranes.....	12
Figure 4. π complexation between olefin and Ag^+	14
Figure 5. Supported liquid membrane.	16
Figure 6. Ion-exchange membranes.....	17
Figure 7. a) Interaction between the functional groups of POZ (amide C=O) with the Ag^+ from AgBF_4 and b) the mutual interaction between the $\text{Ag}^+/\text{NO}_3^-$ and $\text{Al}^{3+}/\text{BF}_4^-$ that weakens the former interaction between the C=O group of polymer.	20
Figure 8. Schematic representation of the possible polarization mechanism of the Ag NP surface by 7,7,8,8-tetracyanoquinodimethane (TCNQ).	27
Figure 9. Chemical structure of PVDF-HFP and BMImBF_4	32
Figure 10. Chemical structure of Pebax [®]	34
Figure 11. Schematic illustration of a usual thin film composite membrane used for industrial gas separations.....	36
Figure 12. Slopes of power-law region from $\log I(q)$ vs. $\log q$ and respective nanofiller morphology.....	44
Figure 13. Representation of rigid and flexible domains structure in a segmented PU. This figure was reproduced from ref. ¹⁹²	50
Figure 14. Scheme of prepolymer formation and chain extension during the synthesis of WPU and WPUU.....	51
Figure 15. Behavior of WPU and WPUU particles in water medium. The scheme shows an anionic ionomer.	52
Figure 16. Steric stabilization scheme (in the enlarged part, a small polar portion of the stabilizing macromolecule anchors the surface of the NP). This figure was reproduced from ref. ²¹⁵	55
Figure 17. Illustration of overall free energy change ΔG as function of the growth particle size r . This figure was reproduced from ref. ^{215,218}	56
Figure 18. Experimental apparatus for the synthesis of Ag NP in WPUU aqueous dispersion: 1 – mechanical stirrer (anchor blade); 2 – thermostatic bath; 3 – peristaltic pump; 4 – glass jacketed reaction; and 5 – AgNO_3 solution.	60
Figure 19. TEM images of WPUU/Ag NP membranes: a)1% Ag NP; b)5% Ag NP.	62
Figure 20. SAXS data of WPUU/Ag NP membranes.	62
Figure 21. Fits of SAXS data using the Beaucage unified model. ^{177,180}	63
Figure 22. XRD patterns of Ag NP and WPUU/Ag NP membranes.	65
Figure 23. Comparison between FTIR spectra of the WPUU and Ag NP 10%.	66
Figure 24. Comparison between FTIR spectra of the WPUU and 50% Ag NP*	67
Figure 25. FTIR spectra of AgBF_4 and H_2O . ²⁴¹⁻²⁴³	79
Figure 26. FTIR spectra of WPUU/ AgBF_4 films.	80
Figure 27. FTIR spectra of WPUU/IL and WPUU/ AgBF_4 /IL films.	80
Figure 28. Flux of propylene, propane, and selectivity vs. permeation time for WPUU/ AgBF_4 membranes.....	82
Figure 29. Flux of propylene and propane vs. permeation time for WPUU/ AgBF_4 membranes in the initial time of the experiments.....	84

Figure 30. Flux of propylene, propane, and selectivity vs. permeation time for the membrane with high AgBF ₄ content.	85
Figure 31. Flux of propylene, propane, and selectivity vs. permeation time for membrane with high AgBF ₄ content in the initial time of the experiments.	85
Figure 32. Flux of propylene and propane vs. permeation for 1 WPUU: 1 AgBF ₄ : 0.25 IL membrane. In this experiment, the permeation cell was opened and closed to restart the run.	87

LIST OF TABLES

Table 1. Data used to calculate the feedstock share for the steam cracker in 2016.....	3
Table 2. Steam cracker yields for ethane and naphtha. ^{9,12}	3
Table 3. Sections of SC process and the energy involved.	4
Table 4. Data used to calculate the total energy consumption of the steam cracker and the SC separation section in 2016.	6
Table 5. Results of long-term permeation tests of various electrolyte membranes.	21
Table 6. Deactivation reaction of silver cation (Ag ⁺).	24
Table 7. Main results of metallic nanoparticles as carriers for membrane facilitated transport of olefins.	28
Table 8. Chemical structures of activator agents for Ag NP.	29
Table 9. Results of membrane performance with ionic liquids for protection against the reduction of Ag ⁺	31
Table 10. Results of the deactivation and regeneration processes of Pebax® 2533 + 80 wt% AgBF ₄ membrane with original selectivity of 40 and olefin permeance of 87 GPU, adapted from Merkel et al. (2013). ⁵³	33
Table 11. Results of facilitated transport membranes based on highly fluorinated polymers from Majumdar <i>et al.</i> (2016). ⁴⁶	37
Table 12. SAXS results for the WPUU/Ag NP membranes.	64
Table 13. Area ratios of the FTIR bands in N–H region of WPUU and 50% Ag NP* membranes.	67
Table 14. Thermal degradation data of the WPUU/Ag NP membranes from batch A of WPUU.	68
Table 15. Thermal degradation data of the WPUU/Ag NP membranes from batch B of WPUU.	69
Table 16. Ag NP/WPUU membranes prepared for gas permeation experiments.....	73
Table 17. AgBF ₄ /WPUU membranes prepared for gas permeation experiments.	74
Table 18. Permeability of CO ₂ , C ₂ H ₆ and C ₂ H ₄ in WPUU/Ag NP membranes.	77
Table 19. Permeability of C ₃ H ₈ and C ₃ H ₆ in WPUU/Ag NP membranes.....	78
Table 20. Results for the WPUU/AgBF ₄ membranes.	84
Table 21. Results for the WPUU/AgBF ₄ membranes at the end of gas permeation experiments.....	87

TABLE OF CONTENTS

1. INTRODUCTION	1
1.1. Production of light olefins.	2
1.2. Energy consumption of steam creaking process.....	4
1.3. Applicability of membrane technology for olefin/paraffin separations.....	7
1.4. Solution-diffusion mechanism.	8
1.5. Facilitated transport membranes for olefin/paraffin separation.....	11
1.5.1. Chemical interaction for olefin separation: Olefin π complexation.....	13
1.5.2. Supported liquid membrane.	15
1.5.3. Ion exchange membranes.	16
1.5.4. Electrolyte membranes.....	17
1.6. Challenges to avoid carrier instability.	24
1.7. Some alternatives to overcome the Ag^+ deactivation.	25
1.7.1. Silver nanoparticles as carrier.	26
1.7.2. Ionic liquids for the stabilization of Ag^+	30
1.7.3. In situ regeneration using oxidizing agents.....	33
1.7.4. Use of highly fluorinated polymers/ Current technological options.....	34
1.8. Summary and conclusions.	38
1.9. Thesis scope and outline.	39
2. METHODS AND EQUIPMENT	41
2.1. Transmission electron microscopy (TEM), Small angle X-ray scattering (SAXS), and X-ray diffraction (XRD)	42
2.2. Infrared spectroscopy (FTIR)	46
2.3. Thermogravimetric analysis (TGA).....	47
3. POLY(URETHANE UREA)/Ag NP COMPOSITES	48
3.1. Waterborne poly(urethane urea)s.....	49
3.2. Ag NP synthesis.....	54
3.3. Experimental	58
3.3.1. Materials.....	58
3.3.2. Preparation of WPUU/Ag NP composites	58
3.3.3. Characterizations.....	60
3.4. Results.....	61
3.4.1. Transmission electron microscopy (TEM) and Small Angle X-ray Scattering (SAXS).....	61

3.4.2. X-ray diffraction (XRD).....	64
3.4.3. Infrared Spectroscopy (FTIR)	65
3.4.4. Thermal Stability.....	67
3.5. Conclusions.....	69
4. OLEFIN/PARAFFIN GAS PERMEATION	70
4.1. Introduction.....	71
4.2. Experimental.....	72
4.2.1. Materials.....	72
4.2.2. Membranes preparation.....	72
4.2.2.1. Membranes based on WPUU/Ag NP	72
4.2.2.2. Membranes based on WPUU/AgBF ₄	73
4.2.3. Gas permeation tests.....	74
4.2.3.1. Pure gas experiments	74
4.2.3.2. Mixture gas experiments	75
4.3. Results.....	76
4.3.1. Membranes based on WPUU/Ag NP	76
4.3.2. Membranes based on WPUU/AgBF ₄	78
4.3.2.1. Infrared Spectroscopy (FTIR)	78
4.3.2.2. Gas permeation	81
4.4. Conclusions.....	89
5. CONCLUSIONS AND CHALLENGES FOR FUTURE RESEARCHES	90
5.1. Conclusions.....	91
5.2. Challenges for future researches	92
REFERENCES	94

Chapter 1

1. INTRODUCTION

Abstract

This introductory chapter presents an overview of the current olefin production and the energy consumption involved. The membrane technology for olefin/paraffin separations is introduced as the main alternative to save energy in present scenario. The drawbacks to the use of membranes and some efforts to make possible the feasible use of them are reviewed critically. At the end of the chapter, the scope and outline of the Thesis are summarized.

1.1. Production of light olefins.

Light olefins are the principal raw material to the petrochemical industry. They are used as the precursor for a variety of thermoplastic polymers, synthetic rubber, and solvents. The applicability of this input ranges from the electronic devices to food and pharmaceutical products. There is no doubt that these building block molecules are needful for the majority of goods used by modern society.¹ Regarding the present scenario, the global demand for ethylene and propylene, which are the most important light olefins, has been increasing over the last decades.^{2,3} In 2016, the global ethylene and propylene production were respectively 146 and 99 million tons and expectation of demand growth rate, until 2025, is 3.6%/year and 4.0%/year for ethylene and propylene respectively.⁴ These numbers show the expansion trend in consumption of light olefins that is closely related to the consumption pattern of the global population over the last years.

The steam creaking (SC) is the principal process to obtain light olefins, and in the near future, probably it should be the leading technology, mainly to the production of ethylene. Nevertheless, there are other potential maturity alternatives to the SC, such as the catalytic dehydrogenation of light alkanes,⁵ the oxidative coupling of methane⁶ and syngas-based routes (Fischer-Tropsch synthesis and methanol synthesis followed by methanol to olefins).⁷ At present, all cited technologies are not economically competitive compared to the SC.⁸ The main feedstock to the SC is the naphtha (*ca.* 61 %), but light alkanes, such as ethane, has been increasing its share (*ca.* 33 %) (**Table 1**).^{4,9} Since 2008, the light alkanes market share has been growing due to the exploitation of shale gas¹⁰ in the United State of America, as a result, the ethane price has become competitive.⁸

Table 2 shows the SC yield by feedstock, and it can be seen that propylene is a by-product of SC and should be produced from additional processes to reach the current demand. Generally, propylene also is manufactured as a by-product from fluid catalytic crackers (FCC) and produced in less scale from propane dehydrogenation process, and metathesis (**Figure 1**).^{4,8,11} In the case of FCC, since the propylene demand is rising, most refineries trying to maximize the propylene production modifying the FCC process to reach the gap in the market.¹¹

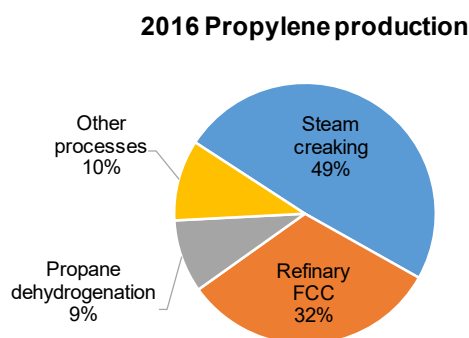
Table 1. Data used to calculate the feedstock share for the steam cracker in 2016.

Feedstock	Global production by feedstock (Mt) ⁴	ethylene by feedstock	Yield by weight of feedstock (wt%) ⁹	Feedstock (Mt)	Feedstock Share (%)
Naphtha	63		30	210	61
Ethane	52		80	65	19
Propane	13		45	29	8
Butane	7		37	19	6
Gas oil	5		25	20	6
Coal	3		–	–	–
Other	2		–	–	–

Note: We considered all ethylene was produced by the steam cracker.

Table 2. Steam cracker yields for ethane and naphtha.^{9,12}

Feedstock	Yield by weight of feedstock (wt%)		
	Ethylene	Propylene	Butadiene
Ethane	80-84	1.0 -1.6	1.0-1.4
Naphtha	29-34	13-16	4-5

**Figure 1.** Production of propylene by process.^{4,8,11}

1.2. Energy consumption of steam creaking process.

Regarding the petrochemical industry, SC is the most energy-intensive process, and, in 2016, it consumed *ca.* $3.0 \cdot 10^{15}$ BTU.^{12,13} In the petrochemical facilities, the SC unit is divided into 3 sections (**Table 3**). Most of the energy is applied in the pyrolysis section where the cracking of the feedstock takes place. Further, there is a compression section followed by a cleanup to remove acid gases (carbon dioxide and hydrogen sulfide) and water. Finally, the cracked gases enter in the separation section to fractionation/purification of the output products. After the pyrolysis, the separation section is the second large energy consumption step in SC. The justification for this consumption is based on the cryogenic distillation of the cracked gases. Roughly, the cryogenic distillation consists on decreasing the gas stream temperature by a complex web of heat exchangers and compressors. Next, the cryogenic stream is fractionated by different distillation/separation columns in the desired final products of the SC.^{12,14,15}

Table 3. Sections of SC process and the energy involved.

Feedstock	Typical energy consumption (GJ/t of ethylene produced) ^{9,13}	The share (%) of energy consumption by SC sections		
		Pyrolysis	Compression	Separation
Ethane	17-19	47	22	31
Naphtha	23-27	65	15	20

Many efforts have been undertaken to save energy in the different section of the SC. In the past years, the typical efficiency improvement rate in the SC units was *ca.* 1.7% per year.¹⁶ In the pyrolysis and the compression section, the attention is devoted to increase the efficiency of the furnace, compressors and other related equipment. The operational condition of the cracking process also has been studied according to the different raw material looking for better energy yield of the pyrolysis.¹⁴ In the separation section, alternative technologies, such as membrane processes and reactive absorption, have been proposed to replace or integrate with the current cryogenic distillation technology.¹⁷⁻¹⁹ The reactive absorption takes places in large absorption/stripping columns containing silver or cooper salts.²⁰⁻²² In addition, other adsorbent materials such as zeolites,²³⁻²⁵ porous organic frameworks,²⁶⁻²⁸ and metal-organic frameworks

(MOFs)²⁹⁻³¹ could also be applied. The membrane separation, which is well known for its energetic efficiency in gas separation,^{32,33} uses polymer membranes,^{34,35} mixed matrix membrane,³⁶⁻³⁸ facilitated transport membranes³⁹⁻⁴² and carbon molecular sieves^{43,44} for the separation. The membrane technology has been achieving the most promising results related to cracked gases separation, specifically regarding the olefin/paraffin separation.⁴⁵⁻⁴⁷ The reactive absorption is also under development however in an earlier stage compared to the membranes.^{20,48}

According to our estimate (**Table 4**), in 2016, the energy consumption in the separation processes, inside the SC unit, was *ca.* $7.5 \cdot 10^{14}$ BTU.^{4,9,12,13} Most of this energy is destined to the refrigeration system of the SC separation section that is used to achieve the cryogenic temperatures in the cracked gases stream.^{12,14} These temperatures are reached by using a chilling system integrated with compressors operating under high pressure (15-30 bar).¹² The refrigerant fluids should cover a broad range of temperature, -150 °C to +10 °C, to be applied in distinct parts of the chilling train and in the fractionation towers.¹⁴ The fractionations take place in towers generically called demethanizer, deethanizer, depropanizer, debutanizer, C2 splitter, and C3 splitter.^{14,36} These fractionation equipment types operate using distinct temperature and pressure conditions to separate the desired compounds. Related to the C2 and C3 splitters, which are distillation columns, the challenging task is separate compounds with similar boiling points. In C2 splitter, the ethylene and ethane ($\Delta t_{\text{ethylene/ethane}} = 15,2$ °C at 1atm)⁴⁹ are separated using a reflux rate of *ca.* 4, a column with 90-125 trays, and pressure operating of 17-28 bar. In C3 splitter, the propylene and propane ($\Delta t_{\text{propylene/propane}} = 5,7$ °C at 1atm)⁴⁹ are separated using a reflux rate of *ca.* 20, a column with 150-230 trays, and pressure operating of 18 bar.¹⁴ In the case of C3 splitter, the high number of separation stages normally requires two connected distillation columns that raises up the capital cost investment related to this equipment type. These features make the C2 and C3 separations one of the most energy intense process inside the SC separation section.³⁶

As one of the advanced SC separation technologies, the membrane technology is thought to replace or integrate the C2 and C3 splitters. The estimate is that *ca.* 8% of all energy used in SC could be saved if membranes are applied just for olefin/paraffin separations.¹² The use of membranes in this separation is considered one of the most important applicability of this technology in the world since it could save a large amount of energy. Consequently, membrane technology could contribute with the lowering of gas emissions and pollution levels.⁵⁰ In a recent study, Lee *et al.*³⁶ identified the minimum required membrane performance to replace one typical C3 splitter. They found that a membrane module with propylene permeance of 11.3

GPU ($1\text{GPU}=1\times 10^{-6}\text{ cm}^3\text{ (STP)/cm}^2\text{ s cmHg}$) and selectivity of 68 could substitute a typical distillation process. Since it is viable the replacement of the distillation by membranes with this minimum performance, the great challenge to the membrane technology is reach the suitable selectivity and permeability for the process and keep them over long-term operation. The operational conditions in which the membrane should be used is severe and can lead to the performance loss along the operation. Regular substitutions due to the incapability to withstand the real operation condition is a drawback to a feasible application of the membrane separation. Therefore, many works try to figure out how to make the membranes more permeable and selectivity to the olefins, besides finding a way to keep the performance in long-term operation.^{46,47,51–53}

Table 4. Data used to calculate the total energy consumption of the steam cracker and the SC separation section in 2016.

Feedstock	Global ethylene production by feedstock (Mt)	Typical energy consumption (GJ/t of ethylene produced)^{12,13}	Total energy consumption (10¹⁵ BTU)	Total energy consumption in separation section of steam cracker (10¹⁴ BTU)
Light^a	72	17-19	1.2-1.3	3.6-4.0
Heavy^b	68	23-27	1.5-1.7	3.0-3.5
Total	140	–	2.6-3.0	6.6-7.5

a - ethane, propane and butane; b - naphtha and gas oil

Note: We assumed the propane, butane SC energy consumption equal to the ethane and the gas oil equal to the naphtha. We considered the energy consumption of SC separation process *ca.* 31% of the total energy consumption for ethane, propane and butane, and *ca.* 20% for naphtha and gas oil.

Among the membranes technologies, the alternatives based only on a solution-diffusion transport have had some difficulties to discriminate the olefin/paraffin pairs. The similarity between the physical and chemical properties of alkenes and alkanes is the main drawback to all dense-type membranes assigned to the separation.³⁵ The carbon molecular sieve membranes suffer of the same problem, since the difference between the molecular diameter of the molecules to be separated is tiny.³³ Nevertheless, many efforts have been developed trying to improve the separation using mixed matrix membrane by the introduction of zeolites,^{54,55} organic and metal–organic frameworks^{56–60} in the polymer matrix. Other works try to develop carbon molecular sieve membranes^{17,43,44} that are brittle and difficult to scale-up the production.³⁶ To overcome these discriminative problems between the molecules, the facilitated

transport of olefins has been explored, increasing simultaneously the permeance and the selectivity of the separation. The facilitated transport membranes have surpassed the upper bound of Robeson diagram for the olefin/paraffin separation in the last years,^{45,61} demonstrating the greater potential of this technology option.

1.3. Applicability of membrane technology for olefin/paraffin separations.

The gas technology separation using membranes is already industrially applied in cases such as the separation of nitrogen from air, CO₂ removal from natural gas, and the hydrogen recovery from steam refinery.^{32,62} It should not sound strange the use of this technology in the light olefin/paraffin separations in which could save considerable energy compared to the current cryogenic distillation process. However, the best available polymer materials, which are used in the saturated/unsaturated hydrocarbon separation, under industrial conditions, only present a real selectivity of 3-4. To be used in steam creaking plants in the replacement or integration with the cryogenic distillation, a higher selectivity should be achieved.^{53,63} Besides the steam creaking plants, which is the main target application, there are other two potential areas where membrane technology could be applied for olefin/paraffin separations. As shown in the **Figure 1**, roughly, 1/3 of the propylene production is from FCC processes. In this case, the olefin/paraffin separation membranes should be used in the recovery of propylene from FCC off-gas streams.^{11,16,63,64}

The membrane technology could also be applied in alkene/alkane separation from vent streams of some kinds of petrochemical reactors. For instance, in the production of polypropylene, the propylene monomer has a small amount of propane (for propylene polymer grade, *ca.* 0.5%⁶⁵) that gradually builds up in the reactional system. The unreacted propane reaches concentrations of 20-30 vol.% inside system. To control the accumulation of propane, there is a continuous purged flux from the process that usually is flared. For each mole of purged propane, 2-3 mol of propylene is lost together resulting in a 1-2% of the total plant propylene feed. The membrane separation is desired technology to be installed before the flare line avoiding the waste of propylene. This application is very attractive because selectivities of 3-5 could be suitable to the propylene recycling process. In addition, the purged stream usually has low level of sulfur and acetylene compounds resulting in a milder condition operation and lower performance need (selectivity and permeance) than in steam creaking process.⁶⁶ Even individually, the small-scale separations of olefins from reactor vent streams when taken together, could represent a huge opportunity of saving money and a way to introduce

commercial olefin/paraffin membrane units. Maybe, this market niche can represent a previous favorable step before the attempt to replace the distillation in the steam cracking process or in the FCC off-gas streams that involves huge challenges to be overcome.^{63,66,67}

1.4. Solution-diffusion mechanism.

The driving force that motivates gas molecules to cross a dense membrane can be expressed by the difference in partial pressure between the feed and the permeate side (**Figure 2**). Under the process conditions, this partial pressure difference (concentration difference) represents the chemical potential gradient that is responsible for the gas flow. Initially, the gases are solubilized (sorption) in the membrane, afterward the diffusion of the molecules through the membrane takes place; and on the lower partial pressure side, desorption occurs. These steps are known as the solution-diffusion mechanism.⁶⁸

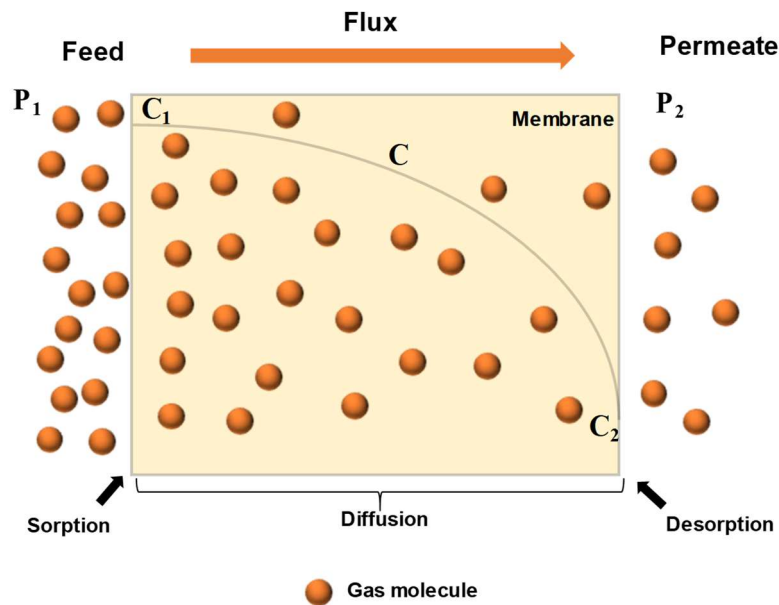


Figure 2. Representation of solution-diffusion mechanism.⁶⁸

Sorption is the thermodynamic step of permeation.⁶⁸ The gas molecules concentration C_i in the membrane is in thermodynamic equilibrium with the molecules of that gas in the gas phase under partial pressure p_i . In the mathematical modeling of this equilibrium, an approach is adopted that involves the fugacity coefficient for the gas phase (ideal gas as a reference state) and activity coefficient for the polymer phase (ideal solution as a reference state). By manipulating mathematical relationships, it is possible to obtain the definition of the coefficient

of sorption or solubility S_i , which is approximately independent of the concentration. In the mathematical approach of this equilibrium, on both sides of the membrane (feed and permeate), the coefficient S_i is considered equal in both interfaces of gas with the polymer. Thus, a linear relationship can be obtained between S_i and p_i , as expressed in equation (1). The sorption parameter is influenced mainly by the balance of three effects: (i) condensability of the gas molecules, (ii) gas / polymer interactions; and (iii) segmental mobility of the polymer.⁶⁹

$$C_i = S_i p_i \quad (1)$$

Taken as example the light olefins/paraffins, the light paraffins are more condensable than olefins, so they have a higher coefficient of solubility compared to olefins.^{69,70} The selectivity provided by the sorption coefficient is not enough for a desired separation. To be more selective towards the olefins, the polymer necessarily needs to make preferential interaction with those molecules. Therefore, polymers that present capable groups (polar groups as polyether)^{70,71} to performing this interaction may be considered as potential material for the separation of light olefins/paraffins.

Diffusion is the kinetic step of permeation that is related to the movement of gas molecules across the membrane.⁶⁸ The total flux through the dense film thickness is represented only by the diffusive flux J_i , given by *Fick's law*, in which D_i is the gas diffusion coefficient in the polymer. By integrating the *Fick's law* expression along the membrane thickness δ , the following equation is obtained:

$$J_i = \frac{D_i (C_i^f - C_i^p)}{\delta} \quad (2)$$

In equation (2), the superscripts f and p refer to the feed side and the permeate side, respectively. The diffusion coefficient D is determined mainly by the following effects: (i) size and shape of the permeant molecule, (ii) gas interaction inside the polymer matrix; and (iii) plasticizing effects of the permeant on the polymer caused by the high volumetric fraction of the gas in the membrane.⁷² The differentiation between light olefins and paraffins in the diffusional step is very inexpressive, since these molecules have very similar sizes. Replacing the equation (1) in (2), it is possible to express J_i as the equation (3), in which P_i is the gas permeability in the membrane. P_i can be defined as the product between D_i and S_i , $P_i = D_i S_i$.

The ratio P_i/δ is also known as gas permeance and it shows the gas flux by the partial pressure difference ($J_i/\Delta p_i$), *i.e.*, reflects the productivity of the membrane in the separation process.

$$J_i = \frac{P_i}{\delta} (p_i^f - p_i^p) \quad (3)$$

Dense membranes for gas separation are generally synthesized from polymeric material. Preliminary information regarding the affinity of a such polymeric membrane for a specific gas is provided by the ideal selectivity $\alpha_{i/j}^{id}$ that is calculated according to equation (4), with P_i and P_j as permeability values of i and j gases, respectively. The $\alpha_{i/j}^{id}$ is different from the real selectivity $\alpha_{i/j}$ (equation (5)) that represents the enrichment factor of the permeate stream for a determined gas when the operation involves a gas mixture. This factor is calculated by the quotient of molar fractions (y) ratios of two key components of the mixture in the permeate and feed stream.

$$\alpha_{i/j}^{id} = \frac{P_i}{P_j} \quad (4)$$

$$\alpha_{i/j} = \frac{(y_i^p/y_j^p)}{(y_i^f/y_j^f)} \quad (5)$$

The practical differences between ideal and real selectivities are the effects caused by permeation of a gas mixture. As the gas permeates through the polymer, the volumetric fraction thereof increases inside polymer matrix.⁶⁹ Thereafter, the higher concentration of gas molecules in the membrane leads to an segmental mobility increasing of the polymer chains. This phenomenon significantly alters the diffusion coefficient and is best known as plasticization.⁷²

The polymeric materials used for gas permeation can exhibit vitreous or elastomeric characteristics. Vitreous and elastomeric polymers have different behaviors related to the permeability of different gas molecules. Vitreous polymers discriminate molecules mostly in the diffusion step. Larger molecules have more difficulty to move through the pre-existing vacancies inside the vitreous polymer matrixes, which have lower segmental mobility. Therefore, in general, the larger the molecule, the lower the permeability in this type of polymer.⁶⁹

In elastomeric polymers, the dominant step is sorption. The more condensable the gas molecules, the easier the solubilization in the polymer matrixes. This usually means that the larger molecules, which are more condensable, have greater permeability in this type of polymer. Elastomers have higher segmental mobility and consequently, higher probability of local segmental density fluctuation. For this reason, the activation energy for a diffusional jump in elastomeric polymers is considered lower and not much influenced by the size of the penetrating molecule, making the diffusional step lesser selective.⁶⁹

The use of block copolymers that can share vitreous and elastomeric features in their polymer backbone may be one of the alternatives to reach the best performance regarding trade-off between selectivity and permeability. Tailormade block copolymers can also provide “virtual” crosslinking that may improve the plasticization resistance of membrane during the gas separation processes.^{73–76} For instance, polyurethanes^{77–80} and poly(ether-block-amide) (Pebax®)^{81–84} have this quality, since they present regions with elastomeric and vitreous characteristics. Depending on the formulation, suitable features can be achieved for specific uses.

1.5. Facilitated transport membranes for olefin/paraffin separation.

The development of new membranes based on polymeric materials or the modification of polymer structures that provide suitable selectivities for the olefin/paraffin separation has been largely investigated.^{85–87} As the polymer films have become more selective to the olefins, they lose productivity due to the trade-off between selectivity and permeation flux, therefore, leading to the technical unfeasibility of the separation process.^{33,88} Films where mass transport is based only on the solution-diffusion mechanism have shown, as best results, ideal selectivity of 27 (C_3H_6/C_3H_8) and 0.8 Barrer of propylene permeability.^{87,88} These values are significantly lower than the performance reported for facilitated transport films that have shown mixture selectivities (C_2H_4/C_2H_6) higher than 100.⁶¹

The facilitated transport mechanism, when it takes place, plays in a complementary mechanism to the solution-diffusion transport. In the facilitated transport, a carrier agent interacts reversibly and selectively with the target molecule, that results in the increase in the driving force for the permeation flux of target molecule, and therefore, the permeate is enriched. This kind of transport is not accessible to the inert molecules that are not able to interact with the carrier agent, so that their concentration decreases in the permeate side (**Figure 3**). Thus, the facilitated transport membrane has a superior selectivity compared to the passive (solution-

diffusion) membrane.^{52,61,89,90} The carriers need to be effectively dispersed over the natural diffusional path of the gases (in the direction of the concentration gradient) and be present at a concentration high enough for transport activation. Furthermore, the carriers also need to be ready to the interaction with the target molecules inside the membrane, *i.e.*, the carriers should be not poisoned.^{91,92}

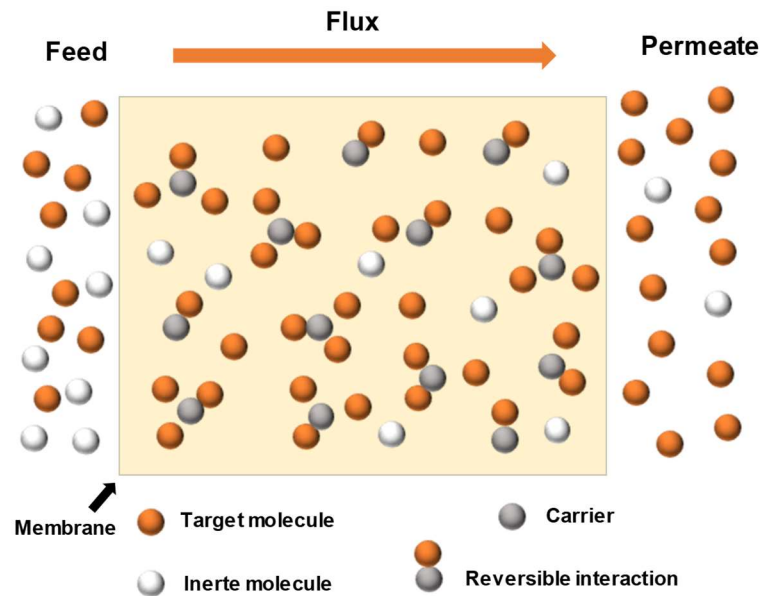


Figure 3. Representation of the facilitated transport mechanism in membranes.

In addition, the facilitated transport has a potential to save energy in the separation process since it gets better simultaneously selectivity and permeability values of the membranes, differently of the passive transport.⁶¹ To occur facilitated transport, the carriers needed to be suitable dispersed through the natural diffusional path of the gases (in the direction of the concentration gradient) and in enough concentration to the transport activation. Further, the carrier also needed to be ready to the interaction with the target molecules inside the membrane, *i.e.*, the carrier should be activated for the interaction, not poisoned.^{91,92}

A useful way to describe or classify the facilitated transport membranes is to evaluate them regarding carrier mobility. In general, there are three possible classifications:⁴⁰ (i) mobile carrier membranes, in which the carriers move freely through diffusional path; (ii) semi-mobile carrier membranes, in which the carriers also move freely, however it is restrict to the local segmental density fluctuation that represents a much higher activation cost energy for diffusion than that required in mobile carrier membranes; and (iii) fixed-site carrier membranes, in which carriers

are chemically bonded to the polymer segments and can only vibrate within a limited nanospace.

Through the mobile carrier membranes, the carriers move like a boat navigating between both sides of the membrane. The low viscosity of the medium is required to the transport in this kind of membrane. Generally, the main component of the medium whereby the carriers move are aqueous solutions or compounds with low viscosity as ionic liquids. Therefore, mobile carrier membranes are usually liquid membranes and they need a support to be used in most membrane separations.⁴⁰

In semi-mobile and fixed carrier membranes, polymeric materials are used as host matrix. Cussler *et al.*⁹³ proposed the jump mechanism for transport within the fixed-site carrier membranes, in which the target molecules cross the membrane by jumps from carrier to carrier. The idea of the solute acting as *Tarzan* came from the early XX century and was the inspiration for the jumping mechanism elaborated in 1989. The thinking of Cussler *et al.*⁹³ was that the carriers placed in chain, from a determined concentration inside the polymer matrix could achieve facilitated diffusion. Since carriers are covalently bounded to the matrix or fixed in a nanospace, the solution-diffusion mechanism is limited compared to the mobile carrier membranes. The distinct features between mobile carrier and fixed-site carrier membranes can be combined to generate an intermediate behavior in semi-mobile carrier membranes, in which the vehicular and the jumping mechanism can take place simultaneously to some extent.^{40,93}

1.5.1. Chemical interaction for olefin separation: Olefin π complexation.

The formation of complexes between some metal and olefins was already known. Nevertheless, only in 1827, it was identified the first metal-olefin complex. The referred compound was the platinum (II) -ethene, which was known as Zeise complex. In the beginning of XX century, arose the first ideas of use the silver (I) (Ag^+) salts in olefin absorption systems. However, only in 1951, Dewar⁹⁴ explained how the interaction mechanism between the ethene and Ag^+ worked. After, Chatt and Duncanson⁹⁵ advanced the Dewar's explanation presenting the interaction mechanism called π -bond complexation.²⁰ This complexation takes places when the bonding orbital of the olefin donate electronic density to the empty outermost orbital of the Ag^+ (5s) making a σ bond. The strength of this bond depends on of the magnitude of the metal (*e.g.* silver, cooper, and gold) positive charge. The second bond formed is a π , resulting from the backdonation of the electronic density from the outermost atomic orbital 4d, which is electronic completed, to the π^* - antibonding molecular orbital of the olefin (**Figure 4**).^{96,97}

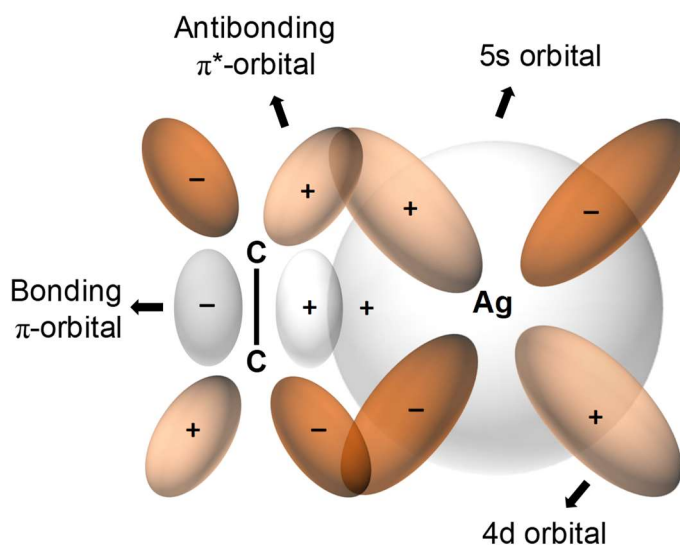


Figure 4. π complexation between olefin and Ag^+ .

In 1960, Scholander⁹⁸ published a pioneer work that explored the facilitated transport in liquids membranes containing hemoglobin as carrier agent for oxygen. Thereafter, works that described membranes of facilitated transport have flourished for several applications.⁶⁹ Over the following decades to the present day, the facilitated transport mechanism have been attracting attention of many researchers due to the separation potential compared to simple mechanism of passive transport.

Practically, the development of the facilitated transport membranes for light olefin/paraffin separations has been based on the feature of reversible interaction among the olefins and some transition metal. Using the π complexation mechanism was possible to understand the interaction among transition metals and olefins, especially silver, copper and gold. Meanwhile, to be reversible and allowing the facilitated transport, the π complexation should be enough strength to favor the interaction between the metal and the olefin but not so tied to keep them bonded during the application of the concentration gradient across the membrane. Among the transition metals, the silver has one singularity related to π complexation. The silver electronegativity is 2.2, inside the range 1.6 - 2.3 in which the reversible complexation can take places. In addition, the silver salts applied in the facilitated transport have the lower lattice energies compared to other salts that also can be used for this goal. A salt with lower lattice energy provides to the metal cation an easier manner to be dissolved and hence a greater availability for the interaction with the olefin.^{52,99} Owing to these features, the silver is the metal more used in the preparation of the membrane for olefin/paraffin separation. Nevertheless, the

use of copper is the second option due to the lower price of this metal³⁶. The price is a critical issue when the intention is to scale up the production of this kind of membranes and should be considered.

Based mainly on the silver salts, the principal carrier, the facilitated transport membranes for olefin/paraffin separations started to be developed initially as supported liquid membranes. After, in the search for superior mechanical stability, ion exchange and electrolyte membranes were applied in the separation.

1.5.2. Supported liquid membrane.

In 1973, Steigelmann and Hughes¹⁰⁰, working in the Standard Oil Company, started to develop films of cellulose acetate with silver nitrate solution in the pores of the membrane (support) (**Figure 5**). The solution is held in the pores of the support by capillary forces. The best initial result achieved for mixture selectivity (C_2H_4/C_2H_6) was *ca* 1280 and a mixture permeance of 30 GPU. Motivated by the preliminary results, they have developed these films for more than 10 years.¹⁰¹ However, spite of all efforts, they have not had success in the commercialization of this technology. The main problem found by them was the poor stability of the Ag^+ solution in the membrane pores. During the separation process, the solution was gradually swept out from the pores due to the dragging effect of the gas stream, dropping the selectivity of the process. To solve this problem, some subsequent works^{52,102–105} have focused on improving the stability of the solutions inside the pores of the membranes. However, the inherent instability of the supported liquid membranes continues to be a limiting feature in the commercial application of this membrane configuration.

Common performances of supported liquid membranes show selectivity values (α) ranging from 100 (α of C_3H_6/C_3H_8 using triethylene glycol/ $AgBF_4$ 43 wt.% with humidified feed stream) to 1000 (α of C_2H_4/C_2H_6 using $AgNO_3$ 4 M with humidified feed stream) and permeances from 4 to 27 GPU of olefin. High permeances are achieved due to low mass transport resistance through liquid medium. The use of humidified feed stream is required to avoid the drying of solution held in support pores. The support can be prepared of microporous membranes made of cellulose, polyvinylidene difluoride (PVDF), and polytetrafluoroethylene (PTFE).^{102,106–108} Indeed, the disadvantage for this membrane configuration are the real risks of dragging out the carrier solution from support pores.

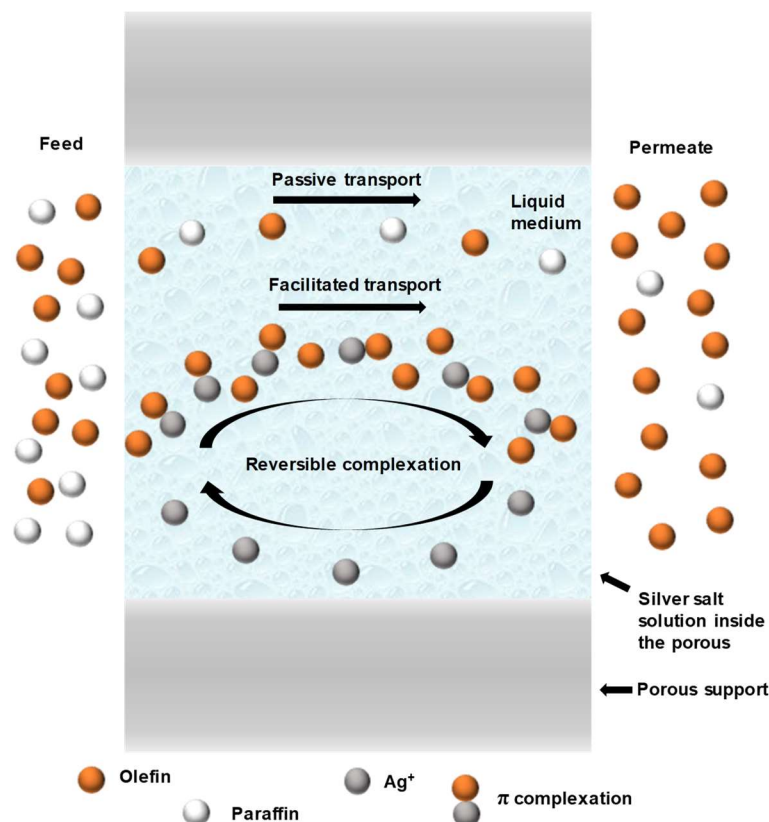


Figure 5. Supported liquid membrane.

1.5.3. Ion exchange membranes.

In the 1980's, to solve the problems with the supported liquid membranes resulting from the Ag^+ solution sweeping out by the passage of the gas stream, LeBlanc and co-workers¹⁰⁹ proposed the use of ion-exchange membranes. From this work, several other groups started to research this kind of strategy.^{39,110–116} The ion-exchange membranes are generally prepared by the addition of the silver salt to the membrane, which is formed by a polymer functionalized with an acid group, (e.g. sulfonic acid group) able to exchange H^+ for the Ag^+ . To achieve the ion-exchange, the polymer should be immersed in the Ag^+ solution or other metallic salt solution. Next, the membrane should be humidified. Without water, the Ag^+ ions are so strongly attached to the anionic sites in the membrane that makes very difficult the interaction with the olefin (**Figure 6**). Working with humidified feed streams, several interesting works have been reported in literature. For instance, Eriksen *et al.*¹¹⁰ applied Nafion (N-117), which was pre swollen in glycerine and soaked in aqueous AgBF_4 6 M, for separation of $\text{C}_2\text{H}_4/\text{C}_2\text{H}_6$ (1:1 molar ratio) humidified stream. The membrane provided a selectivity of 1930 and C_2H_4 permeability of 26800 Barrer or *ca.* 83 GPU.

As the carrier agent cannot be easily swept out from the membrane by the gas streams, the ion-exchange membranes have a vast advantage compared to supported liquid membranes. Despite their advantages, ion-exchange membranes formed by an ion-exchange polymer are usually more expensive and the required humidification is not desirable because it requires an additional operation step aimed at drying the outlet gas streams from the membrane unit.^{52,53} For this kind of membrane configuration, olefin/paraffin selectivity values between 290 and 1900, and olefin permeances ranging from 5 GPU to 83 GPU have been reported (always with humidified feed streams). The main polymeric materials used as matrix for ion-exchange membranes are Nafion and sulfonated polyphenyleneoxide.^{109,110}

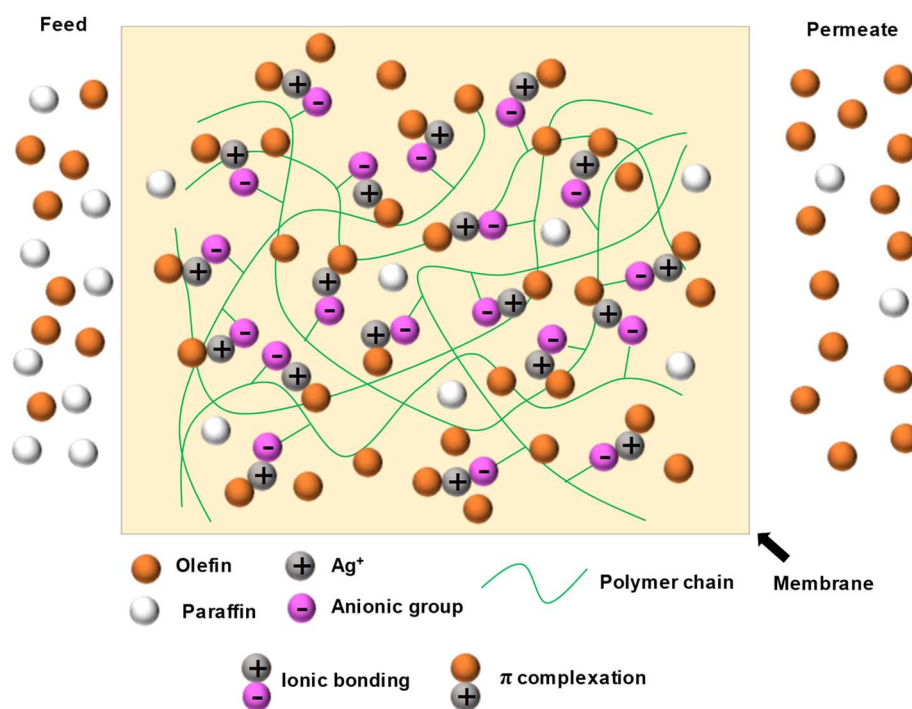


Figure 6. Ion-exchange membranes.

1.5.4. Electrolyte membranes.

During the 1990's and 2000's, to overcome the problems originated from the humidification dependence of the ion-exchange membranes, the development of dense materials denominated as polymer electrolyte membranes took place.^{41,117–119} Among others, the research groups of Ingo Pinnau^{118,120–122} and Yong Soo Kang^{119,123–126} stood out during the last few years. Pinnau and Toy¹¹⁸ reported that it was possible to dissolve silver salts in a hydrophilic polymer with polar functional groups able to coordinate with Ag⁺ ion, *e.g.* polyether. In this kind of

membrane, the facilitated transport was developed without humidification of the flowing gas, which represented a great achievement compared to the ion-exchange membranes. Kang *et al.*^{61,90,99,119,127,128} followed this method and dissolved silver salts in others polar polymer matrices as poly(2-ethyl-2-oxazoline) (POZ), polyvinylpyrrolidone (PVP) and poly(styrene-*b*-butadiene-*b*-styrene) (SBS). The results obtained with polymer electrolyte materials have by far exceeded the previous results of supported liquid and ion-exchange membranes. In 2006, the Kang's group,⁶¹ using the polymer electrolyte membranes with different silver salts and polymers, was able to surpass the upper bound of Robeson diagram with selectivities and permeabilities never achieved before. For instance, the ideal separation factor (pure gas permeation) of propylene/propane was above 10,000 with 45 GPU of propylene permeance.⁹⁹ In the permeation of gas mixtures, the selectivity dropped to 40–60 due to the plasticization effect that occurred in the membranes.⁹⁰

Inside the polymer matrix, the Ag⁺ cations can be arranged as free ions, ion pairs or higher order aggregates.¹²⁹ In this context, the term “free ions” should be understood as the Ag⁺ cations dissolved in the polymer matrix. The best way for the salt to be in the membrane is in the form of free ion, because the silver is more available to the interaction with the olefin.^{125,129–131} To reach the desired amount of free ions in the electrolyte membrane, normally, the polymer should have suitable functional groups (*e.g.* ether, amide, lactam, ester, alcohol and aromatic or aliphatic double bond) to interact with the Ag⁺ cations (**Figure 7a**). Polymers like poly(2-ethyl-2-oxazoline) (POZ), poly(ethylene oxide) (PEO), polyvinylpyrrolidone (PVP), polymethacrylates (PMA), poly(vinyl alcohol) (PVA), poly(styrene-*b*-butadiene-*b*-styrene) (SBS), poly(ethylene phthalate) (PEP),^{61,90,99,119,127,128} polyurethanes (PU) based on polyether or polyester^{42,75,132,133} and poly(ether-block-amide) (best known under the trademark Pebax[®])^{53,81,83} are used as suitable polymer matrix to maintain the dissolution of the silver salts in solid electrolyte membranes. The lower lattice energy of the salt is also crucial in this point to provide an easier way to dissolve the compound. Regarding this aspect, AgBF₄ is the most widely used salt due to its lowest lattice energy among ordinary silver salts for this purpose.^{52,99} At this point, in an attempt to increase the degree of salt dissociation inside the polymer electrolytes, a couple of investigations have proposed the addition of asparagine¹³⁴ in the POZ/AgBF₄ membranes and the use of a mixture of silver salts^{135,136} to improve the salt dissociation inside the polymer matrix.

Nevertheless, the interaction among the polymer functional group and the Ag⁺ salt may cause the reduction of Ag⁺ cation to Ag⁰ metallic. Over the time, the Ag⁰ growth and agglomeration cause the formation of some defects or holes at the interface between the metal particle and the

polymer chains. Without discrimination, the gases can easily pass through this path with lower mass transport resistance that leads to selectivity loss in long-term permeation experiments.⁵¹ Trying to solve this problem, several works have investigated solutions to overcome this drawback. In 2001, Jose *et al.*¹³⁷ retarded the formation of Ag^0 by incorporating phthalates to the membranes of PVP/AgBF₄ (**Table 5**). The stabilization of Ag^+ cation is due to the strong interaction between the carbonyl groups of phthalates and the Ag^+ that plays a key factor in slowing down the reduction induced by the lactam group of PVP. This was the pioneer work that started to report long-term experiments regarding the stability of polymer membranes containing silver salts. In attempt to avoid the Ag^0 growth and agglomeration, Park *et al.*¹³⁸ added a non-ionic surfactant (*n*-octyl β -D-glucopyranoside (8G1)) to the same kind of membrane to provide a steric hindrance effect hampering the metal particles coalescence. The protective layer onto the surface of formed silver particles was responsible to maintain the stability of membrane performance for 30 days (**Table 5**). However, the reduction problems were not solved by this strategy.

The reduction of Ag^+ by polymers like POZ normally results in an increase of H^+ ion concentration in the medium.¹³⁹ This is possible because the membrane contained a small amount of water favored by the hygroscopicity of salts like AgBF₄.¹⁴⁰ To suppress the Ag^+ reduction process, Kim *et al.*¹²⁴ proposed the introduction of HBF₄ in POZ/AgBF₄ membranes. The goal was to shift the equilibrium of the reduction reaction toward the regeneration of Ag^+ , preventing the formation of metallic silver. To investigate this proposal, they performed permeation tests under UV irradiation. As a result, it was found that tiny amounts of HBF₄ could indeed suppress the reduction of Ag^+ . A POZ/AgBF₄ membrane with the molar ratio of 1[carbonyl oxygen]:1[Ag^+] exhibited a selectivity of *ca.* 100 (50:50 vol.% of C₂H₄/C₂H₆) but, after 4 h under UV irradiation, the selectivity dropped to 1. When HBF₄ was introduced in the membrane with the molar ration of 1[carbonyl oxygen]:1[Ag^+]:0.2[HBF₄], the selectivity was maintained in the same initial value after 4 h under UV irradiation, thus having suppressed the Ag^+ reduction process inside the material. Although this procedure has been effective in laboratory studies, it seems an alternative difficult to implement on a large scale.

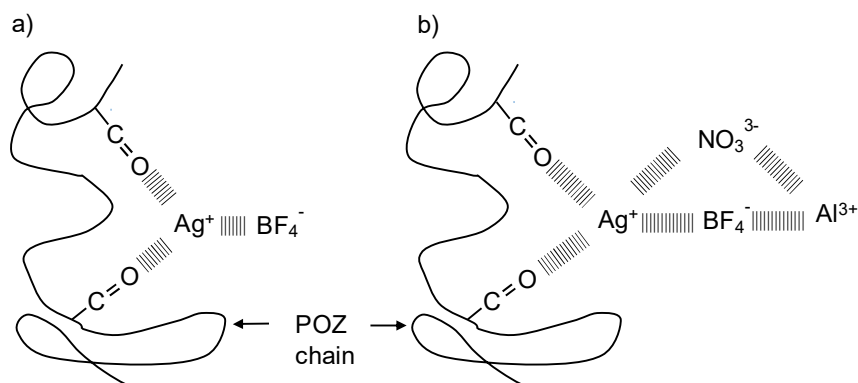


Figure 7. a) Interaction between the functional groups of POZ (amide C=O) with the Ag^+ from AgBF_4 and b) the mutual interaction between the $\text{Ag}^+/\text{NO}_3^-$ and $\text{Al}^{3+}/\text{BF}_4^-$ that weakens the former interaction between the C=O group of polymer.

On the other hand, Kang *et al.*¹⁴¹ interestingly suggested the introduction of $\text{Al}(\text{NO}_3)_3$ in POZ/ AgBF_4 membranes (**Table 5**~~Erro! Fonte de referência não encontrada.~~) to suppress Ag^+ ion reduction.. The function of $\text{Al}(\text{NO}_3)_3$ is to weaken the interaction between the functional group of the polymer and the Ag^+ . The mutual interaction between the ions, *i.e.* $\text{Ag}^+/\text{NO}_3^-$ and $\text{Al}^{3+}/\text{BF}_4^-$, is responsible for changing the chemical environment of the Ag^+ . Compared to the neat POZ/ AgBF_4 , the presence of $\text{Al}(\text{NO}_3)_3$ decreases the binding energy of the valence electron in the silver atom, which is verified by X-ray photoelectron spectroscopy (XPS) analysis. By modifying the electronic density of the silver atom, it is possible to adjust the intensity of the interaction between the Ag^+ and polymer functional group, reducing the oxidative power of the Ag^+ (**Figure 7b**). Using this strategy, it was possible to maintain the selectivity of the membrane for 14 days in long-term permeation tests.¹⁴¹

Also in an attempt to solve the problems related to the essential instability of Ag^+ inside polar polymer matrices, Kang *et al.*¹²⁵ showed a way to disperse silver salts in polydimethylsiloxane (PDMS), which is an inert polymer matrix, and yet reach the facilitated transport (**Table 5**). The Ag^+ does not share the same interaction observed in polar matrixes, leading to the formation of silver salt aggregates trapped in the polymer domains. At first glance, it seemed that it would not work, since the preferable interaction with the olefin takes place with silver free ions. However, in permeation tests, when the olefinic gases began to pass through the membrane, the olefin complexation gradually dissolved the silver salt aggregates into free ions, promoting the facilitated transport. The time to reach the dissolution is *ca.* 100 h, after that, steady-state transport is achieved. Following this approach, it was possible to reach mixed gas selectivity of *ca.* 200, propylene permeance of *ca.* 15 GPU and keep the values constant for one week. This

remarkable result brought the knowledge that introduction of silver salt in inert polymers, *i.e.* polymers that do not have functional groups to dissolve the silver salt, is feasible; and yet, they can promote the facilitated transport of olefins.

Table 5. Results of long-term permeation tests of various electrolyte membranes.

Polymer	Carrier/ stabilizer Fraction (%)	Separation performance (days)	Selectivity ^c	Mixed permeance (GPU)	gas	Olefin purity (mol%)	Reference
Electrolyte membranes of polar matrix							
PVP	AgBF ₄ /DOP 50.0 ^a */2.0 ^b *	4.2	160	7.5		99.4	In 2001, Jose <i>et al.</i> ¹³⁷
PVP	AgBF ₄ /DPP 50.0 ^a */2.0 ^b *	4.2	135	10		99.3	In 2001, Jose <i>et al.</i> ¹³⁷
PVP	AgBF ₄ /DBP 50.0 ^a */2.0 ^b *	4.2	85	9		98.8	In 2001, Jose <i>et al.</i> ¹³⁷
PVP	AgBF ₄ /8G1 49.8/0.5 ^a	30	50	34		98.0	In 2003, Park <i>et al.</i> ¹³⁸
PVP	AgBF ₄ /8G1 49.9/0.2 ^a	30	60	34		98.4	In 2003, Park <i>et al.</i> ¹³⁸
PEP	AgNO ₃ 50.0 ^a	7	16.2	5.4		94.2	In 2006, Kang <i>et al.</i> ¹⁴²

a - molar fraction; b - weight fraction; a* - molar fraction relates only to the polymer; b* - weight fraction relates only to the polymer; c - mixed gas (50:50 vol % of propylene/propane mixture)

*Al(NO₃)₃·9H₂O

PVP – polyvinylpyrrolidone; PEP – poly(ethylene phthalate); POZ – poly(2-ethyl-2-oxazoline); PEO – poly(ethylene oxide); PVA – poly(vinyl alcohol); PDMS – polydimethylsiloxane

DOP – dioctyl phthalate; DPP – diphenyl phthalate; DPB – dibutyl phthalate; 8G1 – n-octyl β-D-glucopyranoside.

Table 5. Continued.

Polymer	Carrier/ stabilizer Fraction (%)	Separation performance (days)	Selectivity ^c	Mixed permeance (GPU)	gas	Olefin purity (mol%)	Reference
Electrolyte membranes of polar matrix							
POZ	AgBF ₄ / Al(NO ₃) ₃ [*] 47.6/4.8 ^a	14	21	4.8		95.5	In 2013, Kang <i>et al.</i> ¹⁴¹
PEO	AgBF ₄ / Al(NO ₃) ₃ [*] 49.9/0.2 ^a	10	10	20		90.9	In 2015, Song <i>et al.</i> ¹⁴³
PVP	AgCF ₃ SO ₃ / Al(NO ₃) ₃ [*] 49.9/0.2 ^a	4	5	0.5		83.3	In 2015, Sung <i>et al.</i> ¹⁴⁴
PVP	AgCF ₃ SO ₃ / Al(NO ₃) ₃ [*] / BMImBF ₄ 43.6/4.1/8.7 ^a	4	9	0.5		90.0	In 2016, Park and Kang ¹⁴⁵
PVA	AgBF ₄ / Al(NO ₃) ₃ [*] 49.3/1.5 ^a	6	17	11		94.0	In 2017, Park <i>et al.</i> ⁵¹
Electrolyte membranes of inert matrix							
PDMS	AgBF ₄ 73 ^b	7	200	15		99.5	In 2004, Kim <i>et al.</i> ¹²⁵

a - molar fraction; b - weight fraction; a* - molar fraction relates only to the polymer; b* - weight fraction relates only to the polymer; c - mixed gas (50:50 vol % of propylene/propane mixture)

*Al(NO₃)₃·9H₂O

PVP – polyvinylpyrrolidone; PEP – poly(ethylene phthalate); POZ – poly(2-ethyl-2-oxazoline); PEO – poly(ethylene oxide); PVA – poly(vinyl alcohol); PDMS – polydimethylsiloxane

DOP – dioctyl phthalate; DPP – diphenyl phthalate; DPB – dibutyl phthalate; 8G1 – n-octyl β-D-glucopyranoside.

Also in an attempt to solve the problems related to the essential instability of Ag⁺ inside polar polymer matrices, Kang *et al.*¹²⁵ showed a way to disperse silver salts in polydimethylsiloxane (PDMS), which is an inert polymer matrix, and yet reach the facilitated transport (**Table 5**).

The Ag^+ does not share the same interaction observed in polar matrixes, leading to the formation of silver salt aggregates trapped in the polymer domains. At first glance, it seemed that it would not work, since the preferable interaction with the olefin takes place with silver free ions. However, in permeation tests, when the olefinic gases began to pass through the membrane, the olefin complexation gradually dissolved the silver salt aggregates into free ions, promoting the facilitated transport. The time to reach the dissolution is *ca.* 100 h, after that, steady-state transport is achieved. Following this approach, it was possible to reach mixed gas selectivity of *ca.* 200, propylene permeance of *ca.* 15 GPU and keep the values constant for one week. This remarkable result brought the knowledge that introduction of silver salt in inert polymers, *i.e.* polymers that do not have functional groups to dissolve the silver salt, is feasible; and yet, they can promote the facilitated transport of olefins.

In the set of electrolyte membranes, the longest-term permeation test was performed in a PVP/AgBF₄/n-octyl β -D-glucopyranoside (8G1) membrane. Along 30 days, the presence of non-ionic surfactant (8G1) provided a stable membrane performance (mixture selectivity $\text{C}_3\text{H}_6/\text{C}_3\text{H}_8 = 60$ and mixed gas permeance of 34 GPU) with the highest permeance reported for electrolyte membranes.¹³⁸ The introduction of 8G1 only avoided the Ag^0 growth and agglomeration, however the reduction problems remained unsolved. Among attempts that indeed try to protect Ag^+ cation against reduction, POZ/AgBF₄/Al(NO₃)₃ membrane showed a stable performance (mixture selectivity $\text{C}_3\text{H}_6/\text{C}_3\text{H}_8 = 21$ and mixed gas permeance of 4.8 GPU) for 14 days.¹⁴¹ The highest selectivity value was found in PDMS/AgBF₄ membrane with a stable performance (mixture selectivity $\text{C}_3\text{H}_6/\text{C}_3\text{H}_8 = 200$ and mixed gas permeance of 15 GPU) for 7 days.¹²⁵ In general, the selectivity values can vary from 5 to 200 and the mixed gas permeance from 0.5 to 34 GPU.^{125,138,144} The time reported in long-term permeation tests ranges from 4 to 30 days.^{125,144,145}

PVP is the most used polymer for electrolyte membranes of polar matrix; however, membranes made of PDMS, which is an inert matrix, have shown the highest selectivity values. Despite all efforts, the selectivity loss caused by Ag^+ cation reduction remains unsolved for permeation tests longer than 2 weeks. Considering simultaneously selectivity, permeance, and separation stability, the best result is performed by PDMS/AgBF₄ membrane, indicating that the use of inert matrixes is a promising strategy to develop new electrolyte membranes for olefin/paraffin separation. To avoid the reduction of Ag^+ inside the polymer matrix, besides the silicone-based polymers, other polymer class, which is well known by its intrinsic inertness, is thought to be used as membrane material. Fluoropolymers have been used in the latest works trying to solve the problem of Ag^+ instability.^{45,146} In general, since Ag^+ is a stronger oxidant,

the aim is that the polymer to be used as membrane does not have any group that could be oxidized by the Ag^+ cation.

1.6. Challenges to avoid carrier instability.

Taking into account the results reached at laboratory scale by using polymer membranes with silver salts⁶¹, the search for higher selectivities and permeabilities in the separation process is no more a big challenge. However, the maintenance of the membrane performance in long-term operation conditions has become a new target to be surpassed. Ag^+ cations incorporated in the electrolyte membranes report instability problems related to the tendency of them to react with other species, deactivating or poisoning the agent carrier in long-term operation.^{53,63} The photoreduction or the exposition to reductant gases, *e.g.* hydrogen, inactivates the Ag^+ cation due to its reduction to metallic silver (Ag^0). The decontrolled formation of Ag^0 in the membrane can damage it with negative influence on the separation performance. The Ag^+ cation also can react with hydrogen sulfide (H_2S) and acetylene (C_2H_2) forming undesired compounds, principally silver acetylide that is extremely explosive and can pose a significant risk to the process. The deactivation reaction of Ag^+ are summarized in **Table 6**. It is worth emphasizing that small amounts (*ca.* 10 ppm) of these contaminants in the gas stream is enough to drastically decrease the process selectivity, in less than one week, impairing the membrane use.⁵³

Table 6. Deactivation reaction of silver cation (Ag^+).

Reaction	Description
$\text{Ag}^+ + \text{e}^- \xrightarrow{uv} \text{Ag}^0$	Photoreduction
$2\text{Ag}^+ + \text{H}_2 \rightarrow 2\text{Ag}^0 + 2\text{H}^+$	Reduction by H_2
$\text{C}_2\text{H}_2 + 2\text{AgX} \rightarrow \text{Ag}_2\text{C}_2 + 2\text{HX}$	Formation of silver acetylide
$\text{H}_2\text{S} + 2\text{AgX} \rightarrow \text{Ag}_2\text{S} + 2\text{HX}$	Formation of silver sulfide

X is an anionic component of silver salt

Normally, the olefin/paraffin stream from naphtha steam cracking, which aims to be separated by membrane technology, contains some silver poisonous agents in low concentration, in ppm range. In the naphtha cracking furnace, it is necessary to operate with *ca.* 20 ppm of sulfur compounds in the feedstock to prevent the formation of undesired carbon monoxide. The function of sulfur is to passivate the nickel and iron catalysts sites in the

cracking coil material of the furnace. The H₂S formed in the cracked gases is removed together with the CO₂ in the compression section using caustic solvents in absorption towers. Usually, CO₂ and H₂S concentration in the overhead stream of the absorption towers is below 0.2 ppm.^{12,14}

Usually, hydrogen reduced compounds and acetylene (C₂ and C₃) are some byproducts of the SC. Hydrogen is removed at the lowest temperatures achieved in the chilling train, together with methane; they are overhead products of the demethanizer.³⁶ The acetylene species, *i.e.* acetylene, methylacetylene (MA), and propadiene (PD), are removed by catalytic hydrogenation processes that transform them into more saturated hydrocarbons. The content of acetylenic compounds in the outlet of the hydrogenation process is <0.5 ppm.¹⁴ Typically, the specification of polymer grade ethylene and propylene from the SC is <1 ppm of H₂ and <4 ppm of acetylene species.⁶⁵

This severe scenario corresponds to a typical petrochemical plant where membranes are intended to be implemented. In addition, there are other challenges not related to silver poisoning. To replace or integrate C₂ and C₃ splitters, the membrane should treat a feed stream under a pressure of 5-20 bar and produce a permeate stream at 1–3 bar. Governed by these conditions, plasticization effects may occur even in the most rigid polymer membranes.^{18,147} Thus, withstanding the negative influence of contaminants and avoid plasticization issues are essential challenges to be overcome by the next generation membranes.

1.7. Some alternatives to overcome the Ag⁺ deactivation.

In this context, some research groups have focused their efforts on proposing strategies to mitigate and/or overcome the problems imposed to the separation by the deactivation of the carrier. In the scientific literature, the most prominent efforts, proposing different solution lines to these problems, seem to not have a clear consensus on what would be the most promising strategy. The alternatives, which use dense polymeric films, are (i) the use of metallic nanoparticles as carrier, mainly silver nanoparticles, (ii) the use of ionic liquids for the stabilization of Ag⁺, (iii) *in situ* regeneration of electrolyte polymeric membrane by using oxidizing agents, and (iv) the use of highly fluorinated polymers.

1.7.1. Silver nanoparticles as carrier.

As already seen, the reduction of Ag^+ to Ag^0 throughout the separation process causes deactivation of the carrier and consequently the loss of membrane selectivity. In 2004, Kang *et al.*,⁹¹ when performing permeation tests on a polymeric membrane with silver salts, noticed that the selectivity was reduced from 52 to 31 in 150 h of experiment. In parallel, it was observed the formation of metallic silver nanoparticles (Ag NP), whose size increased from 14.75 to 27.75 nm. It should be noted that, even at the beginning of the experiment, Ag NP were formed, pointing to the difficulty in avoiding Ag^+ reduction. What was remarkable in this experimental observation was that, even with Ag NP of 27.75 nm in the membrane, the selectivity did not fall abruptly, only 40% reduction was observed. The hypothesis proposed for the maintenance of the Ag carrier properties was the formation of a partial charge polarization on the Ag NP surface. The phenomena observed by these authors has initiated a new study framework involving facilitated transport nanocomposite membranes of light olefins in place of Ag^+ salts. The great advantage of this replacement is that the problems of reduction deactivation involving the Ag^+ ion would be bypassed. This would allow the maintenance of the separation properties of the membranes in long-term operation.¹⁴⁸

In 2007, Kang *et al.*⁹² presented the first paper introducing the idea of Ag NP as carrier for the facilitated transport of olefins. To polarize the surface of Ag NP more efficiently, p-benzoquinone (p-BQ), an electron acceptor, was used to this goal, since the polymer matrix (EPR-poly(ethylene-co-propylene)) used was non-polar. The membrane selectivity achieved working with 50:50 v/v propylene/propane mixtures was 11 (**Table 7**). After this work, others studies have begun to explore new molecules to polarize the surface of the Ag NP,^{47,149–151} always aiming to improve the selectivity of separation. **Figure 8**. Schematic representation of the possible polarization mechanism of the Ag NP surface by 7,7,8,8-tetracyanoquinodimethane (TCNQ). **Figure 8** shows a schematic representation of the possible polarization mechanism of the Ag NP surface by 7,7,8,8-tetracyanoquinodimethane (TCNQ).

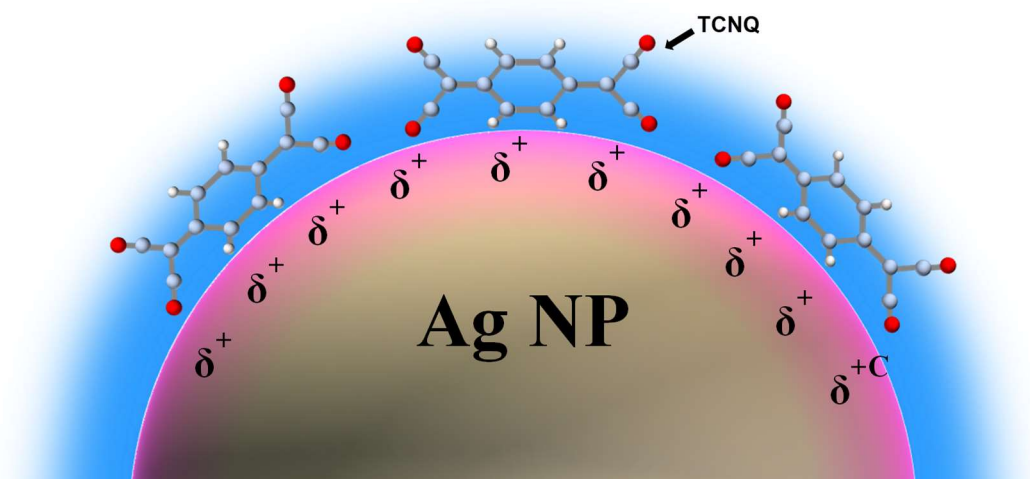


Figure 8. Schematic representation of the possible polarization mechanism of the Ag NP surface by 7,7,8,8-tetracyanoquinodimethane (TCNQ).

Table 7 shows the most promising results observed for the separation of light olefin/paraffin mixtures by membranes using Ag NP and **Table 8** presents the chemical structures of activator compounds for Ag NP. Analyzing **Table 7**, there is a clear evolution in the carrier properties of the Ag NP due, mainly, to the suitable choice of the polarizing agent of the NP surface, but other factors are important such as the nanoparticle concentration, its size in the polymer matrix, and its adequate dispersion along the diffusional gas pathway. Although the concentration may vary from one work to another, it is noted that a concentration higher than 30 wt% of Ag NP, relative to the composite material, is required. In all works, where the facilitated transport of olefins by Ag NP with activator is verified, the NP have diameters smaller than 30 nm.¹⁵² Therefore, Ag NP with sizes below this value can further improve the transport of the olefinic gases. Experimentally, the formation of the induced dipole on the interface between the Ag NP and the activator is checked by the X-ray photoelectron spectroscopy analysis (XPS). By changing the binding energy of the $d_{5/2}$ and $d_{3/2}$ silver orbitals to higher values, it is possible to verify the polarization of the NP surface.^{92,149}

Table 7. Main results of metallic nanoparticles as carriers for membrane facilitated transport of olefins.

Polymer	Carrier/activator Fraction (%)	Separation performance (days)	Selectivity ^c	Total permeance (GPU)	Olefin purity (mol%)	Reference
EPR	Ag NP/p-BQ 35.1/29.8 ^b	3.5	11	0.45	91.7	In 2007, Kang <i>et al.</i> ⁹²
PVP	Au NP 81.1 ^b	—	22	1.2	95.7	In 2008, Kang <i>et al.</i> ⁸⁹
SLM*	Ag NP/ BMImBF ₄ 41.2/58.8 ^b	5	17	2.7	94.4	In 2008, Kang <i>et al.</i> ¹⁵¹
POZ	Ag NP/PVP 29.8/35.1 ^b	15	21	1.3	95.5	In 2008, Kang and Kang ^{91,153}
PVP	Ag NP/ TCNQ 33.1/0.7 ^b	5.5	50	3.5	98.0	In 2011, Chae <i>et al.</i> ¹⁴⁹
PVP	Ag NP/TTF 33.3/33.3 ^a	—	145	2.5	99.3	In 2014, Choi <i>et al.</i> ¹⁵⁰
PEO	Ag NP/p-BQ 27.8/2.8 ^a	10	10	15	90.9	In 2014, Hong <i>et al.</i> ¹⁵⁴
PU	Ag NP/(OTf) ⁻ 21.0/29.1 ^b	—	24.4 ^d	—	—	In 2016, Rezende <i>et al.</i> ¹⁵⁵

a - molar fraction; b - weight fraction; c - mixed gas (50:50 vol % of propylene/propane mixture)

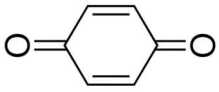
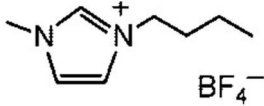
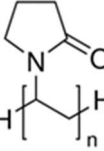
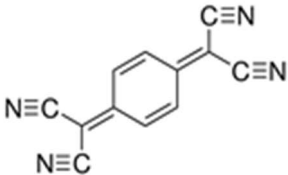
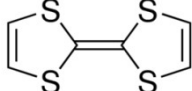
*Supported liquid membranes. Support of polyester microporous membrane

EPR – poly(ethylene-co-propylene); PVP – polyvinylpyrrolidone; POZ – poly(2-ethyl-2-oxazoline); PEO – poly(ethylene oxide)

Ag NP – silver nanoparticle; Au NP – gold nanoparticle

p-BQ – p-benzoquinone; BMImBF₄ – 1-butyl-3-methylimidazolium tetrafluoroborate; TCNQ – 7,7,8,8-tetracyanoquinodimethane; TTF – tetrathiafulvalene.

Table 8. Chemical structures of activator agents for Ag NP.

Activator	Chemical structure	Reference
p-BQ		In 2007, Kang <i>et al.</i> ⁹² and in 2014, Hong <i>et al.</i> ¹⁵⁴
BMIImBF ₄		In 2008, Kang <i>et al.</i> ¹⁵¹
PVP*		In 2008, Kang and Kang ^{91,153}
TCNQ		In 2011, Chae <i>et al.</i> ¹⁴⁹
TTF		In 2014, Choi <i>et al.</i> ¹⁵⁰

p-BQ: p-benzoquinone – BMIImBF₄ – 1-butyl-3-methylimidazolium tetrafluoroborate; PVP* – polyvinylpyrrolidone crosslinked (this activator was introduced as a stabilizer during the Ag NP synthesis); TCNQ – 7,7,8,8-tetracyanoquinodimethane; and TTF – tetrathiafulvalene.

The membranes with Ag NP have reached higher selectivity values compared to membranes made of PVP¹⁴⁹ with the same weight ratio of Ag⁺ and with the advantage of being resistant to light and hydrogen gas.⁴⁷ To further investigate the viability of Ag NP as promising carriers for the facilitated transport of olefins, Kang *et al.*⁴⁷ verified the deactivation resistance against C₂H₂. Surprisingly, the NP activated with TCNQ as a polarizing agent proved to be resistant to the formation of silver acetylide. Therefore, this is an additional evidence of the superior chemical stability that the Ag NP reports compared to Ag⁺ salts. To become even more feasible, the chemical stability of Ag NP membranes against hydrogen sulfide and other sulfur compounds needs to be investigated. Other source of instability for the separation is the inherent instability of the polarizing agents, which is few mentioned in the literature. Compounds like p-BQ, TCNQ and tetrathiafulvalene (TTF) work as electron acceptor; thus, they have a tendency of withdrawing electrons from other molecules. This feature makes polarizing agents susceptible to chemical attack similarly as it is found in Ag⁺ cation that results in reduced species unable to polarize the surface of Ag NP.

Other aspect that should be addressed is related to the permeance of this kind of membranes. Generally, the flux of Ag NP membranes need to be improved. For industrial application, high fluxes are required because it is necessary to reach the target high production of industrial

plants. Thus, Hong *et al.*¹⁵⁴ prepared a membrane of poly(ethylene oxide) with Ag NP activated by p-benzoquinone seeking out the permeance increase. The composite membrane showed a selectivity of 10 and a mixed-gas permeance of 15 GPU for 10 days, the highest permeance reported for Ag NP membranes.

The use of Ag NP was also tested in membranes of polyurethane (ether based) (PU). Rezende *et al.*¹⁵⁵ measured the sorption values of propylene and propane in Ag NP/PU membranes (**Table 7**), in which the Ag NP were synthesized *in situ* into PU matrix using UV light radiation and silver triflate (AgCF_3SO_3) as salt precursor. It was found an ideal solubility selectivity of 24.4 in the Ag NP/PU membranes that could indicate an essential contribution of the sorption selectivity in propylene/propane separation by this kind of membrane.

1.7.2. Ionic liquids for the stabilization of Ag^+ .

The introduction of ionic liquids (IL) to stabilize Ag^+ salts in facilitated transport membranes is another alternative that the literature has reported as promising. For instance, the use of POZ/ AgNO_3 membranes could reach stable separation performance (mixed gas permeance of 5.6 and selectivity of 32) during 150 h by the addition of small amount of 1-butyl-3-methylimidazolium nitrate (BMImNO_3).¹³¹ Another example is the use of PVP/ AgBF_4 membrane with BMImNO_3 that was able to maintain a selectivity of 7.2 with 3.6 GPU nearly constant along 160 h of permeation (**Table 9**).¹⁵⁶

Table 9. Results of membrane performance with ionic liquids for protection against the reduction of Ag⁺.

Polymer	Carrier/ stabilizer Fraction (%) ^a	Separation performance (days)	Selectivity ^b	Mixed permeance (GPU)	gas Olefin purity (mol%)	Reference
POZ	AgNO ₃ / BMImNO ₃ 58.8/7.0	6	32	5.6	84.8	In 2006, Kang <i>et al.</i> ¹³¹
PVP ^f	AgBF ₄ / BMImNO ₃ 8.9/86.6	6.5	7.2	3.6	87.8	In 2007, Kang <i>et al.</i> ¹⁵⁶
PVDF- HFP	AgBF ₄ / BMImBF ₄ 60.2/7.8	10	700	55 ^d 6630 ^e	99.9	In 2013, Fallanza <i>et al.</i> ⁴⁵
TPU	AgBF ₄ / BMImBF ₄ 10/20	—	18.3 ^c	3000 ^e	94.8	In 2017, Wang <i>et al.</i> ⁷⁵
TPU	Ag(Tf ₂ N)/ BMImTf ₂ N 10/20	—	9 ^c	8398 ^e	90.0	In 2017, Wang <i>et al.</i> ⁷⁵
TPU	Ag(Tf ₂ N) 30	—	38 ^c	8512 ^e	97.4	In 2017, Wang <i>et al.</i> ⁷⁵

a - weight fraction; b - mixed gas (50:50 vol % of propylene/propane mixture); c – tests under 2 bar transmembrane pressure; d – olefin permeance; e – olefin permeability in Barrer

POZ – poly(2-ethyl-2-oxazoline); PVP – polyvinylpyrrolidone; PVDF-HFP – poly (vinylidene fluoride-*co*-hexafluoropropylene); TPU – thermoplastic polyurethane Elastollan®

BMImNO₃ – 1-butyl-3-methylimidazolium nitrate; BMImBF₄ – 1-butyl-3-methylimidazolium tetrafluoroborate; BMImTf₂N – 1-butyl-3-methylimidazolium bis(tri fluoromethanesulfonyl)imide.

In the search for higher stability, in the last few years, dense composite membranes incorporating ionic liquids have received much attention.^{45,145,156–159} In this configuration, IL/Ag⁺ system is embedded in the polymer so that Ag⁺ cations are distributed between the polymer matrix and a liquid phase entrapped inside it. This Ag⁺ distribution through the membrane promotes the fixed and mobile carrier facilitated transport mechanisms, leading to higher permeabilities and selectivities.¹⁶⁰ In this line, Ortiz *et al.*^{45,161} developed a material with promising characteristics for the separation of light olefin/paraffin mixtures. Previous to the

material choice, a thorough investigation on the most suitable IL to form the IL/silver salt pair was carried out^{162,163}. Among several pairs, 1-butyl-3-methylimidazolium tetrafluoroborate/silver tetrafluoroborate (BMImBF₄/AgBF₄) was selected. Additionally, the fluoropolymer poly (vinylidene fluoride-co-hexafluoropropylene) (PVDF-HFP) (**Figure 9**) was used as polymer matrix to avoid the potential reduction of Ag⁺ by the polymer chain.

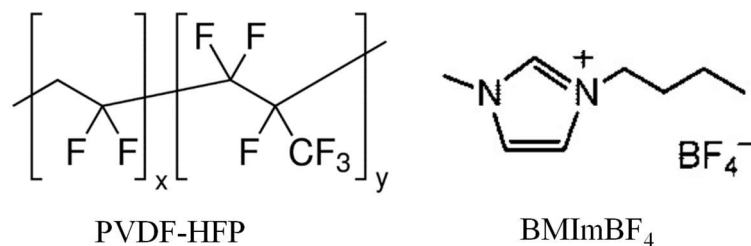


Figure 9. Chemical structure of PVDF-HFP and BMImBF₄.

The results obtained with the composite films of PVDF-HFP/BMImBF₄-AgBF₄ behave satisfactorily providing a mixture selectivity C₃H₆/C₃H₈ = 700, and propylene permeability of 6630 Barrer or *ca.* 55 GPU in the separation process (**Table 9**). This remarkable performance was maintained for 10 days. The IL could stabilize the Ag⁺ in a long-term experiment in this kind of membrane. To prove the potential of this type of material it is necessary to perform tests under the presence of the deactivating agents and verify the behavior of the composite membranes with ionic liquid against the simulated industrial operational conditions.⁴⁵

On the other hand, different tests were made using thermoplastic polyurethanes (TPU)/IL membranes, but without taking into account the problems related to instability of the olefins transport. Wang *et al.*⁷⁵ synthesized several PU membranes with different silver salt/IL pairs. The IL used contained the 1-butyl-3-methylimidazolium cation (BMIm⁺). Among all membranes prepared with IL, the highest selectivity (C₃H₆/C₃H₈ = 18.3) was found for the AgBF₄/BMImBF₄/TPU (weight fraction 10/20/70) membrane. The highest olefin permeability (8400 Barrer) was observed for the Ag(Tf₂N)/BMImTf₂N/TPU (weight fraction % 10/20/70) membrane. In general, the IL enhanced the selectivity of the TPU membranes by favoring the coordination of olefin with the Ag⁺ ions inside the dense polymeric matrix. However, the best result (C₃H₆/C₃H₈ = 38 and 8512 Barrer) were reported for the Ag(Tf₂N)/TPU (weight fraction % 10/20/70) membrane without adding IL (**Table 9**).

1.7.3. In situ regeneration using oxidizing agents.

Merkel *et al.*⁵³ have continued the research line focused on the development of polymer electrolyte membranes using polyethers which can provide a facilitated transport without the matrix humidification. This group further discussed the instability of the Ag⁺ cation caused by deactivating agents listed in **Table 10**. The material used to produce the membranes was the Pebax[®] 2533 (**Figure 10**) with various levels of silver tetrafluorobate (AgBF₄). It is an elastomeric thermoplastic material composed of blocks of polyether (PE) and polyamide (PA). Specifically, the poly (ether-b-amide) used was prepared from nylon 12 and polytetramethylene oxide.

Table 10. Results of the deactivation and regeneration processes of Pebax[®] 2533 + 80 wt% AgBF₄ membrane with original selectivity of 40 and olefin permeance of 87 GPU, adapted from Merkel *et al.* (2013).⁵³

Deactivation process	Selectivity ^a drop	Regeneration process	Selectivity ^a regeneration
Membrane exposed to ambient light for 34 days	-95%	Immersion in a H ₂ O ₂ /HBF ₄ bath ^b for 30 s	100%
Membrane exposed to ambient light for 34 days	-95%	Contact with the H ₂ O ₂ /HBF ₄ vapors ^c for 16 h	50%
7 days of hydrogen permeation	-95%	Contact with the H ₂ O ₂ /HBF ₄ vapors for 60 h	50%
Membrane exposed to 10 ppm of acetylene in the ethylene feed for 5 days	-85%	Immersion in a bath of H ₂ O ₂ /HBF ₄ for 60 s	69%
Membrane exposed to 10 ppm of hydrogen sulfide in the ethylene feed for 7 days	-92%	Immersion in a bath of H ₂ O ₂ /HBF ₄ or contact with the H ₂ O ₂ /HBF ₄ vapors	0%

a – mixed gas (65:35 vol % of ethylene/ethane); b - 1:1 mixture of 35 wt% H₂O₂ in water and 50 wt% HBF₄ in water; c - membrane in contact with the vapor of a 1:1 H₂O₂/HBF₄ aqueous solutions at room temperature.

The Pebax[®] 2533/AgBF₄ membranes were tested against the deactivating agents in the separation of ethylene/ethane mixtures, and as expected, the selectivity in the separation process has collapsed. However, by exposing these membranes to hydrogen peroxide vapors combined with tetrafluoroboric acid (H₂O₂/HBF₄) or immersing directly in a bath of H₂O₂/HBF₄, the membranes were able to return partially or completely to the original selectivity values (**Table 10**).

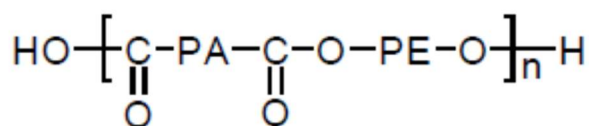


Figure 10. Chemical structure of Pebax[®]

This *in situ* regeneration, by using these oxidative treatments, has reversed the deactivation caused by light, H₂ and C₂H₂; however, the membranes deactivated by H₂S have not shown any reversion. In the light and H₂ cases, the explanation for the regeneration is that the Ag⁰ formed in the deactivation process is oxidized and returns to the Ag⁺ form, becoming active again for the facilitated transport. However, the deactivation process caused by H₂ seems to be more aggressive than light deactivation, since the required time to restore the same level of selectivity was longer in the case of H₂ deactivation (60 h). According to Merkel *et al.*,⁵³ the understanding of the phenomenon involved in the regeneration of membranes inactivated by C₂H₂ still demands more detailed studies. Nevertheless, taking into account the chemical reaction of silver acetylide formation it can be thought that the regeneration is not caused by the oxidizing agent itself, but by the presence of HBF₄, which shifts the equilibrium of the reduction reaction toward the Ag⁺ regeneration.¹⁶⁴

From the possibility of *in situ* membrane regeneration, the research group believes that it will be possible to extend the service life of the membrane by applying cyclic regeneration steps, thus enabling the practical application of the membranes made of Pebax[®] 2533/AgBF₄. Analyzing this proposal, it is noted that the deactivation by H₂S was not solved and the cyclic regeneration steps should be evaluated against the commercial application feasibility of the technology.

1.7.4. Use of highly fluorinated polymers/ Current technological options.

In 2016, the Compact Membrane Systems (CMS) Company has unveiled the separation system called Optiperm. By this olefin/paraffin separation system, the Company has claimed resistance against common poisonous agents in feed stream, including hydrogen and acetylene. The Company promises a high return with small financial investment. For instance, the Company describes a typical application of olefin/paraffin separation in a polypropylene reactor purge stream that costs <\$1M to installation, <\$500K per year of operating cost and an internal rate of return of >150%.^{165,166}

The base for the stability of the Ag^+ inside the polymer matrix is the use of a highly fluorinated polymer that is extremely chemically and thermally resistant. Specifically, the fluorinated polymer with sulfonate functional group is used.⁴⁶ The Ag^+ is added to the polymer matrix by ion-exchange with the H^+ of the sulfonic groups. Unlike the previous works,^{52,110,113,115} in which the membrane was immersed in the Ag^+ water solution to achieve the ion-exchange, now, the polymer and the Ag^+ salt are solubilized in the same solvent and after, the solution is casted to form the polymeric film. This material is called silver ionomer and it is responsible for the facilitated transport of olefins.⁴⁶

As a typical structure of thin film composite membrane used for industrial gas separations, the CMS's membrane has different layers joined together, each one with specific function, as shown in the **Figure 11**. The selective layer has the task of distinguishing the molecules to be separated and it should be thin (0.1-1 μm) to provide high permeances. A thin layer does not have enough mechanical strength and it is necessary deposit it onto the surface of a porous support (150–200 μm) with negligible mass transport resistance. Normally, the support has small porous (< 100 nm) on the surface.^{167,168}

When the thickness of the selective layer become closer to the porous diameter of the support, it takes place a geometric restriction in the diffusion of the gases, leading to a substantial decreasing of the gas flux.^{169,170} To solve this problem, usually, it is added a third layer between the support and the selective layer, called gutter layer. The gutter layer is a high diffusion layer composed by a very permeable polymer. Its purpose is to channel the outgoing gases from selective layer into the surface pores of the support. By this channel effect, the geometric restriction is reduced compared to the two-layer configuration. The optimum thin composite membrane performance is reached when the thickness of the gutter layer is in the range of 1–2 times the pore radius of the support.¹⁶⁷ In addition to the former three layers, another high diffusion layer can be added to protect the selective layer and plug any defects eventually present. This protective layer prevents damage during the manipulation of the membrane and protects the exposed surface of the selective layer from contaminants present in the stream to be separated.^{167,168}



Figure 11. Schematic illustration of a usual thin film composite membrane used for industrial gas separations.

In the CMS's Optiperm system,⁴⁶ the high diffusion and the selective layers are composed of a custom fluoropolymer designing for a specific function according to the layer assignment. The high diffusion layers should be made preferably of a glassy polymer containing tough functional groups against the oxidation by the Ag^+ . Perfluoroether and chlorotrifluoroethylene are useful polymers to be applied in the high diffusion layers, rather than primary and secondary alcohol, iodo, bromo, and aldehyde. For the selective layer, the polymer should be more inert than the high diffusion layer, preferably should be use an amorphous perfluoropolymer searching the maximus protection for the Ag^+ . The fluoropolymer inertness and the protection offered by the protective layer are responsible for the stability and resistance against poisonous agents during the separation process. Another source of inherent reduction of the Ag^+ is the direct contact between the selective layer and the porous support. Usually, the polymer from which the support is made has small amount of incidental organic vapor or other chemicals. Besides, the oxidable organic groups in the own polymer chain of the support could reduce the Ag^+ . Thus, another protection factor is also attributed to the gutter layer, but in this case, the protection is associated to avoid the direct contact between the selective layer and the support.

In the patent assigned to CMS,⁴⁶ the claims are mainly related to the material used in the preparation of the membrane. The best results (**Table 11**) were achieved by using the following materials for the membrane layers. The high diffusion layers are composed by the Teflon® AF 2400, a copolymer with a high molar percentage (83%) of perfluoro(2,2-dimethyl-1,3-dioxole) (PDD) and 17% of tetrafluoroethylene. The porous support is made of PAN350, an ultrafilter made from polyacrylonitrile. Two selective layers with the same amount of silver salt (AgNO_3) are employed. One layer has higher permeance and lower selectivity (selective layer 1) and another has lower productivity and higher selectivity (selective layer 2). The selective layer 1 is composed by a silver ionomer of sulfonic acid based on the PDD/VF (vinyl fluoride)/PPSF

(perfluoro sulfonylfluorideethylvinyl ether) terpolymer (T_g 58 °C). The selective layer 2 is made of the Aquivion®D79-25BS,¹⁴⁶ a perfluorosulfonic acid polymer made from perfluorosulfonylfluoridevinyl ether monomer. In the patent, there are no long-term stability and resistance against poisonous agents tests. The permeation tests were conducted using humidification (relative humidity greater than 90%) of the feed stream and N₂ as a sweep gas.

Table 11. Results of facilitated transport membranes based on highly fluorinated polymers from Majumdar *et al.* (2016).⁴⁶

Polymer	Carrier Fraction (%) ^a	Selectivity ^b	Total permeance (GPU)	Olefin purity (mol%)
(PDD/VF/PPSF)/	AgNO ₃	95.5	278.9	96.0
	16.7 ^b			
Aquivion®D79-25BS	AgNO ₃	52.1	317.37	92.9
	16.7 ^b			

a - weight fraction; b - mixed gas (20:80 vol % of propylene/propane mixture)
 PDD – perfluoro(2,2-dimethyl-1,3-dioxole); VF – vinyl fluoride ; PPSF – perfluoro sulfonylfluorideethylvinyl ether.

Regarding the humidification need issue related to the ion-exchange membrane,¹⁷¹ Feiring *et al.*¹⁷² tested different sweep gas configurations for checking the hole of the moisture and the sweep gas in highly fluorinated silver ionomer membranes. In the configuration 1, they humidified the sweep gas (N₂ under 2.8 kPa) and the feed mixture (10:90 vol % of propylene/propane under 414 kPa). In the configuration 2, the feed was not humidified, and the sweep gas was a vapor from above a sealed tank of water under vacuum of 6.7 kPa absolute pressure. Finally, the configuration 3 employed a dried feed and vacuum. As expected, it was founded the best results for configuration 1. Surprisingly, the configuration 2 and 3 presented equivalent high olefin/paraffin selectivity but 30% and 60% lesser olefin permeance respectively. Comparing the configurations 1 and 2, it seems that only the humidification of the permeate stream can supply the facilitated transport activity during the permeation, resulting in still notable high olefin permeance. The presence of the inert sweep gas in the permeate implies a further separation step. Thus, the configuration 2, which does not use the N₂ as sweep gas, shows an advantage since the permeate stream only has the olefin and an eventual small amount of paraffin. Nevertheless, the presence of water in the permeate was not avoided. A subsequent drying stage may be considered in the separation train, but it seems an easier task than removing the inert gas from the output stream of the membrane unit. To replace the inert sweep gas, the

use of a vacuum pump should be taken in account and a tradeoff between energy consumption and permeance may be considered.

1.8. Summary and conclusions.

The global demand of light olefins has experienced a significant growth related to the increasing demand of different polymers over the last decades. The principal process to produce olefins is the naphtha steam cracking process, the most energy intensive process in the petrochemical industry. In an attempt to save energy in the process, some alternatives have been proposed to replace or integrate with the current cryogenic distillation separation of olefins and paraffins. Among several technologies, facilitated transport membranes have stood out owing to the combination of high selectivity and permeance. However, to be used in the industrial separation, some instability issues should be considered.

The Ag^+ cation, the main carrier for the facilitated transport membrane, suffers deactivation by poisonous agents present in the gaseous stream to be separated. Even without the presence of deactivating agents, the Ag^+ cation can be reduced by the chemical environment of the polymer matrix from which the membrane is made. After achieving superior performance by using silver salts dissolved or dispersed in polymer matrix, the current arduous task is to maintain the selectivity in long-term separation process. To attain this goal, some clever alternatives have been proposed to overcome the hurdle.

By adding small amounts of HBF_4 or non-ionic surfactants, it is possible to confer certain stability to Ag^+ cation. In addition, the introduction of $\text{Al}(\text{NO}_3)_3$ in electrolyte membranes can weaken the interaction between the functional group of the polymer and the Ag^+ salt, providing a more stable chemical environment to the Ag^+ . A remarkable result was reached with a $\text{POZ}/\text{AgBF}_4/\text{Al}(\text{NO}_3)_3$ membrane. The selectivity was maintained for 14 days. The use of another interesting carrier, Ag NP, overcome the problem related to the reduction of Ag^+ . To be useful, the Ag NP should be activated by a suitable polarizing agent. Experimental tests showed the resistance of Ag NP against acetylene, which is one of the poisonous agents. Therefore, Ag NP reveal higher resistance compared to Ag^+ . The best results reached by Ag NP composite membranes achieved a selectivity of 10 and a mixed-gas permeance of 15 GPU for 10 days.

To avoid the Ag^+ cation reduction inside the polymer matrix, more inert polymers have begun to be applied as a host matrix to silver salts. Specially fluoropolymers, which are well known by their intrinsic inertness, have been used as material to the preparation of Ag^+ facilitated

transport membranes. A PVDF-HFP matrix was used for hosting a system of $\text{AgBF}_4/\text{BMImBF}_4$. IL have been demonstrated as another type of agents able to stabilize Ag^+ against reduction. Joining together these features, a membrane of PVDF-HFP/ BMImBF_4 - AgBF_4 reported a mixture selectivity of 700 and propylene permeability of 6630 Barrer (*ca.* 55 GPU) in a 10 days separation test. Claiming resistance against common poisonous agents in the feed stream, a thin film composite membrane based on a highly fluorinated polymer was developed by Compact Membrane Systems Company. Beyond the intrinsic inertness of the membrane material, additional protection arises from the configuration of the composite membrane. A thin separation layer composed by fluorinated silver ionomer, which is responsible for the facilitated transport of olefins, is between two high diffusion protective layers. This configuration seems to avoid the poisoning of the Ag^+ cation that are ionic bonded in the ion-exchange polymer; however, the membrane humidification dependence was not solved. If the problems related to poisoning are still present in the membrane process, other alternative is to try an *in situ* regeneration using vapor of the oxidizing system ($\text{H}_2\text{O}_2/\text{HBF}_4$) to recover the separation performance and extend the service life of the membrane.

Most of the results reported in the literature didn't consider the presence of poisonous agents in the permeation experiments. The main concern is still the stability of Ag^+ inside the polymer matrix, but it seems that this challenge has started to be overcome using stabilizing agents and inert polymer matrix. Issues related to the plasticization effects are not yet a problem discussed intensively by the works concentrated in the facilitated transport membrane for the olefin/paraffin separation. Probably, the future efforts will be dedicated to understand deeply the problems regarding the poisonous agents, trying to figure out a more robust solution. Due to the lower performance required and milder condition operation, the initial commercial application of the membrane technology to olefin/paraffin separation could be in the vent streams of some kinds of petrochemical reactors. This application could make a step forward in the use of commercial olefin/paraffin membrane units before the challenging task aimed to replace the distillation unit in the steam cracking process or in the FCC off-gas streams.

1.9. Thesis scope and outline.

This Thesis emphasizes the use of two different proposing strategies to mitigate and/or overcome the problems imposed to olefins/paraffins separation: the use of Ag NP/activator and $\text{AgBF}_4/\text{BMImBF}_4$ systems. The general goal is to prepare WPUU composites membranes with

these two systems and after performing gas permeation tests to evaluate gas transport properties of olefins and paraffins.

Considering the potential applicability of the membrane technology for light olefins/paraffins separation, the goal of Chapter 1 is to critically review the development of facilitated transport membrane for this separation highlighting the challenges and main drawbacks surpassed during the last decades. A comprehensive analysis of the instability/deactivation problems confronted by distinct kinds of membranes is carried out. The alkene/alkane membrane separation technology is presented describing the source of poisonous agents for the principal carrier used, i.e. the Ag^+ . Finally, some recent strategies are pointed out as options that try to overcome the Ag^+ deactivation by smart solutions.

The objective of Chapter 2 is to present briefly the main analytical techniques used to characterize the WPUU composites studied in this Thesis and how to interpret the results to get the desired information. Transmission electron microscopy (TEM), small angle scattering X-ray (SAXS), X-ray diffraction (XRD), Fourier transform infrared spectroscopy (FTIR), and thermogravimetric analysis (TGA) are presented with special attention related to the Ag NP size and the interaction between the polymer chains and silver species (Ag^0 and Ag^+).

Chapter 3 reports the use of WPUU for gas separation and the approach for Ag NP synthesis. The first goal is to justify the use of Ag NP/WPUU as material for gas separation membrane. The second aim is to prepare and characterize Ag NP/WPUU membranes by TEM, SAXS, XRD, FTIR, and TGA to check the morphology of Ag NP and their influence on chemical and thermal features of WPUU.

Chapter 4 collects all gas permeation tests of the Thesis. The objective is to prepare Ag NP/activator/WPUU and $\text{AgBF}_4/\text{BMImBF}_4/\text{WPUU}$ membranes and after investigating the gas transport behavior through these membranes. The activators used were p-Bq and BMImBF_4 . FTIR was applied to investigate the influence of Ag^+ cation on WPUU matrix. Moreover, the FTIR results were used to correlate the polymer structure modification with gas transport behavior.

Finally, Chapter 5 reports the general conclusions of this thesis and an overview of the challenges and prospects for future research.

Chapter 2

2. METHODS AND EQUIPMENT

Abstract

The objective of this chapter is to present briefly the main analytical techniques used to characterize the WPUU composites studied in this Thesis and how to interpret the results to get the desired information. Transmission electron microscopy (TEM), small angle scattering X-ray (SAXS), X-ray diffraction (XRD), Fourier transform infrared spectroscopy (FTIR), and thermogravimetric analysis (TGA) are presented with special attention related to the Ag NP size and the interaction between the polymer chains and silver species (Ag^0 and Ag^+).

2.1. Transmission electron microscopy (TEM), Small angle X-ray scattering (SAXS), and X-ray diffraction (XRD)

In the study of nanomaterials, a set of techniques is used to check the morphology of NP analyzed. Beginning with transmission electron microscopy (TEM), which is a microscopy technique used to generate high resolution images of NP. To be performed, TEM requires a primary step of sample preparation. The sample prepared must be thin enough to allow the crossing of an electron beam generating images by transmission. For polymer material containing NP, it is necessary to prepare the samples in an ultramicrotome equipment. Thus, it is possible to prepare very thin slices in a range of few tens of nanometers. When the polymer material has a very low glass transition temperature (T_g), *i.e.*, an elastomeric polymer, it is necessary to cut the material using an ultramicrotome with cryoscopy. Cryoscopy temperatures get the polymer very rigid allowing the normal utilization of the ultramicrotome knife. Without low temperatures, it is not possible to perform proper cuts in the material. Although TEM can provide high resolution images, this technique scans a very small part of the sample, in the order of cubic micrometers. As a very small percentage of the sample is analyzed, some errors in the conclusions obtained may occur, especially if the best regions are selected by the microscopist to the detriment of other areas unattended.¹⁷³

To avoid these types of interpretation problems, TEM analyses should always be complemented by SAXS (small angle X-ray scattering) analyzes. The sample volume analyzed by SAXS is usually in the order of cubic millimeters or more, making the analysis much more representative of the sample reality. However, by using SAXS, a resolution loss takes place compared to TEM.¹⁷³

In SAXS technique for nanocomposites characterization, when two phases (the matrix and the nanofiller) are irradiated by the X-ray beam, the electron density contrast between two phases provides information about the geometry and the three-dimensional arrangement of smaller phase (the nanofiller). Depending on the resolution quality of the SAXS equipment used, information on the arrangement of nanofiller, which ranges from 1 nm and a few micrometers, is obtained. The information is obtained by measuring the scattered intensity I as a function of the scattering vector q that is related to the scattering angle θ by the Bragg law, equation (6):

$$q = \frac{4\pi \sin(\theta/2)}{\lambda} \quad (6), \text{ equation}$$

Where λ is the wavelength of the X-ray radiation used. The scattering profile of $I(q)$ function (when plotted on log-log scale) typically shows regions of exponential scattering (Guinier region) and decaying scattering in the form of power-law. From the Guinier region, it is possible to determine the average structural size of the nanofiller according to Guinier's law according to equation (7):¹⁷³

$$I(q) = G \exp\left(-\frac{q^2 R_g^2}{3}\right) \quad (7)$$

Where G is the extrapolation of the value of $I(0)$ and it is related to the volume v of the nanofiller inside polymer matrix, the volumetric fraction Φ , and the composition $\Delta\rho^2$ (electronic density difference between the phases) by equation (8). Additionally, R_g is the Guinier Radius (or for independent particles $R_g = R =$ radius of rotation), which is related to the mean size ($D =$ diameter) of nanofiller by equation (9).

$$G = \Delta\rho^2 v \Phi (1 - \Phi) \quad (8)$$

$$R_g = \frac{D}{2} \sqrt{\frac{3}{5}} \quad (9)$$

The power-law region that follows the Guinier region (as q increases) is calculated as:

$$I(q) = \frac{B}{q^P} \quad (10)$$

Where B is the prefactor of the power-law that is not very significant in scattering of nanocomposites, and P is the power-law exponent that provides information about the nanofiller geometry.

The surface area of colloid can be calculated from the scattering intensity under power-law regime.¹⁷⁴ Considering the equation (10), if the nanofiller surface morphology is smooth, then $I \approx q^{-4}$ with $P = 4$, which better known as Porod law. With $P = 4$ as reference, deviations from this value provide information related to nanofiller morphology within polymer matrix. For example, P values in the range of $3 \leq P < 4$ are related to a surface morphology that contains roughnesses and it is called surface fractal. If the power-law presents an exponent $P < 3$, it is

said that the nanofiller has a morphology of mass fractal. For NP with simple Euclidean geometries, P can provide a signature for the morphology of the nanofiller. It is possible to distinguish between rods, discs and spheres if the slope of $\log I(q)$ vs. $\log q$ is -1, -2 or -4, respectively (**Figure 12**).¹⁷⁴⁻¹⁷⁶

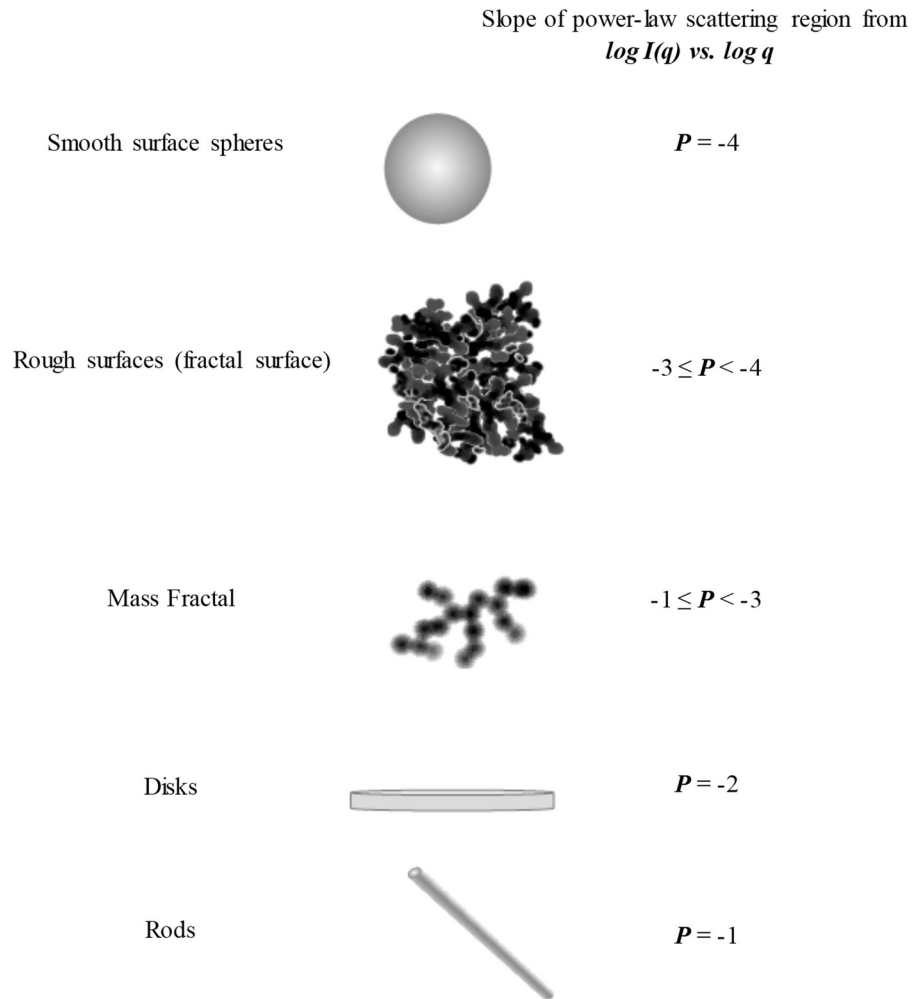


Figure 12. Slopes of power-law region from $\log I(q)$ vs. $\log q$ and respective nanofiller morphology.

The equation for a single level of scattering profile can be reached by combining the Guinier's law to the related power-law regime equation as follows:

$$I(q) = G \exp\left(-\frac{q^2 R_g^2}{3}\right) + B \left\{ \frac{[\text{erf}(qR_g/\sqrt{6})]^3}{q} \right\}^P \quad (11)$$

Equation (11) represents suitably the scattering profile of monodisperse systems. However, for polydisperse systems with multiple hierarchical structures with different size scales (in the case of nanocomposites), the x equation needs to be expanded to take into account the multiple hierarchical levels of organization, so the equation (11) is expanded to:

$$I(q) \approx \sum_{i=1}^n \left(G_i \exp\left(-\frac{q^2 R_{G_i}^2}{3}\right) + B_i \exp\left(-\frac{q^2 R_{G_{(i+1)}}^2}{3}\right) \times \left(\frac{\left[\operatorname{erf}\left(\frac{q R_{G_i}}{\sqrt{6}}\right) \right]^2}{q} \right)^{P_i} \right) \quad (12)$$

Where i define the structural level related to the size scale; thus, $i = 1$ is the lower size hierarchical level (higher q values). This model represented by equation (12) is known as unified model proposed by Beaucage *et al.*^{177,178}

When a spatial correlation between the domains is present, *i.e.*, for systems with higher nanoparticles concentration, an interference peak appears in the experimental curves. All previous equations for $I(q)$ considered dilute systems of nanofiller. For systems with spatial correlation, a structural factor $S(q)$ is added to the $I(q)$ equation. Beaucage *et al.* proposed a semiempirical equation (13) for the structure factor $S(q)$. Where k is defined as a packing factor, which is proportional to the volume fraction occupied in the matrix by the correlated heterogeneities (reaching its theoretical maximum of 5.9 for close-packed crystal), and θ is a term associated with spatial correlations that occur at average distance d . For spherical domains, θ is given by equation (14). The mean distance between domains, d , can be determined by equation (15), where q_{max} corresponds to the maximum of the peak interference function, $I(q)$, visible in the experimental curves.¹⁷⁹

$$S(q) = (1 + k\theta)^{-1} \quad (13)$$

$$\theta = 3 \frac{\sin(qd) - qd \cos(qd)}{(qd)^3} \quad (14)$$

$$d = \frac{2\pi}{q_{max}} \quad (15)$$

As a measure of polydispersity of nanoparticles embedded in a polymer matrix, a generalized index of polydispersity (**PDI**) for symmetric particles was proposed by Beaucage *et al.*¹⁸⁰ as follows:

$$PDI = \frac{BR_g^4}{(1.62G)} \quad (16)$$

Where B is Porod constant, G is the Guinier prefactor, and R_g is the radius of gyration. Polydispersity, as well as asymmetry, of the particles serves to increase the dimensionless ratio of $BR_g^4/(1.62G)$. This ratio, normalized by the value for monodisperse spheres of 1.62 (the lowest possible value), serves as an index for polydispersity, **PDI**.

Another technique that also uses X-ray radiation during analysis is X-ray diffraction (XRD). Differently from SAXS, which analyzes scattered radiation detected at smaller angles, XRD detects X-rays that diffract in the crystalline structure of the NP, and this diffracted radiation is detected at higher angles. The distance between the chemical bonds of the atoms participating in the crystalline lattice of the material has the same order of magnitude of the incident X-ray radiation. For this reason, the phenomenon of diffraction occurs caused by the crystalline network of the material that acts as a diffraction grating for incident X-rays. From the data of XRD is possible to determine the position and distance of atoms in the crystalline structure of the material. Information about distinct phases that may be present and mean diameter of crystals can also be found.^{173,181,182}

Regarding the problems addressed in the Thesis, XRD analysis will be used to check crystalline structures of NP using comparison with diffraction patterns found in diffractogram libraries. Another utility is the estimation of the mean diameter of NP crystals using the Debye-Scherrer equation (equation (17)), where D is the mean particle diameter, λ is the wavelength of incident radiation, k is the geometric factor (constant that depends on the shape of the crystal), B is the full width at half maximum (FWHM) of the diffraction peak, and θ is the Bragg's angle.^{181,182}

$$D = \frac{K\lambda}{B \cos \theta} \quad (17)$$

2.2. Infrared spectroscopy (FTIR)

FTIR analysis is an essential tool to evaluate the changes in proton donator and proton acceptor groups of PUU^{73,183} The vibrational modes of $-NH$, $C=O$ (urethane and urea), and ether ($C-O-C$) bonds receive great attention because it possible to analyze changes and rearrangements of hydrogen bonds that can occur among polymer chains.^{73,184} The analysis of

the bonded urethane carbonyl (*st* C=O) band at 1702 cm⁻¹ and bonded urea (*st* C=O) at 1645 cm⁻¹ allows a discussion about microseparation between the rigid and flexible domains of PUU.^{183,185} The band region of ether group (*st* C-O-C) at 1100 cm⁻¹ also deserves attention because of the possible ether-silver interactions (Ag⁺ or Ag⁰).

Comparing the spectrum of a neat polymer, band shifts toward higher or lower wavenumber can take place upon the addition of fillers/compounds in the polymer matrix. Generally, shifts to lower wavenumbers suggest an interaction intensification between the functional group and the filler/compound or other group in the polymer backbone. On the other hand, shifts to higher wavenumbers imply in an opposite behavior, *i.e.*, an interaction decrease related to the functional group.¹⁴¹

2.3. Thermogravimetric analysis (TGA)

The TGA allows to evaluate the degradation profile of the polymeric material. Some minor changes, not shown in TGA curves, can be evaluated by derivative thermogravimetry (DTG) curves. The thermal degradation of PUU films is basically a two-stage depolycondensation process. The first stage of degradation is related to the rigid domains of the polymer and the subsequent stage corresponds to flexible domains. Due to its association with rigid domains of PUU, the initial temperature of degradation (T_{onset}) can provide information on changes in the urethane and urea groups.^{186,187}

In the DTG curves, several peaks appeared, demonstrating the complexity of the degradation. They are associated with temperature at maximum rate of weight loss (T_{vmax}) at each stage of degradation. The higher T_{vmax} , which is relative to the last peak of the DTG curves, is related to the degradation of polymer flexible domains; thus, variations in this T_{vmax} are closely associated to changes in ether groups present in PUU.^{186,187}

Chapter 3

3. POLY(URETHANE UREA)/Ag NP COMPOSITES

Abstract

This chapter reviews the use of WPUU for gas separation and the approach for Ag NP synthesis. The goal was synthesized Ag NP inside the WPUU aqueous dispersion, *i.e.*, *in situ*. By the method adopted for the synthesis, it was possible to overcome the challenges to control the suitable dispersion and low polydispersity of Ag NP in aqueous medium. WPUU/Ag NP membranes with silver content up to 50wt% were prepared.

3.1. Waterborne poly(urethane urea)s.

Polyurethane (PU) and poly(urethane urea) (PUU) belong to a versatile polymer class, which have been extensively employed as fibers, foams, coatings, adhesives, elastomers, membranes, and biomaterials.¹⁸⁸⁻¹⁹⁰ This polymer family can provide desirable properties for a range of application by tailoring the features of rigid and flexible segments present in the material. By a suitable formulation choice, it is possible to obtain from vitreous to elastomeric characteristics. The PU and PUU are formed by flexible polyol segments, most commonly based on polyethers or polyesters; and by rigid segments formed by diisocyanates and chain extenders.^{74,191} Morphologically, PU and PUU present, to some extent, a degree of microphase separation between rigid and flexible domains due to thermodynamic incompatibility between them.¹⁸⁸ The **Figure 13** shows a representation of these domains in the polymer matrix. By controlling the microphase separation using a wide range of precursor monomers, it is possible to explore unusual properties for different applications.¹⁹²

The final morphology and mechanical properties of material are governed primarily by multiples hydrogen bonds formed between proton donator (urethane and urea N-H) and proton acceptor (urethane and urea C=O, ester carbonyl and ether oxygen) groups.^{73,193} PUU with bidentate hydrogen bonds generally exhibit a superior Young's modulus, tensile strength, and extension properties compared to related PU.¹⁹⁴ In terms of thermal processability, in most cases, PU and PUU are processing from solution instead of thermal processes due to the thermal degradability of urea and urethane linkage.^{186,195}

PU and PUU obtained from aqueous dispersion (WPU and WPUU) have been receiving great attention by replacing volatile organic compounds (VOC) in the preparation of coatings, membranes, adhesives, food packaging, and biomedical devices.¹⁸⁴ Thus, this replacement reduces safety risks and environment concerns compared to conventional PU and PUU formulations based on VOC.^{196,197}

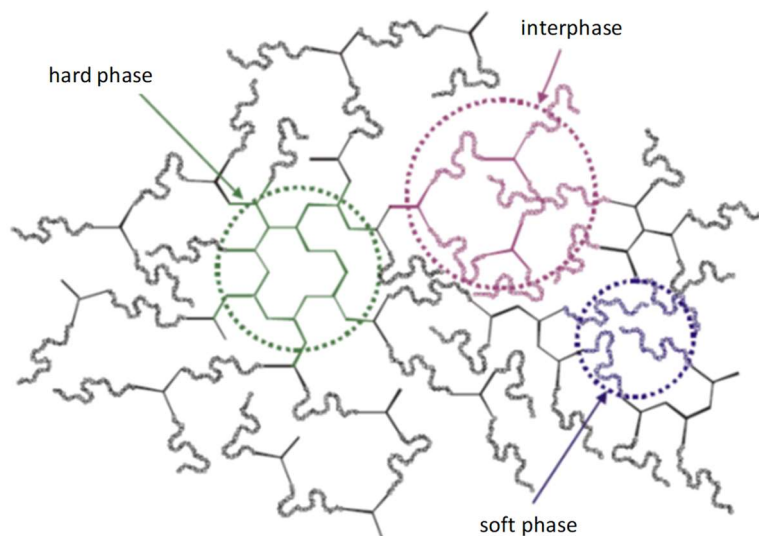


Figure 13. Representation of rigid and flexible domains structure in a segmented PU. This figure was reproduced from ref.¹⁹².

WPU and WPUU synthesis is usually initiated by the formation of a prepolymer using the reaction between a polyol and ionic segments (internal emulsifier) with an excess of diisocyanate, forming urethane bonds and terminal cyanate (NCO) groups.¹⁹⁶ Further, water is added to the prepolymer to formation of dispersion. The incorporation of ionic groups allows the stabilization of dispersion in aqueous medium. After, the terminal NCO groups can react with diols or diamines forming WPU or WPUU, respectively. This step is known as chain extension. The extension by using diamines results in polymer chains with urea groups. The extension by using diols results in urethane groups. **Figure 14** schematizes the formation of prepolymer and chain extension step in the synthesis of the WPU and WPUU. In aqueous media, WPU and WPUU constitute particles in nanometric scale (<100nm) due to their ionic groups that act as internal emulsifier.^{198,199} In these particles, internal emulsifier, urethane, and urea groups face the aqueous medium, while the flexible segments, composed by more hydrophobic domains turn inwardly (**Figure 15**).¹⁹⁶

WPUU have been researching as a material for the permeation of gases. From 2002 to 2004, Coutinho *et al.*^{200,201} studied the use of WPUU based on hydroxyl-terminated polybutadiene (HTPB) and poly (propylene glycol) (PPG) in CO₂ and N₂ permeations. In these works, the most expressive results were an ideal selectivity ($\alpha^{id}CO_2/N_2$) of 31.2 and 22.6 with CO₂ permeance of 0.025 and 1.57 GPU, respectively. Continuing the research line, in 2011, Barboza *et al.*^{198,199} evaluated CO₂ permeability in WPUU/clay composites with different contents of poly (propylene glycol) (PPG) and block copolymer based on poly(ethylene glycol) and

poly(propylene glycol) (EG-b-PG). By an increment in the copolymer content, it was observed an increase in the CO₂ permeability in films with and without clay. In sequence, Pereira *et al.*^{80,202} tested $\alpha^{\text{id}}\text{CO}_2/\text{CH}_4$ of WPUU membranes stimulated by the context of CO₂ removal from natural gas (CH₄). Using NCO/OH ratio of 1.5 in the prepolymer and varying the proportion of PPG and EG-b-PG in the precursor monomers, it was found a formulation with 25% PPG/75% EG-b-PG that presented an $\alpha^{\text{id}}\text{CO}_2/\text{CH}_4$ of 54 and CO₂ permeability of 189 Barrer. This result was considered promising, since it was possible to cross the Robeson's 2008 upper bound for this separation.

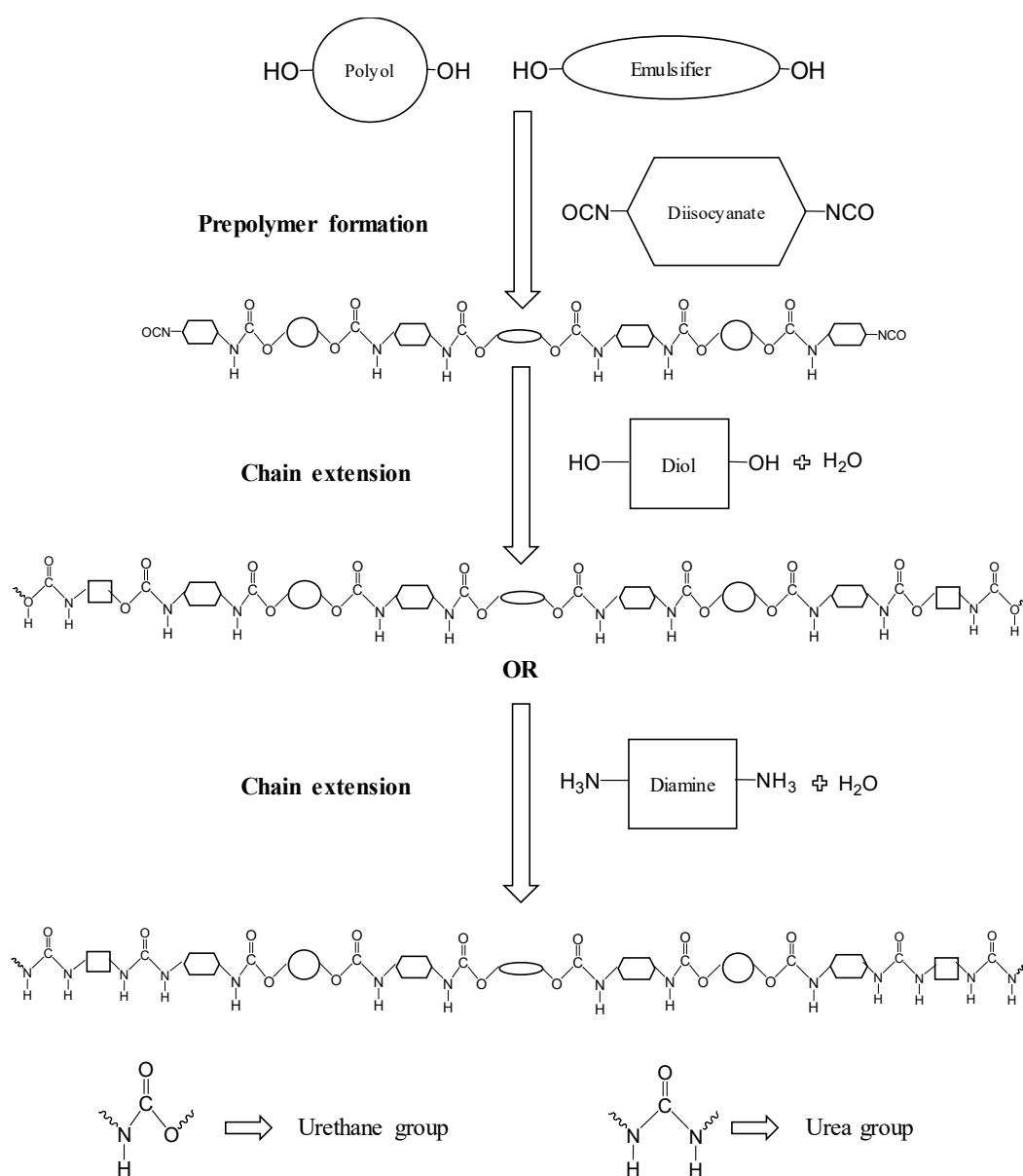


Figure 14. Scheme of prepolymer formation and chain extension during the synthesis of WPU and WPUU.

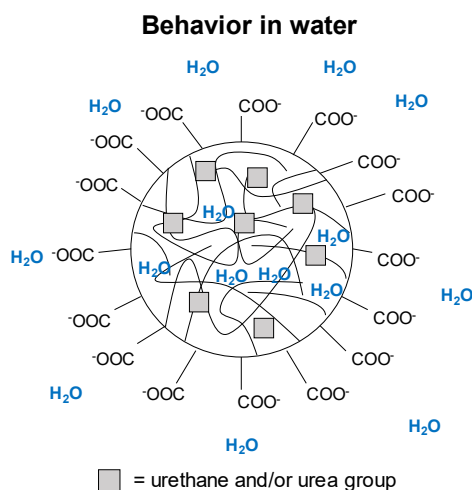


Figure 15. Behavior of WPU and WPUU particles in water medium. The scheme shows an anionic ionomer.

From Pereira's formulation^{80,202} with noteworthy result for CO₂/CH₄ separation, in 2013, Campos¹⁸⁵ introduced powder Ag NP (coated with 4% of polyvinylpyrrolidone) in an WPUU dispersion by using a high intensity ultrasonic processor. After, α^{id} of olefin/paraffin was tested in the WPUU/Ag NP membranes with higher Ag NP content of 1wt%. It was not possible to achieve the facilitated transport of olefin through the membranes; however, it was the first work that investigated the permeability of petrochemical gases in the WPUU/Ag NP composite membranes. Also, CO₂ and N₂ permeabilities was evaluated as probe gases to investigate how Ag NP presence influenced the gas transport properties of the membranes. The results obtained by Fourier transform infrared spectroscopy (FTIR) and thermogravimetry (TGA) suggested an interaction between ether oxygen atoms of WPUU and Ag NP. The CO₂-philic feature of the material was impaired, since the polyol segments was obstructed by interactions with Ag NP, which were among ether linkages. CO₂, C₂H₄ permeability values were reduced remarkably due to the ether groups obstruction. C₂H₆ and N₂ permeability values were decreased moderately because of the Ag NP aggregates formation, which intensified the tortuosity of the diffusion path in WPUU matrix.¹⁸⁵

PUU have a suitable feature for gas separation membranes. PUU hard segments work as a strong "virtual" crosslinking that may improve the plasticization resistance of membrane during the gas separation processes.⁷³⁻⁷⁵ Additionally, WPU and WPUU based materials obtained from water dispersion do not need thermal processes to be used, protecting the products from thermal degradation.¹⁹⁵ A desired requirement for a polymer to be use as Ag NP nanocomposite

membrane for the olefin facilitated transport is to allow the gas access to the Ag NP surface. Polymers with high diffusional resistance do not favor the facilitated transport because they decrease the target molecule concentration around the carrier, hampering the jump mechanism.^{52,76,203} Normally, elastomeric polymers should favor the permeation of more condensable gases. This is appropriate, since the larger molecules from the steam creaking products are light olefins and paraffins. As CO₂, olefins are apolar gases, however they can interact with the polar polymer domains through quadrupole moment. Many papers explore the ether oxygen of poly(ethylene glycol) (PEG) segments to improve the CO₂ solubility in membranes.^{202,204,205} For WPUU with flexible polyether segments, it is possible to enhance the solubility of olefins compared to paraffins. The presence of PEG in the flexible segments ensures a greater interaction with olefinic gases, since the gas transport through membrane take places in these domains.²⁰⁴ Probably, elastomeric polymers with higher CO₂-philic feature, in theory, also should show a higher olefin solubility, which may contribute in some way to the separation. If the polymer alone ensures enough olefin concentration within the membrane and consequently around the carrier, surely, one of the conditions for facilitated transport will be present. However, very permeable polymers can impair the selectivity of the membrane, even if the facilitated transport is present. Due to high permeability to olefins and paraffins, a membrane could not be suitable to the separation, since the high flux of paraffin can decrease any selectivity to olefins. Thus, a tradeoff between elastomeric behavior of material and separation selectivity should be considered.

The polymer WPUU formulation used in Campos' s work¹⁸⁵ is elastomeric ($T_g = -35^\circ\text{C}$) and it has a higher CO₂-philic feature due to the presence of ether groups from PEG, hence the olefins permeability is greater than the paraffins (α^{id} ethene/ethane is 1.4). Although, paraffins should be more permeable, the opposite behavior takes place. Olefins, which are lesser condensable, are more permeable than paraffins due to the interaction between ether groups and alkenes.

Another factor to be considered is that in all works dealing with membranes for olefins facilitated transport, only commercial polymers are used as matrix for membranes. The use of a versatile polymer as WPUU may be useful to achieve properties in which is necessary to make a certain modification in the formulation and consequently in the polymer structure/properties. Moreover, the material preparation in aqueous medium, avoiding the use of undesirable volatile organic compounds, is eco-friendly. Therefore, the strategy of using WPUU as matrix for Ag NP composite membranes applied to olefin/paraffin separation is reasonable to be proposed.

3.2. Ag NP synthesis.

In the preparation of nanocomposites materials there are two types of approach: bottom-up and top-down. Top-down strategy starts from bulk-scale materials and by using physical, chemical or mechanical processes the method can reduce the bulk material into nanoparticles. Bottom-up strategy starts with atoms or molecules to obtain nanoparticles.^{206,207}

In top-down approach, usually, higher energy mechanical methods are used, such as mills that fragment the microparticles into smaller particles in nanometer scale. High energy laser, ultrasonic, thermal and lithographic methods can also be used.²⁰⁸ Generally, the final material in this approach consists of nanoparticles with higher polydispersity, without a suitable size and shape control of the produced nanoparticles. Top-down strategy variations are related to the quality of dispersion provided by macroscopic processing factors such as design of the processing structure, mixing speed and residence time. There is a considerable limitation to the optimization of the process from these factors.^{206,207}

In bottom-up approach, nanoparticle structures are generally constructed by chemical processes. This strategy produces structures with more complex shapes prepared from atoms or molecules. Better particle size, shape, and lower polydispersity control can be achieved. The methods involved in bottom-up strategy comprise precipitation, aerosol and sol-gel processes.²⁰⁶

Metal nanoparticles (NP) have been extensively exploited in the formation of polymeric nanocomposites with many functional properties. The difficulties in dealing with metal NP are their instability (due to the tendency of agglomeration caused by high free surface energy), oxidation by air, humidity, etc. By introducing NP into dielectric polymer matrices, many problems of stabilization and manipulation of metal NP are solved.²⁰⁹ The principal metals used in polymer nanocomposites are silver, gold, platinum and copper. The main features added to the polymers by the addition of NP are conductivity,²¹⁰ antibacterial,^{211,212} magnetic²¹³ and catalytic characteristics.²¹⁴ These special NP aspects arise from the increase of surface atoms as the size of NP decreases. In macroscopic materials, most atoms are internal, and a few are found in the basal planes of the surface. In NP, almost all atoms are in the surface (in corners or edges) providing to the material the characteristics of superficial atoms. This fact is the reason for special and unique features of NP.²⁰⁶

The bottom-up strategy is more efficient regarding the control of particle size; however, it brings up additional challenges to NP synthesis. In the specific case of Ag NP, focus of the Thesis, the Ag NP synthesis via chemical reduction in water medium is the most widely used

method.^{207,215} To synthesize Ag NP via chemical reduction, there are basically three elements: (i) precursor salt, (ii) stabilizing and (iii) reducing agent. There are a variety of possible combinations involving several types of these three elements. Nevertheless, the most used and cheapest syntheses involves the use of AgNO_3 as precursor salt²¹⁶ and NaBH_4 as stabilizing agent.²¹⁷ Since chemical reduction is an easy method to reproduce, it takes into account when goes is to scale-up the production of Ag NP. Stabilizers may also vary widely, depending on the system, but generally they have surfactant properties, which protect the surface of NP against agglomeration. Recently prepared NP anchor in the polar regions of the polymer, preventing the approximation of others NP and avoiding agglomeration (**Figure 16**).²¹⁵ Typically, polymers such as polyvinylpyrrolidone (PVP), polyvinyl alcohol (PVA), and poly(N-isopropylacrilamide) are among the most used stabilizers.²¹⁵

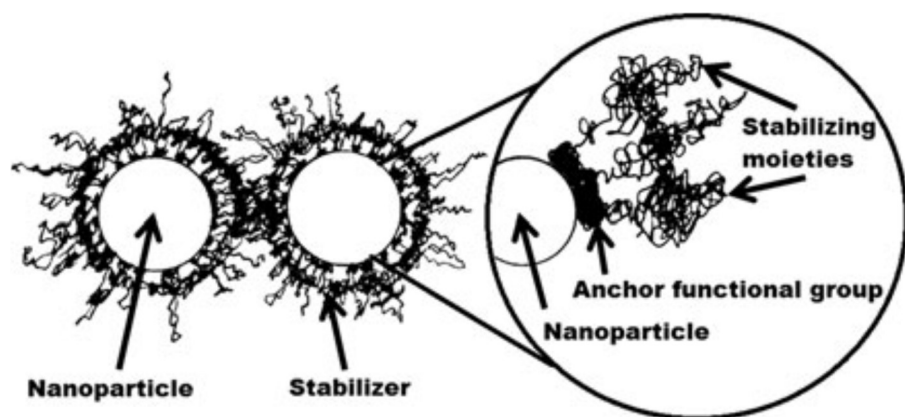


Figure 16. Steric stabilization scheme (in the enlarged part, a small polar portion of the stabilizing macromolecule anchors the surface of the NP). This figure was reproduced from ref. ²¹⁵.

As seen in the previous section, WPUU have internal emulsifiers in their structure, which are responsible for the dispersion stability in aqueous medium. In these particles, internal emulsifier, urethane, and urea groups face the aqueous medium, while the flexible segments, composed by more hydrophobic domains turn inwardly. As shown in **Figure 15**, WPUU particles are typical micellar structure in which the internal emulsifier, urethane and urea groups, which are hydrophilic, are oriented towards the aqueous medium. On the other hand, flexible polyether segments, which are hydrophobic, are turned inwardly towards the polymer nanoparticle core.¹⁹⁶ In principle, the WPUU conformation in aqueous dispersion can provide the basic characteristics of a stabilizing agent for Ag NP synthesis. Polar segments placed at the external surface of WPUU colloid particles can anchor the recently synthesized NP,

ensuring a nanoscale approximation without collision and agglomeration throughout their synthesis.^{185,215} Preliminary, the possibility of using WPUU dispersion eliminates the need of an additional stabilizing agent, affording an advantage to the synthesis of Ag NP in WPUU dispersion.

During the synthesis, the metallic NP formation has two steps: nucleation and growth. In the nucleation stage, the metal cation undergoes reduction and the recently formed metal atom moves randomly until collides with other atoms and cations forming a cluster. The nucleus will be formed as cations, atoms and clusters collide. The nucleus that exceeds the activation energy (the maximum free energy ΔG^*) should have a critical radius size r^* (**Figure 17**).²¹⁸ Nuclei larger than critical size decrease their free energy and the process of NP growth becomes spontaneous. Nuclei smaller than the critical size are dissolved. After the nuclei formation, they can grow into NP via molecular addition or Ostwald ripening. Molecular addition consists in addition of metal atoms on the surface of the nucleus. The addition is extremely dependent on the nucleation rate. High nucleation rates result in many nuclei that tend to grow independently, providing small NP with better size distribution and more uniform shape. On the other hand, Ostwald ripening takes place by collision and agglomeration between NP with the following dynamic: larger NP become larger and smaller NP become smaller until their dissolution.²¹⁵

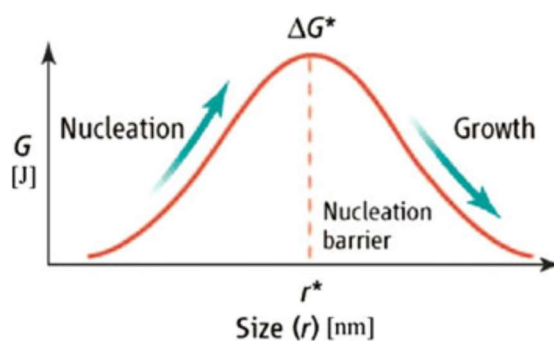


Figure 17. Illustration of overall free energy change ΔG as function of the growth particle size r . This figure was reproduced from ref. ^{215,218}.

Comparatively, Ostwald ripening velocity is greater than molecular addition velocity; thus, it is much easier to synthesize large NP than smaller ones. Apparently, a high nucleation rate is essential to achieve smaller NP and it depends on the power of reducing agent, but this cannot be generalized because each reaction has its own growth dynamics. The influence of temperature on the growth process of NP depends on the reaction system employed, and it is not possible to obtain a clear trend of its influence.²¹⁵

The Ag NP synthesis using WPUU dispersion as a stabilizing agent leads to perform the reaction in aqueous medium. This kind of synthesis is also known as *in situ* synthesis. Many applications require that NP should be dispersed in aqueous media and remain suspended with same chemical or physical properties over an extended period. The NP synthesis in aqueous medium has some difficulties that arise from the intense ionic interactions aggravated by increasing the ionic strength in the medium. These challenges are solved by using low reagent concentrations during the preparation of NP (*ca.* $5 \cdot 10^{-4} \text{M}$). To increase the concentration, stabilizing agents are sometimes used, but with further difficult to remove them at the end of the preparation when it is required.²¹⁹

In contrast to the synthesis in aqueous medium, NP synthesized in organic media can be prepared at higher concentrations (above 1 mol/L of reagents) with higher monodispersity, predefined shapes and sizes when compared to the preparation in aqueous medium. NP prepared in organic medium are insoluble in water; thus, many works have been tried to create NP transfer methods from organic medium to aqueous medium because of the synthesis difficulties in water.²¹⁹ Although there is the possibility of synthesis in aqueous medium, it consists a challenge to be overcome due to problems that may occur during the process of Ag NP synthesis in WPUU dispersion.

The properties of Ag NP for light olefins/paraffins separation by facilitated transport membrane are directly related to the control of the surface area that is a consequence of size control during the synthesis. In addition, NP must be properly dispersed in the polymer matrix with suitable concentration to allow the olefin molecule migration from one carrier to another, characterizing the facilitated transport. The challenges for the preparation of WPUU/Ag NP membranes start in the reactional system by the control of Ag NP dispersion and concentration in WPUU dispersion. Ensuring the stability of Ag NP in aqueous medium, avoiding aggregation and precipitation, is the initial problem.²²⁰⁻²²²

From the previous paragraphs is possible to conclude:

- (i) The $\text{AgNO}_3/\text{NaBH}_4$ reaction system is the simplest and most common; therefore, it is a reasonable option for Ag NP synthesis;
- (ii) Due to the surfactant characteristics, WPUU aqueous dispersion can be used as a stabilizing agent for Ag NP synthesis;
- (iii) NaBH_4 is a strong reducing agent²¹⁵ able to provide the necessary conditions for a higher nucleation rate (delaying Ostwald ripening), which favors the formation of small Ag NP with uniform size distribution;

- (iv) With a high nucleation rate, it is not necessary to raise the reaction temperature. The temperature and stirring of the reaction system should be lowest as possible to minimize Ostwald ripening. Stirring should be sufficient to homogenize the reaction medium and must be stopped when the last amount of AgNO₃ is added in the reactional system.

These points are important to avoid the the agglomeration of Ag NP.

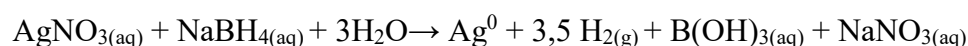
3.3. Experimental

3.3.1. Materials

Powder sodium borohydride and silver nitrate ($\geq 99.0\%$) were provide by Sigma-Aldrich. Block copolymer based on poly(ethylene glycol) and poly(propylene glycol) (EG-b-PG), number average molecular mass (\bar{M}_n) = 1850 g·mol⁻¹ and EG content of 7% in terms of molar mass, and poly (propylene glycol) (PPG), (\bar{M}_n = 1000 g·mol⁻¹) were kindly donated by Dow Brazil and data were reported by the manufacturer. Dimethylolpropionic acid (DMPA) purchased from Sigma-Aldrich; ethylenediamine (EDA, 99%) was provided by Acros Organics; isophorone diisocyanate (IPDI) was gently donated by Centro Técnico Aeroespacial (CTA); and triethylamine (TEA) purchased from Vetec.

3.3.2. Preparation of WPUU/Ag NP composites

The Ag NP synthesis proposed in this work follows the reaction:²¹⁵



In the reaction, the molar ratio of Ag:BH₄⁻ is 1:1. Usually, excess of reducing agent is used to ensure that all Ag⁺ is reduced to Ag⁰, in addition, the BH₄⁻ excess is responsible for stabilizing Ag NP in aqueous medium²²³. In the Ag NP synthesis of this thesis, it was not used a BH₄⁻ excess, since there was an expectation for the stabilization of Ag NP by the WPUU aqueous dispersion.

All WPUU aqueous dispersion used in this Thesis were prepared previously in the Laboratory of Sustainable Polymeric Materials from Rio de Janeiro State University under supervision of Professor Marcia Cerqueira Delpech. The PUU NCO-terminated (terminated

with isocyanate group) prepolymer was synthesized by reacting EG-b-PG, PPG, DMPA, and IPDI (NCO/OH equivalents-gram proportion of 1.5) at 95 °C during 30 min. The equivalents-gram proportion between the polyols (EG-b-PG, PPG, and DMPA) in the synthesis was 3:1:4. The carboxylic groups of DMPA were neutralized using TEA. The NCO-terminated prepolymer was dispersed in deionized water and then submitted to the chain extension reaction with EDA at 30°C, as reported in previous works.^{80,183,196,198} WPUU dispersion with a solid content around 30% was prepared. Two different WPUU batches were produced, batch A and B. The batch will be indicated when final results of the analyses performed are influenced by batch type. Other formulation was synthesized by using the same methodology and reagents except by a different NCO/OH ratio of 2. The code for this formulation is WPUU(2). WPUU(2) was not characterized like WPUU, however this material will be used for some permeation tests in the next chapter.

Ag NP were prepared by the reduction *in situ* of Ag⁺ using NaBH₄. The molar ratio of Ag:BH₄⁻ was 1:1. Fifteen milliliters of WPUU (approximately 15 g) were added to 15 mL of deionized water, and then NaBH_{4(s)} was added under mechanical stirring at 500 rpm. After the solubilization of the reducing agent, 20 mL of AgNO₃ solution were added with a flow rate of *ca.* 0.01 mL·s⁻¹, under stirring at 500 rpm - 2000 rpm. Reactional system was at 10 °C during all procedures.^{211,223-226} **Figure 18** shows the experimental apparatus used for synthesizing the Ag NP/WPUU dispersions.

At the end of the reaction, Ag NP/WPUU dispersions were cast onto Teflon plates and dried in a vacuum oven at 40 °C for one week. After drying process, the membranes were removed from the plates for characterization. By using this methodology, the following membranes were prepared: 1 wt% (1% Ag NP), 2.5 wt% (2.5% Ag NP), 5 wt% (5% Ag NP), and 10 wt% (10% Ag NP). The percentages are relative to the amount of silver in the final dried composite material.



Figure 18. Experimental apparatus for the synthesis of Ag NP in WPUU aqueous dispersion:

1 – mechanical stirrer (anchor blade); 2 – thermostatic bath; 3 – peristaltic pump; 4 – glass jacketed reaction; and 5 – AgNO_3 solution.

To the preparation of material with higher Ag NP content, a modification of the procedure described above was adopted. At the synthesis end, a precipitate was formed, and it was separated from the dispersion by filtration. The precipitate was introduced into a test tube containing water. After manual stirring, the tube was centrifuged (3000 rpm for 10 min). The precipitate at the tube bottom was separated from the supernatant. This procedure was performed 3 times. After the washing steps, the precipitate was solubilized in ethanol at 75°C for 15 min. After solubilization, the alcoholic solutions of Ag NP/WPUU were cast onto Teflon plates and dried in a vacuum oven at 35°C for 24 h. Membranes with 30 wt% (30% Ag NP^{*}) and 50 wt% (50% Ag NP^{*}) were prepared by this methodology. For evaluation, the precipitate formed during the synthesis of 30% Ag NP^{*} membrane was also investigated. The code for this material is 30% Ag NP_{ppt}.

3.3.3. Characterizations

The FTIR analysis were performed on a Perkin Elmer (Spectrum One) FT-IR spectrometer equipped with an attenuated total reflection (ATR) accessory, with a flat ZnSe plate, and dried films were collected at an angle of 42° . The measurements were obtained at 4 cm^{-1} of spectral resolution, 50 scans per spectrum and performed in triplicates for each film. The spectrum of the crystal was used as background.

WPUU/Ag NP composites were characterized using transmission electron microscopy

(TEM) (JEM 2100, JEOL), operating at 80 kV. The SAXS data were collected at the wavelength $\lambda = 1.49 \text{ \AA}$ using a MAR CCD 165 detector on the SAXS-2 beamline of the Brazilian National Synchrotron Light Laboratory (LNLS/Brazil) over a range of $0.007 < q < 0.2 \text{ \AA}^{-1}$ ($q = 4\pi \sin \theta / \lambda$, where 2θ is the scattering angle). The scattering patterns were measured at 25 °C for samples. The obtained scattering patterns were measured at 25 °C for samples and corrected for the instrument background, before being used for further analysis.

X-ray diffraction (XRD) measurements of the films were performed using a Rigaku Miniflex II diffractometer with Cu-K α radiation ($\lambda = 1.5405 \text{ \AA}$). XRD data were collected in a conventional Bragg–Brentano $\theta/2\theta$ geometry using a continuous scan ranging between $5^\circ < 2\theta < 60^\circ$ and step size of 0.05° .

Thermogravimetric analysis (TGA) measurements were carried out in N₂ flow ($20 \text{ mL} \cdot \text{min}^{-1}$) for all the samples using a Dp Union SDT Q 600 TGA with a temperature scan rate of $20 \text{ }^\circ\text{C} \cdot \text{min}^{-1}$. WPUU/Ag NP films with mass ranging from 8 to 15 mg were placed in alumina crucibles and heated from 25 to 600 °C. During the heating period, the weight loss and temperature difference were recorded as a function of temperature. The films onset degradation temperature (T_{onset}) was defined by the intersection of a line tangent to the baseline with a line tangent to the inflection point of the differential weight loss (DTG) curves, as recommended by ASTM E2550-07 standard.²²⁷ The thermal analyses were made in triplicates for each film.

3.4. Results

3.4.1. Transmission electron microscopy (TEM) and Small Angle X-ray Scattering (SAXS)

TEM images of the 1% Ag NP and 5% Ag NP membranes shows a suitable dispersion and diameters between 10 and 20 nm for the NP (**Figure 19**). The SAXS data for WPUU, 1% Ag NP, 2.5% Ag NP, and 5% Ag NP membranes are shown in **Figure 20**. The fittings using the Beaucage unified model are in the **Figure 21**, it was considered NP with spherical shape and smooth surface. The SAXS results are summarized in **Table 12**. It was found Ag NP diameters ranged from 3 to 7 nm with low polydispersity. In neat WPUU membrane, the mean distance between the rigid domains of the polymer was 6 nm. Probably, these rigid domains are clustered into structures with a fractal surface morphology because the slope of the **log I(q) vs. log q** curve model is -3 in the second hierarchical level indicating a fractal surface.^{177,180}

Analyzing the TEM and SAXS data, it can be concluded that the synthesized Ag NP are smaller than 10 nm. The black spots in TEM images possibly shows a nanoagglomerates of Ag NP that justifies larger diameters found by TEM compared to SAXS analysis.

It was achieved a suitable Ag NP dispersion in the WPUU matrix, since there was no formation of microclusters (larger than 100 nm). From the TEM images it is possible to observe a Ag NP homogeneous distribution in Ag NP/WPUU membranes. Additionally, a low polydispersity related to Ag NP diameters was found in the material showing that the synthesis was able to provide Ag NP with uniform size. The adequate Ag NP dispersion in the membranes can be attributed to the stabilizer feature of WPUU aqueous dispersion that avoided the formation of large size agglomerates.

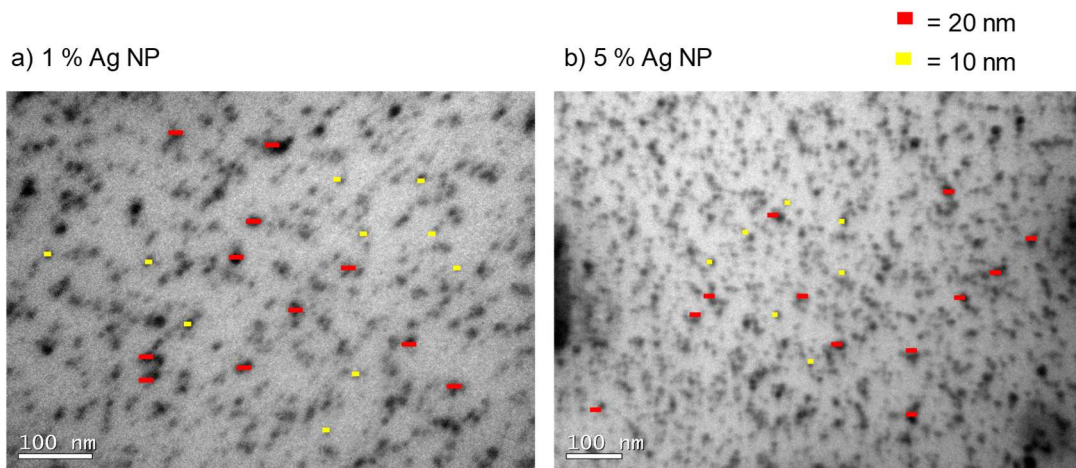


Figure 19. TEM images of WPUU/Ag NP membranes: a) 1% Ag NP; b) 5% Ag NP.

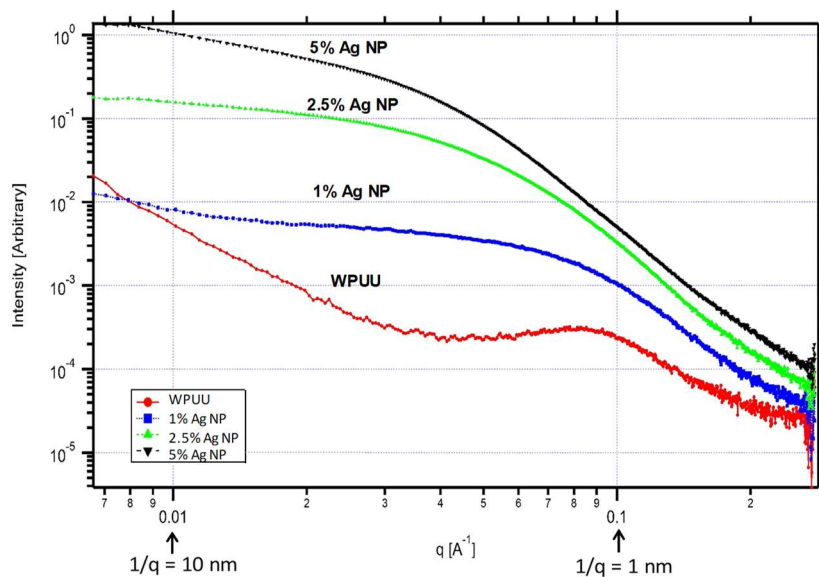


Figure 20. SAXS data of WPUU/Ag NP membranes.

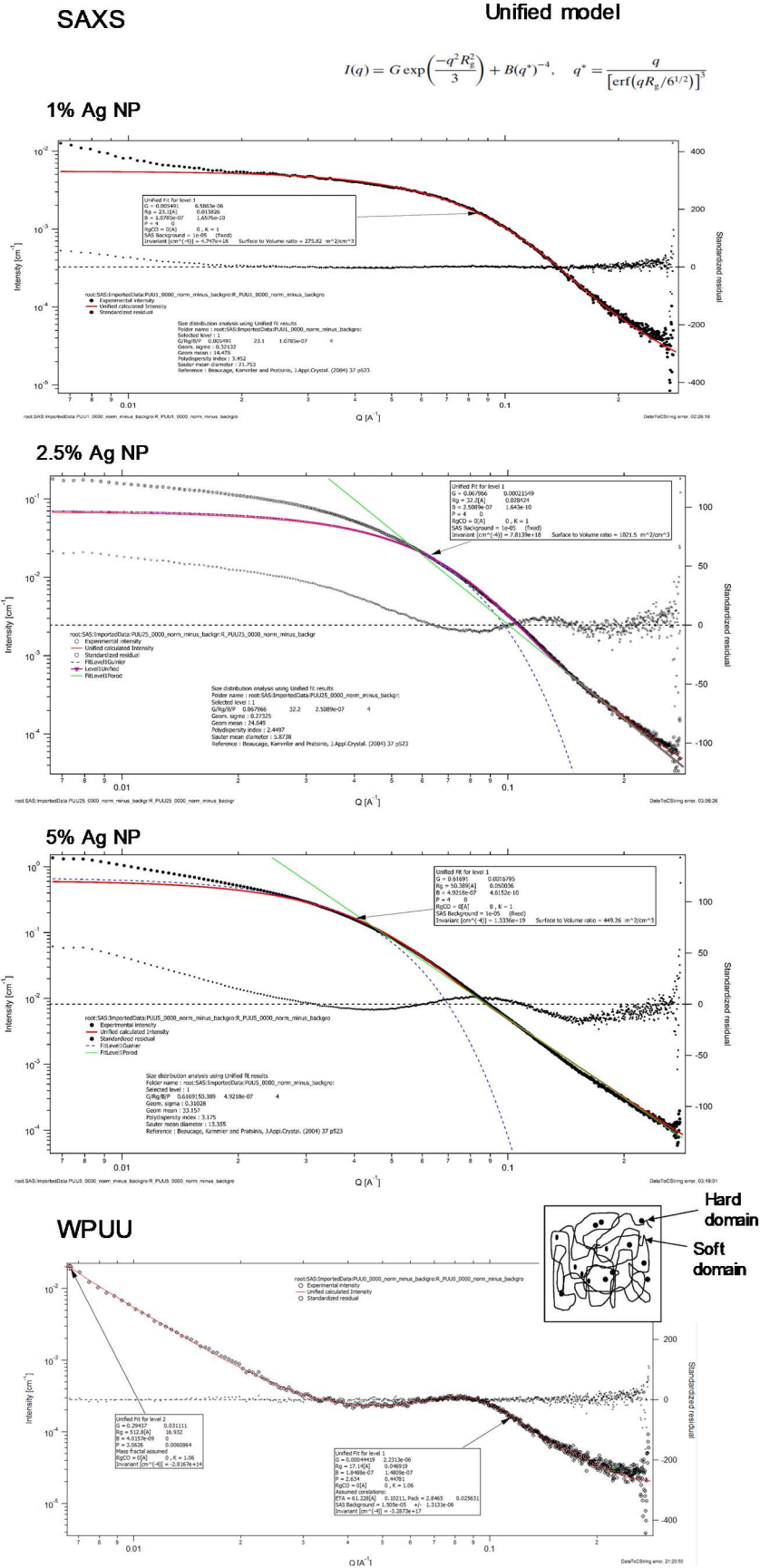


Table 12. SAXS results for the WPUU/Ag NP membranes.

Membrane	R_g (Å)	Diameter (nm)	Polydispersity index	k	d (nm)
1% Ag NP	23.1	3	3.4	—	—
2.5% Ag NP	32.2	5	2.4	—	—
5% Ag NP	50.4	7	3.2	—	—
WPUU	17.4	—	—	2.8	6.1

P is fixed at -4 for the Ag NP membranes.

3.4.2. X-ray diffraction (XRD)

The diffractograms of WPUU, 1% Ag NP, 10% Ag NP, 30% Ag NP_{ppt}, 30% Ag NP*, and 50% Ag NP* are shown in **Figure 22**. Ag NP have diffraction peaks at $2\theta = 38^\circ$ and 44° related to the (1 1 1) and (2 2 0) metallic silver crystal planes (JCPDS file no. 04-0783), which corresponds to a face-centered cubic structure.¹⁸² The same diffraction pattern appeared in 10% Ag NP, 30% Ag NP_{ppt}, 30% Ag NP*, and 50% Ag NP* and membranes, indicating the metallic nature of the Ag NP embedded in the polymer matrix. In the 10% Ag NP and 30% Ag NP_{ppt} materials, NaNO₃ diffraction peaks, resulting from the Ag NP synthesis, were also found.²²⁸ The mean size of Ag NP was estimated by using the Scherrer's equation (17) applied to the data of peak associated to the (1 1 1) plane.^{229,230} The geometric factor used for the calculus was 0.9. The mean size determined was 8.7; 15.6, 15.6 and 18.8 nm for the 10% Ag NP, 30% Ag NP_{ppt}, 30% Ag NP*, and 50% Ag NP*, respectively.

By increasing the silver content in the membrane, the Ag NP size got larger, but even at nanometric scale. In the diffractogram of the 30% Ag NP* and 50% Ag NP* membranes, NaNO₃ peaks were practically absent, showing that salt removal by washing procedure was successful. Moreover, the washing step and the solubilization in ethanol did not alter the size of the synthesized Ag NP, since the Ag NP in the 30% Ag NP_{ppt} and 30% Ag NP* had the same size. No silver peaks in the 1% Ag NP membrane are observed because of the lower amount of silver, which is not detected by the XRD analysis. The broad halo centered at $2\theta = 20^\circ$, which is mainly related to the amorphous structures of PPG in WPUU soft domains,²³¹ did not have significant changes.

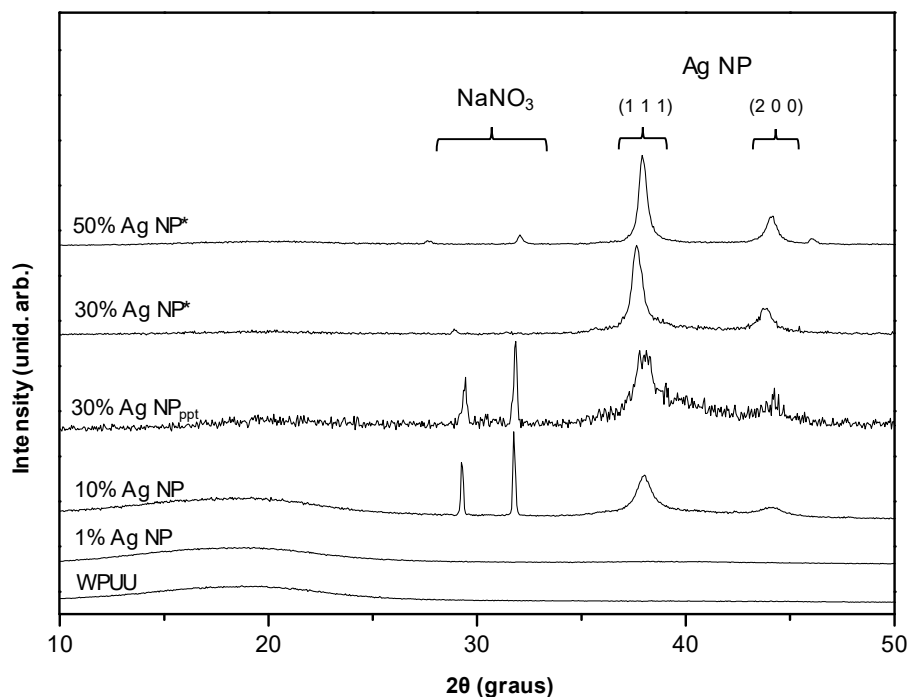


Figure 22. XRD patterns of Ag NP and WPUU/Ag NP membranes.

3.4.3. Infrared Spectroscopy (FTIR)

FTIR analysis is an essential tool to evaluate the changes in proton donor and proton acceptor groups of WPUU.^{73,183} From the neat WPUU up to the membrane with 5 wt% of silver content, there were no significant changes in the FTIR profile. **Figure 23** shows the FTIR spectra of the WPUU and 10% Ag NP membranes, depicting the most significant changes in the main vibrational modes of -NH , C=O (urethane and urea), and ether (C-O-C) bonds. No FTIR spectrum shows any shoulder or split in C=O bands suggesting not only the absence of free carbonyl urethane (absorption at $1740\text{-}1716\text{ cm}^{-1}$) and urea groups ($1680\text{-}1695\text{ cm}^{-1}$ region), but also the absence of disordered urea hydrogen-bonded carbonyl group that absorbs at $1652\text{-}1679\text{ cm}^{-1}$ region. Noteworthy is that the presence of these groups should not be discarded due to the large profile of the bands in the region between 1600 and 1750 cm^{-1} , which could include a fraction of these species. In the carbonyl region (C=O) (**Figure 23b**), the frequency of urethane carbonyl decreases ($\Delta = -7\text{ cm}^{-1}$), reflecting a hydrogen bonding rearrangement inside the polymer matrix, mainly in the interphase region, since the urea C=O band keeps the same frequency. The shifts to lower frequency indicate an intensification of hydrogen bonds related to urethane carbonyl groups. In the amide II region, the frequency shift

indicates an alteration of intermolecular hydrogen bonds and polymeric chain conformation.¹⁸³

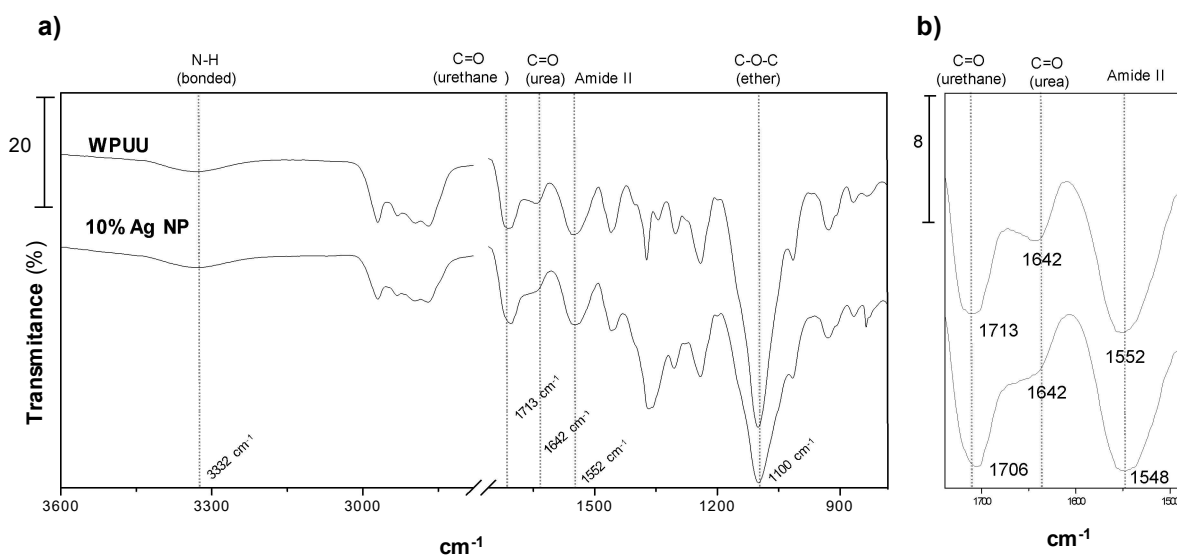


Figure 23. Comparison between FTIR spectra of the WPUU and Ag NP 10%.

In the 50% Ag NP* membrane, there were no expressive shifts in the C=O (urethane and urea) bands. However, ether and –NH regions underwent some changes. In the ether region of FTIR spectra (**Figure 24c**), the former ether band was shifted to lower frequencies ($\Delta = -8 \text{ cm}^{-1}$) indicating that ether groups interacted more intense with another site inside the material, probably with the Ag NP surface or proton donor groups (N–H).^{89,118} The N–H groups also seem to feel the Ag NP presence. To investigate this aspect, the area ratios (between baseline and the band) of absorption FTIR bands of N–H region was calculated (**Figure 24b** and **Table 13**). The ratio is necessary to make a fair comparison among bands intensities of different samples. The extinction coefficients of all vibration bands compared were considered the same for the membranes. To calculate the areas, the fitting of Gaussian peaks was assume a constant base line between 3800 cm^{-1} and 3400 cm^{-1} (N–H region).²³² The number of bonded proton donors groups (bonded urethane and urea N–H)^{73,233} increased with the loading of Ag NP 50 wt%. Moreover, the bonded N–H band shifts to lower frequency indicating an intensification of hydrogen bonds related to N–H groups. As the carbonyl region was not changed markedly upon the silver addition, there is just one more option to a proton donate interact, probably the ether group, which is a proton acceptor. This kind of interaction, between ether groups and N–H, favors the miscibility among hard and soft domains of the WPUU, in a certain extend.¹⁸³ The amide II region also changed corroborating the alteration in intermolecular hydrogen

bonds(**Figure 24a**).¹⁸³ There are some differences in band frequencies between **Figure 23** and **Figure 24** because the FTIR analysis were carried out in different spectrophotometers.

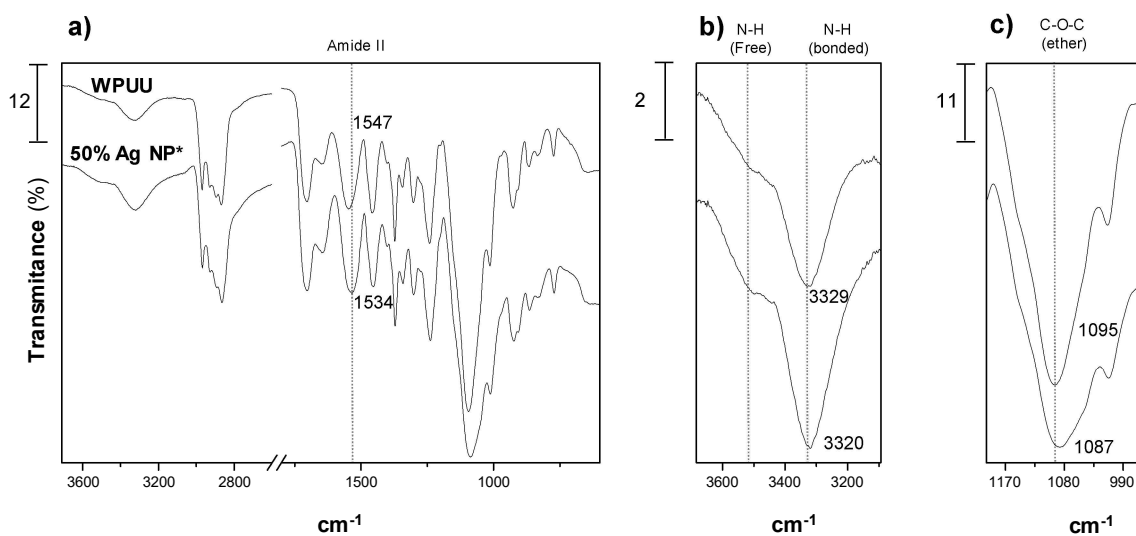


Figure 24. Comparison between FTIR spectra of the WPUU and 50% Ag NP*.

Table 13. Area ratios of the FTIR bands in N–H region of WPUU and 50% Ag NP* membranes.

Membrane	N-H bonded/free ^a
WPUU	4.0
50% Ag NP*	9.5

^a The free is centered at 3580 cm⁻¹ and bonded at 3330 cm⁻¹

Comparing 10% Ag NP and 50% Ag NP* membranes, it can be seen a carbonyl band shift in Ag NP 10% that does not take place in the 50% Ag NP*. This difference may be caused by the NaNO₃ present in the composite that can interact with the carbonyl groups of the material. This situation did not take place in 50% Ag NP* membrane because it passed by a washing procedure to remove the salt.

3.4.4. Thermal Stability

TGA data of the membranes are reported in **Table 14** and **Table 15** for batch A and B of WPUU, respectively. The introduction of Ag NP into the polymer matrix decreased the initial degradation temperatures (T_{onset}) as general trend. This modification is related to the high thermal conductivity of silver compared to traditional polymeric materials.^{234,235} Since silver

conducts more efficiently the heat inside the composite material, it anticipates the thermal decomposition process, reducing the T_{onset} as compared to neat WPUU.

Meanwhile, at the second thermal degradation stage, the temperature at maximum rate of weight loss (T_{vmax}), which is related to the soft domains decomposition,^{186,236} seems to not have a single behavior upon the addition of Ag NP into the WPUU matrix. Up to 5% Ag NP membrane, there were no significant changes, but in the 10% Ag NP material the T_{vmax} decreases and it has the tendency to increase in the free NaNO_3 membranes. This observation suggests that Ag NP and NaNO_3 were placed in the soft chains of the polymer interfering in the degradation of this domain. By removing the NaNO_3 from the membranes using the washing procedure, there is a trend to increase the T_{vmax} upon the addition of Ag NP. This behavior is related to interaction among Ag NP and the WPUU ether groups that favors the increasing of T_{vmax} .^{235,237} The FTIR results confirm this kind of interaction showing a shift band in ether region for the 50% Ag NP* membrane.

Table 14. Thermal degradation data of the WPUU/Ag NP membranes from batch A of WPUU.

Membrane	T_{onset} (°C)	T_{vmax} (°C)^a
(Batch A)		
WPUU	212(5)	386(1)
1% Ag NP	200(3)	384(3)
2.5% Ag NP	169(2)	386(1)
5% Ag NP	165(2)	385(2)

The number in parenthesis is the standard deviation;

a – T_{vmax} of the second degradation stage;

Table 15. Thermal degradation data of the WPUU/Ag NP membranes from batch B of WPUU.

Membrane	T_{onset} (°C)	T_{vmax} (°C)^a
(Batch B)		
WPUU	206(5)	373(1)
1% Ag NP	194(3)	370(3)
10% Ag NP	167(4)	361(3)
30% Ag NP _{ppt}	191(1)c	375(17)c
30% Ag NP*	179(1)c	386(15)c
50% Ag NP*	179(1)c	381(5)

The number in parenthesis is the standard deviation;
a – T_{vmax} of the second degradation stage;
b – duplicate

3.5. Conclusions

The method adopted for the synthesis *in situ* of Ag NP, using WPUU aqueous dispersion as stabilizing agent, was able to overcome the challenges to controll the suitable dispersion and low polydispersity of Ag NP in aqueous medium. The WPUU/Ag NP dispersions were employed to preparer WPUU/Ag NP membranes with silver content up to 50wt%. During the preparation of higher concentrated Ag NP membranes, it was necessary to remove NaNO₃, which is a synthesis residue.

TEM, SAXS and XRD results demonstrated that synthesized Ag NP were in nonometric scale, with less than 20 nm. For the 50% Ag NP* membrane, FTIR data showed an interaction among the Ag NP and WPUU ether groups, in addition, tendency of microphase miscibility among WPUU hard and soft domains was found. The Ag NP-ether interaction is also responsible for delaying the second thermal degradation stage of WPUU in free NaNO₃ composites; however, the Ag presence had an anticipative effect related to T_{onset} of the material.

By these results, the synthesis *in situ* of Ag NP in WPUU dispersion, without any additional stabilizing agent, was demonstrated as a proper procedure to the preparation of WPUU/Ag NP membranes with silver content up to 50wt%.

Chapter 4

4. OLEFIN/PARAFFIN GAS PERMEATION

Abstract

This chapter collects all gas permeation tests of the Thesis. The objective is to investigate the gas transport behavior through WPUU membranes with Ag NP/activator and AgBF₄/BMImBF₄ systems. Experimental procedures to the preparation of Ag NP/activator/WPUU and AgBF₄/BMImBF₄/WPUU membranes are introduced. The activators used were p-Bq and BMImBF₄. The facilitated transport of olefin was not achieved in Ag NP/activator/WPUU membranes, probably caused by the low electron acceptor feature of BMImBF₄ and by the poor stability of p-Bq. On the other hand, the facilitated transport of olefins was reached in AgBF₄/BMImBF₄/WPUU membranes. However, the membrane evidenced a humidification dependence to be stable in long-term permeation experiments.

4.1. Introduction.

Regarding membrane gas separation processes, olefin/paraffin gas separation is sometimes referred as the “holy grail” of membrane technology since ethylene and propylene are the most important building blocks for petrochemical industry.⁵³ The available commercial polymeric membranes using the solution–diffusion mechanism⁶⁹ do not achieve the desired performance for useful industrial operation. Much research is being undertaken aiming the production of appropriate materials for this kind of separation. The majority of studies investigate the facilitated transport membranes using carrier agents, which bind with olefins by the π -complexion reaction.^{40,76} Generally, transport membranes using silver (Ag) salts as carrier agents have been demonstrating better selectivity and permeability, when compared to passive transport membranes.⁶¹ Despite the superior separation properties of those systems, in general, some Ag salts carrier agents do not have enough stability to keep a long-term performance separation.⁵³ As an attempt to solve this problem, many authors have been pointing out to carrier agents based on Ag nanoparticles (NP), as promising chemical stable carriers for facilitated transport membranes.^{40,91,92,151,152,238} Ag NP can introduce resistance to the membrane against exposure to light and poisonous agents, as hydrogen and acetylene, resulting in desirable chemical stability, during the separation process.⁴⁷ The investigation of new membranes based on Ag NP with long-term resistant performance is the challenge for many authors.^{47,91,151,155}

Considering all suitable characteristics of Ag NP and WPUU (as described in **Chapter 1** and **Chapter 3**, respectively), a study investigating the transport properties of petrochemical gases through WPUU/Ag NP material is reasonable to be proposed. To act as carrier, Ag NP require a suitable activator agent to polarize its surface to form a partial charge, which is responsible by the interaction with olefins.^{92,148} The activator compounds for Ag NP are presented in **Table 8**. For the experiments in this Thesis, it was chosen p-benzoquinone (p-BQ) and 1-butyl-3-methylimidazolium tetrafluoroborate (BMImBF₄) due to the lower price of this activator agents comparing with other compounds. The concentration of Ag NP inside the polymer matrix should be higher than 30 wt% and NP should have diameters smaller than 30 nm to achieve the facilitated transport. (**Chapter 1**)

Other alternative that literature has shown as promising is the introduction of ionic liquids (IL) to stabilize Ag⁺ salts in facilitated transport membranes. Relate to this option, Ortiz *et al.*^{45,162} developed a material with promising characteristics for the separation of light olefins/paraffins. Composite films of poly (vinylidene fluoride-co-hexafluoropropylene) (PVDF-HFP)/BMImBF₄–AgBF₄ reached C₃H₆/C₃H₈ mixture selectivity of 700 and propylene

permeability of 6630 Barrer (*ca.* 55 GPU) in long-term permeation tests for 10 days. This remarkable performance motivated the use of this system (AgBF₄/BMImBF₄) in membrane of WPUU as attempt to overcome Ag⁺ cation deactivation.

Therefore, the general objective of this chapter is to investigate the behavior of Ag NP/activator and AgBF₄/BMImBF₄ systems applied in WPUU matrix. The specific goals of this part of Thesis are:

- (i) to perform permeation tests using WPUU/Ag NP membranes, which was analyzed in **Chapter 3**; moreover, to introduce BMImBF₄ and p-BQ as activator/polarizing agents;
- (ii) to prepare WPUU/AgBF₄ membranes and test them in gas permeation experiments;
- (iii) to check the influence of BMImBF₄ in the gas transport behavior of the WPUU/AgBF₄ membranes.

4.2. Experimental

4.2.1. Materials

The gases (C₂H₄, C₂H₆, and CO₂) (99.9%) were supplied by Linde do Brasil. Propylene and propane gas were purchased from Praxair with a minimum purity of 99.5%. Poly(urethane urea) used in this work was prepared as described in section 3.2.2. The ionic liquid (IL) BMImBF₄ (CAS number 174501-65-6) was provided by Iolitec, with a minimum purity of 99%. Silver tetrafluoroborate (CAS number 14104-20-2) of 99% purity was purchased from Apollo Scientific Ltd. Anhydrous ethanol (CAS number 64-17-5) and p-benzoquinone (p-Bq) (CAS number 106-51-4) were supplied by Sigma Aldrich. Microporous support of PVDF was purchased from Merk.

4.2.2. Membranes preparation

4.2.2.1. Membranes based on WPUU/Ag NP

Besides the membranes prepared as described in section 3.2.2., other membranes with IL or p-Bq were prepared by adding these compounds directly into alcoholic solution of WPUU/Ag NP under 5 min. of mild stirring. After, the mixture was casted onto a Teflon mold and placed inside a vacuum oven in order to form the nanocomposite membranes. For all mixture gas

experiments, the tests were performed placing the membranes onto a PVDF-HFP microporous support to avoid any damage to the film.

An additional WPUU formulation, WPUU(2), was used to prepare the membranes. WPUU(2) was synthesized by using a NCO/OH ratio of 2, while WPUU formulation has NCO/OH ratio of 1.5. The expectation is that WPUU(2) should be less elastomeric than WPUU due to the higher content of hard segments when compared to WPUU. The same procedure, used to prepare WPUU/50% Ag NP salt free membrane (**Chapter 3**), was performed to prepare WPUU(2)/50% Ag NP salt free membrane. All Ag NP/WPUU membranes prepared for gas permeation experiments are listed in **Table 16**. The codes for each membrane are expressed as weight ratio based on 0.750g of polymer.

Table 16. Ag NP/WPUU membranes prepared for gas permeation experiments.

Membrane (weight ratio based on 0.750g of WPUU)
1 WPUU
1 WPUU : 1 Ag NP (equivalent to 50% Ag NP)
1 WPUU : 0.28 Ag NP : 0.2 IL**
1 WPUU : 0.42 Ag NP : 0.25 IL**
1 WPUU(2)
1 WPUU(2) : 1 Ag NP
1 WPUU(2) : 1 Ag NP : 0.5 IL
1 WPUU(2) : 1 Ag NP : 1 IL
1 WPUU(2) : 1 Ag NP : 1 IL : 0.85 p-Bq ⁹²
*50% Ag NP: membrane prepared from alcoholic solution and salt free, see the preparation in chapter 3; **membrane prepared by adding WPUU alcoholic solution to dilute the original 1 WPUU : 1 Ag NP solution

4.2.2.2. Membranes based on WPUU/AgBF₄

During the synthesis of WPUU dispersions, dimethylolpropionic acid (DMPA) was neutralized by triethylamine (TEA) resulting in an aqueous media with pH = 9.5. High pH and amines are source of reduction for Ag⁺ cation; thus, a pretreatment should be carried out previously to the use of WPUU dispersion.

WPUU dispersion was neutralized by $\text{HCl}_{(\text{aq})}$ 37% w/w until complete precipitation of polymer. The neutralized polymer was washed several times with H_2O ($\text{pH} < 3$). The resultant material was solubilized in ethanol at 75°C . After solvent removal, the dried final material, free of TEA, was used to prepare the WPUU/ AgBF_4 membranes.

The membranes were prepared by the solubilization of 0.750 g of WPUU pretreated in ethanol. To alcoholic polymer solution was added AgBF_4 and BMImBF_4 . After, the mixture was casted onto a PVDF-HFP microporous support and placed inside a vacuum oven in order to form the composite membranes. Due to the poor mechanical stability of the material, it was necessary carried out the casting directly upon to PVDF-HFP microporous support. All AgBF_4 /WPUU membranes prepared for gas permeation experiments are listed in **Table 17**. The codes for each membrane are expressed as weight ratio based on 0.750g of polymer. The base for weight ratio used in this work was 1polymer: 1 AgBF_4 , the same as used in the work of Pinnau and Toy.¹¹⁸ The base for weight ratio of polymer and IL was in according with Fallanza *et al.*⁴⁵

Table 17. AgBF_4 /WPUU membranes prepared for gas permeation experiments.

Membrane (weight ratio based on 0.750g of WPUU)
1 WPUU
1 WPUU : 0.25 IL
1 WPUU : 1 AgBF_4
1 WPUU : 1 AgBF_4 : 0.25 IL
1 WPUU : 1 AgBF_4 : 0.50 IL
1 WPUU : 2 AgBF_4 : 0.50 IL

4.2.3. Gas permeation tests

4.2.3.1. Pure gas experiments

The gas transport properties were determined in an apparatus for gas permeation measurements by using a variable pressure and constant volume method,²³⁹ in which the permeate flux is measured by monitoring the pressure increase of collected permeate gas in a closed volume using a pressure transducer. The permeability of the gases was measured at 2 bar through the membrane, at $308 \pm 0.2 \text{ K}$. Permeabilities, **P** (in Barrer), was calculated from

the initial slope of the pressure curve on the permeation side vs. time, using the equation (18), where the dp^p/dt (cmHg·s⁻¹) is the rate of pressure measured by the pressure sensor in the low-pressure downstream chamber, V^p (cm³) is the downstream volume, T (K) is the temperature of the experiment, δ (cm) is the thickness of the film, A_m (cm²) is the film effective area of permeation and Δp (cmHg) is the pressure difference through the film. For the experiments, $V^p = 7$ cm³, $A_m = 4.9$ cm², and $\delta \approx 0.300$ cm or 300 μ m. To check the reliability, the measurements were made twice for each film, and the standard deviation between the replicates was less than 0.05.

$$P = \frac{273.15}{76} \frac{dp^p}{dt} \frac{V^p}{TA_m} \frac{\delta}{\Delta p} \quad (18)$$

4.2.3.2. Mixture gas experiments

The membranes prepared were placed into a permeation cell (46.5 cm²). The tests were performed inside an oven with temperature control (298 \pm 0.2 K). Gas flow rates were controlled by a mass flow controller. The feed stream (20 ml/min - mixed gas 50/50% v/v C₃H₈/C₃H₆) flows through the upper chamber, while the nitrogen used as sweep gas (20 ml/min) flows through the permeate side. The pressure was controlled using micrometric valves. The feed and the permeate stream were analyzed by gas chromatography. The analysis was performed in a gas chromatograph HP 6890 equipped with a thermal conductivity detector (TCD) and a column HP Al/S (30m length, nominal diameter of 0.53 mm).

The experimental permeabilities of each gas were calculated using the equation (3). At least two samples were collected to calculate the olefin or paraffin flux. The relative deviation of the gas composition analysis was *ca.* 5%. For some membranes, it was not possible to measure the thickness of the film; thus, the experiments results were reported in GPU (1 GPU=1 \times 10⁻⁶ cm³ (STP)/cm² s cmHg). All results reported in GPU were based on 0.750g of polymer. For all results reported in Barrer, the thickness of the membranes was *ca.* 100 μ m.

4.3. Results

4.3.1. Membranes based on WPUU/Ag NP

The permeability values of CO₂, C₂H₄, and C₂H₆ in WPUU/Ag NP membranes are presented in **Table 18**. CO₂ was used in these tests due to its high affinity to the WPUU matrix, providing valuable information related to property changes in polymer matrix. CO₂ and C₂H₄ can interact with ether groups present in soft domains of WPUU matrix. Thus, both gases have considerable solubility in WPUU. C₂H₆ does not share the same affinity by ether groups, making it less soluble in the material. WPUU used is elastomeric, consequently, sorption is the dominant step, which favors CO₂ and C₂H₄ transport in neat WPUU membrane.^{70,204} The FTIR analysis of this material (**Chapter 3**) did not show any significant change in ether region of spectra. Therefore, upon the addition of Ag NP, the WPUU membrane did not interact preferentially through ether groups. Since ether groups were not altered upon Ag NP addition, it is reasonable to discard expressive changes in the sorption behavior of the material. Thus, the main affect to be considered is the change in the diffusional pathway caused by tortuosity increase upon the Ag NP introduction. If this hypothesis is correct, the drop in the permeability should follow the molecular size of gases molecules, from large to small compound. This effect should be more evident in high Ag NP content; hence, it will be considered 30% Ag NP* membrane to analyze this behavior. The order of permeability drop is: C₂H₆ (68%) > C₂H₄ (64%) > CO₂ (48%) with similar C₂H₆ and C₂H₄ drop. The size order of molecules is: C₂H₆>C₂H₄>CO₂ with very close C₂H₆ and C₂H₄ sizes.²⁴⁰ By this comparison, it is clear that the same trend was found, confirming the change in the diffusional pathway caused by Ag NP. Additionally, the gas transport results for membranes up to 30 wt% of Ag NP content did not show any facilitated transport of olefins as depicted by $\alpha^{**}(\text{C}_2\text{H}_4/\text{C}_2\text{H}_6)$ nearly to 1.

For membranes with 50 wt% of Ag NP content, permeation test was performed using propylene/propane gas mixture (50:50 vol%) (**Table 19**). Even with 50wt% of Ag NP (weigh ratio 1 WPUU: 1 Ag NP) in the membrane, it was not possible to observe the facilitated transport of olefin in both membranes, 50% Ag NP WPUU and WPUU(2) free salt. In 1 WPUU: 1 Ag NP membrane, the FTIR analysis showed an Ag NP/ether group interaction (**Chapter 3**); however, this interaction was not enough to activated Ag NP to the facilitated transport.

Therefore, an external activated agent is required.⁴⁰ For this purpose, an ionic liquid (IL) , BMImBF₄,^{45,238} and p-benzoquinone (p-Bq)⁹² was selected to be introduced in WPUU/Ag NP membranes. IL improved discreetly the selectivity (the highest selectivity founded was 2.37 for

1 WPUU(2) : 1 Ag NP : 1 IL) of the membranes due to its affinity by olefin (**Table 19**). However, Ag NP activation by IL was not detectable in the test. The olefin flux did not increase as expected. The membrane with p-Bq achieved the best selectivity (2.92) among WPUU/Ag NP membranes. Nonetheless, the presence of this activator was not enough to provide the facilitated transport of olefin through the membrane. One hypothesis to the failure of p-Bq use as activator is the poor stability of this electron acceptor that can be reduced easily to hydroquinone. The reduced form of p-Bq is not active to polarize the surface of Ag NP demonstrating a real drawback to the application of this activator in WPUU/Ag NP membranes. Compounds like p-BQ, TCNQ and tetrathiafulvalene (TTF) work as electron acceptor; thus, they have a tendency of withdrawing electrons from other molecules. This feature makes polarizing agents susceptible to chemical attack similarly as it is found in Ag⁺ cation that results in reduced species unable to polarize the surface of Ag NP.

Table 18. Permeability of CO₂, C₂H₆ and C₂H₄ in WPUU/Ag NP membranes.

Membrane	Permeability (Barrer)			$\alpha^{**}(\text{C}_2\text{H}_4/\text{C}_2\text{H}_6)$	Permeability drop related to neat WPUU		
	CO ₂	C ₂ H ₆	C ₂ H ₄		CO ₂	C ₂ H ₆	C ₂ H ₄
WPUU	296	109	132	1.21	—	—	—
1% Ag NP	256	105	129	1.23	14%	4%	2%
10% Ag NP	219	82	98	1.20	26%	25%	26%
30% Ag NP*	154	35	47	1.30	48%	68%	64%

*30% Ag NP: membrane prepared from alcoholic solution, see the preparation in chapter 3; **Ideal selectivity.

Table 19. Permeability of C₃H₈ and C₃H₆ in WPUU/Ag NP membranes.

Membrane (weight ratio based on 0.750g of WPUU)	Permeability		$\alpha^a(\text{C}_3\text{H}_6/\text{C}_3\text{H}_8)$
	C ₃ H ₈	C ₃ H ₆	
1 WPUU	140	245	1.75
1 WPUU : 1 Ag NP (50% Ag NP [*])	—	—	1.73
1 WPUU : 0.28 Ag NP : 0.2 IL ^{**}	65.1	120	1.84
1 WPUU : 0.42 Ag NP : 0.25 IL ^{**}	62.6	140	2.00
1 WPUU(2)	92.1	171	1.84
1 WPUU(2) : 1 Ag NP	78.5	143	1.79
1 WPUU(2) : 1 Ag NP : 0.5 IL	67.7	144	2.12
1 WPUU(2) : 1 Ag NP : 1 IL	56.9	145	2.37
1 WPUU(2) : 1 Ag NP : 1 IL : 0.85 p-Bq	0.239 ^b	0.700 ^b	2.92

Condition: 0.2 bar transmembrane pressure. WPUU: NCO/OH ratio of 1.5. WPUU(2): NCO/OH ratio of 2.

^{*}50% Ag NP: membrane prepared from alcoholic solution and salt free, see the preparation in chapter 3; ^{**} membrane prepared by adding WPUU alcoholic solution to dilute the original 1 WPUU : 1 Ag NP solution.

a - mixed gas (50:50 vol % of propylene/propane mixture); b – permeance, long-term test of 104 h.

4.3.2. Membranes based on WPUU/AgBF₄

FTIR analysis is an essential tool to evaluate the changes in proton donator and proton acceptor groups of WPUU.^{73,183} The goals of this section is to evaluate the possible interactions of AgBF₄ and BMImBF₄ inside the polymer matrix and how these interactions affects the structure of the WPUU.

4.3.2.1. Infrared Spectroscopy (FTIR)

The FTIR spectra of AgBF₄ and H₂O are depicted in **Figure 25**. Due to the hygroscopicity,¹⁴⁰ H₂O bands (ν O-H and δ O-H) appear in the AgBF₄ spectrum. Moisture bands are also present in membrane FTIR spectra when a high content of AgBF₄ is used in analyzed films.

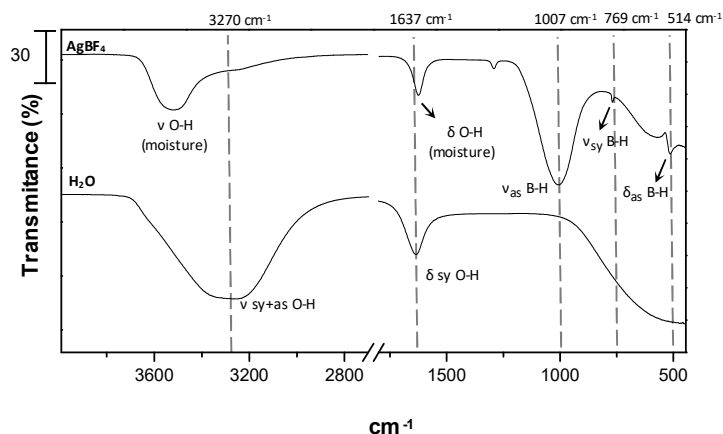


Figure 25. FTIR spectra of AgBF_4 and H_2O .^{241–243}

Figure 26a shows the FTIR profile of the films prepared with different contents of AgBF_4 . As AgBF_4 was added in WPUU matrix, the ether band shifted from 1095 cm^{-1} (neat polymer) to 1047 cm^{-1} in the film with weight ratio of 1 WPUU:1 AgBF_4 . This frequency decrease indicates an intensification of interaction among ether groups and the Ag^+ cations (**Figure 26d**).^{117,118,120} The ether/ Ag^+ interaction leads to a weakening of the former ether/N-H interaction that is depicted by the frequency increase of N-H bonded band from 3332 cm^{-1} to 3396 cm^{-1} (**Figure 26b**). Mainly in 1 WPUU:1 AgBF_4 film, Ag^+ cation also interacted with urethane C=O, which is at the interface between the hard and soft phase of WPUU. Urethane C=O band frequency decreased from 1712 cm^{-1} to 1677 cm^{-1} (**Figure 26c**), indicating an interaction intensification related to these groups. On the other hand, the urea C=O band frequency seems to increase from 1641 cm^{-1} to higher values (**Figure 26c**) (it was not possible to check it in 1 WPUU:1 AgBF_4 film due to moisture interference) that can be interpreted as a weakening of interactions among urea and urethane C=O since urea groups are inner inside WPUU hard domains. Presumably, Ag^+ cation did not reach the hard domain cores. The interaction weakening of urea groups was related to unavailability of urethane N-H groups that suffered Ag^+ /urethane interference at the interfacial region.

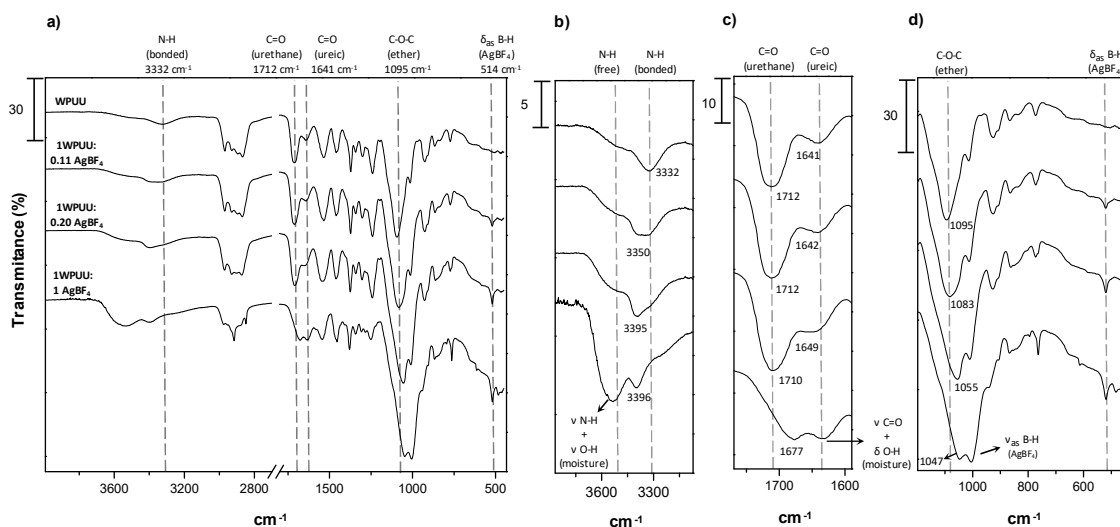


Figure 26. FTIR spectra of WPUU/AgBF₄ films.

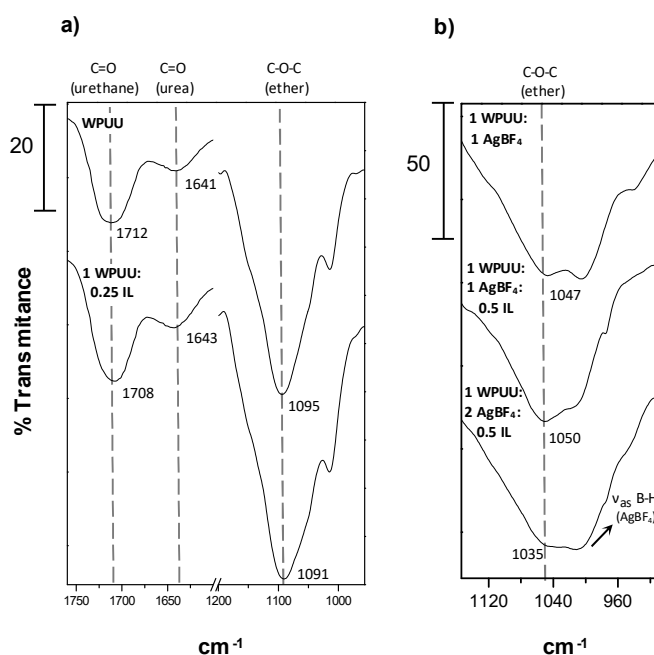


Figure 27. FTIR spectra of WPUU/IL and WPUU/AgBF₄/IL films.

The introduction of IL in the WPUU matrix seems to follow the same interaction behavior like in AgBF₄ case; however, less intense. In the film with weight ratio of 1 WPUU: 0.25 IL, the ether band and urethane C=O band frequencies decreased from 1095 cm⁻¹ to 1091 cm⁻¹ and from 1712 cm⁻¹ to 1708 cm⁻¹, respectively. Additionally, the urea C=O band frequency increased from 1640 cm⁻¹ to 1643 cm⁻¹ (**Figure 27a**). These FTIR results suggest an IL cations (imidazolium) interaction with ether and urethane group to some extent.

The influence of IL upon the WPUU/AgBF₄ composite was also verified using FTIR. The main change was in the ether region. Compared to the 1 WPUU:1 AgBF₄ film, the material with weight ratio of 1 WPUU: 1 AgBF₄: 0.5 IL showed an ether band shift to high frequencies, from 1047 cm⁻¹ to 1050cm⁻¹ (**Figure 27b**). This frequency increase suggests a weakening of the interaction between the Ag⁺ cations and the ether groups caused by the addition of IL.⁵¹ However, the same IL behavior was not maintained when the AgBF₄ content was doubled. In 1 WPUU: 2 AgBF₄: 0.5 IL film, the Ag⁺/ether interaction was intensified due to the high AgBF₄ content. It can be checked by the large shift to lower frequencies in ether band, from 1050 cm⁻¹ to 1035 cm⁻¹ (**Figure 27b**).

Therefore, by observing the ether region of WPUU FTIR spectrum is possible to investigate the main interaction, Ag⁺/ether group, in the WPUU/AgBF₄ composites. Ag⁺/ether group interaction is the principal responsible for the dissolution of the AgBF₄ salt in the polymer matrix. This interaction may be smoothed by the addition of IL in the formulation of WPUU/AgBF₄ composite material.

4.3.2.2. Gas permeation

To find out the AgBF₄ concentration that could provide the facilitated transport in WPUU matrix, it was prepared some WPUU/AgBF₄ membranes with different silver salt contents. The initial membrane composition able to perform the facilitated transport of olefin was the weight ratio of 1WPUU:1 AgBF₄ based on 0.750g of polymer.¹¹⁸ During the permeation (**Figure 28**), olefin flux increased until 3.15h of experiment due to the growing number of olefin molecules that began to complex with Ag⁺ cation and hop from carrier to carrier in order to cross the membrane.¹¹⁷ Within the membrane, the Ag⁺ can interact with coordination site of the WPUU matrix (i.e. ether oxygen atoms) to form desirable free ions pairs, which is useful to the olefin complexation than the original crystal structure of salt.^{125,129-131} However, instead of reaching a stable value, establishing the steady facilitated transport flux, the olefin flux started to decrease. Apparently, the decrease is because the removal of residual solvent or moisture trapped inside the polymer matrix. One important moisture holding inside the membrane is the AgBF₄, which is a very hygroscopic salt.¹⁴⁰ The few residual liquids were dragged while the dried gas mixture crossed the membrane.

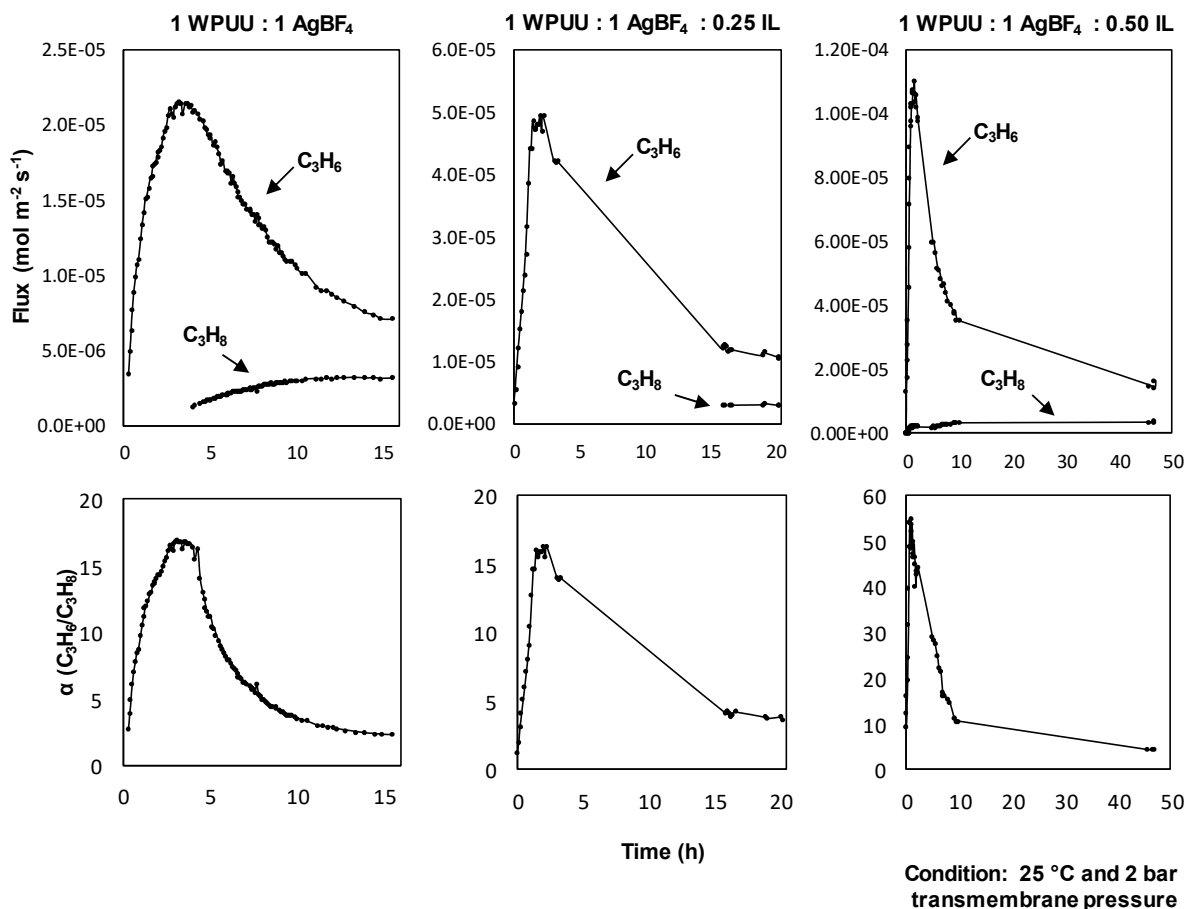


Figure 28. Flux of propylene, propane, and selectivity vs. permeation time for WPUU/AgBF₄ membranes.

Water can form Ag⁺ aquo complex that supports the salt dissolution.³⁹ In its solvated form, Ag⁺ cations are more available to the interaction with the olefin. The drying process leads to a loss of one of the dissolution sources remaining only the dissolution provided by the polar polymer chains. As the moisture was dragged from the membrane, the polymer dissolution did not show the ability to sustain the silver availability for the olefin reversible complexation. In this case, the WPUU interaction with the Ag⁺ cation makes it so attached to ether groups that the metal becomes less available for the olefin interaction, in a certain extent. Presumably, this is one of possible reasons for the decreasing of olefin flux during the permeation experiment.

Another cause could be the reduction of Ag⁺ by the polymer interaction, which can deactivate the Ag⁺ transforming it into Ag⁰. Roughly, the Ag⁰ formation can just be detected by simple inspection of the membrane at the end of permeation, since agglomerations of Ag⁰ is dark and the WPUU material is colorless. This verification was made, and no black spots were observed at the end of the 63 h of permeation. This does not mean that any Ag⁰ formation takes place, but it can be assumed that there was no evidence of a critical reduction process in the

membrane. Another evidence that corroborated to this assumption was the difference about flux behavior of both gases. Silver nanoparticles growth during the permeation process leads to the formation of interfacial void that become large. Through this voids, both gases can pass instinctively resulting in the increase of flux but in the decreasing of selectivity.¹³⁸

Initially, the silver reduction was discharged as hypothesis during the permeation experiment. Thus, to solve the unviability of the Ag^+ for the olefin complexation during the runs, ionic liquids were thought as an alternative to smooth the interaction between Ag^+ and WPUU ether groups. The ionic liquid (IL) chosen was the BMImBF₄ due to its known behavior in composite membrane of PVDF-HPF/AgBF₄ in the work of Ortiz *et al.*⁴⁵ Moreover, this IL adds a proper factor to the membrane. The system BMImBF₄/AgBF₄ can avoid the potential reduction of Ag^+ by the polymer chain interactions.^{131,156}

Figure 29 and **Table 20** show the effect of IL content in the olefin maximum flux (J_{max}) achieved. Compared to the membrane without IL, the olefin J_{max} increased 2.3 and 5.1 times in the membrane with weight ratio of 1 WPUU:1 AgBF₄:0.25 IL and 1 WPUU:1 AgBF₄:0.5 IL, respectively. In addition, membranes with a high IL content reach the J_{max} sooner. This J_{max} anticipation and the higher J_{max} values reached show the properly IL support to the olefin flux in the WPUU membranes. However, after membranes with IL reach the J_{max} , the olefin flux followed the same behavior of the membrane without IL. The olefin flux started to decrease, probably because the removal of residual solvent or moisture trapped inside the polymer or in the IL medium. At the end of permeation experiments, either the IL could not sustain the high values of olefin flux.

As an attempt to increase the olefin flux, a membrane with weight ratio of 1 WPUU:2 AgBF₄:0.5 IL was prepared. The membrane showed the same behavior of previous membranes. The initial olefin flux increased, afterward, it started to decrease during the permeation time (**Figure 30**). Compared to 1 WPUU:1 AgBF₄:0.5 IL membrane, this high content AgBF₄ film increased the olefin J_{max} 5.6 times. Moreover, the J_{max} was anticipated from 1.52 h to 0.42 h (**Figure 31**).

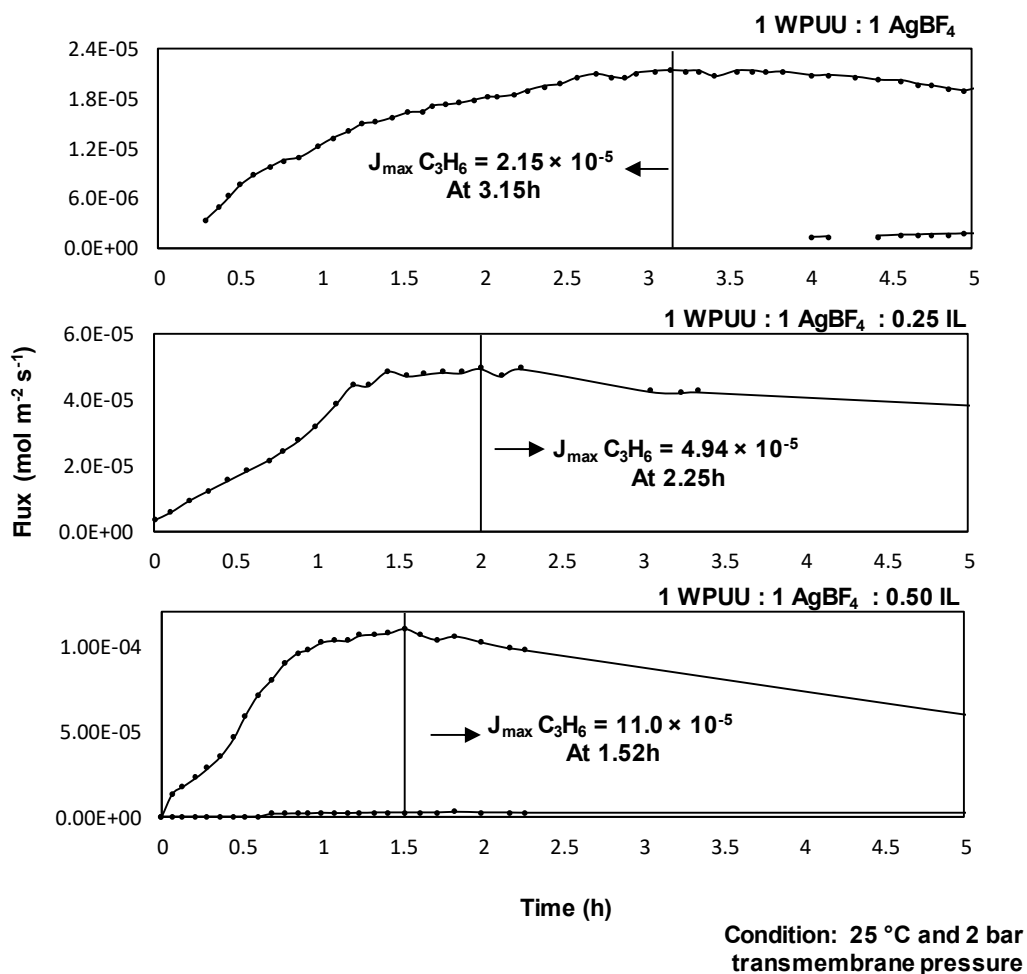


Figure 29. Flux of propylene and propane vs. permeation time for WPUU/AgBF₄ membranes in the initial time of the experiments.

Table 20. Results for the WPUU/AgBF₄ membranes.

Membrane (weight ratio based on 0.750g of WPUU)	$J_{\max} \text{C}_3\text{H}_6$ ($10^{-5} \text{ mol m}^{-2} \text{ s}^{-1}$)	α_{\max} ($\text{C}_3\text{H}_6/\text{C}_3\text{H}_8$)	Permeance (GPU)		Time of maximum values (h)
			C_3H_8	C_3H_6	
1 WPUU	5.15*	1.80	0.59	1.06	—
1 WPUU : 0.25 IL	4.35*	1.95	0.45	0.86	—
1 WPUU : 1 AgBF ₄	2.15	>16.8	0.02	0.44	3.15
1 WPUU : 1 AgBF ₄ : 0.25 IL	4.94	>16.2	0.06	1.01	2.25
1 WPUU : 1 AgBF ₄ : 0.50 IL	11.0	48.9	0.04	2,28	1.52
1 WPUU : 2 AgBF ₄ : 0.50 IL	61.6	97.5	0.15	13.94	0.42

Condition: 25 °C and 2 bar transmembrane pressure. *Stationary flux values.

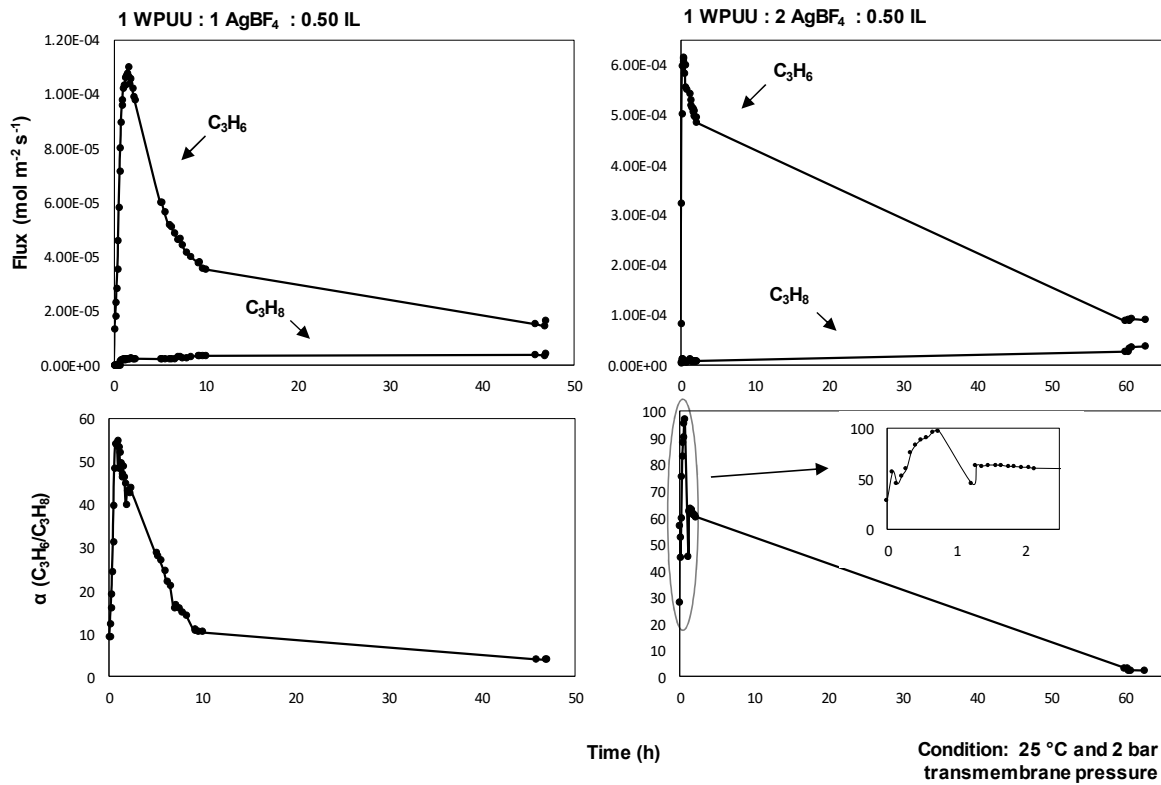


Figure 30. Flux of propylene, propane, and selectivity vs. permeation time for the membrane with high $AgBF_4$ content.

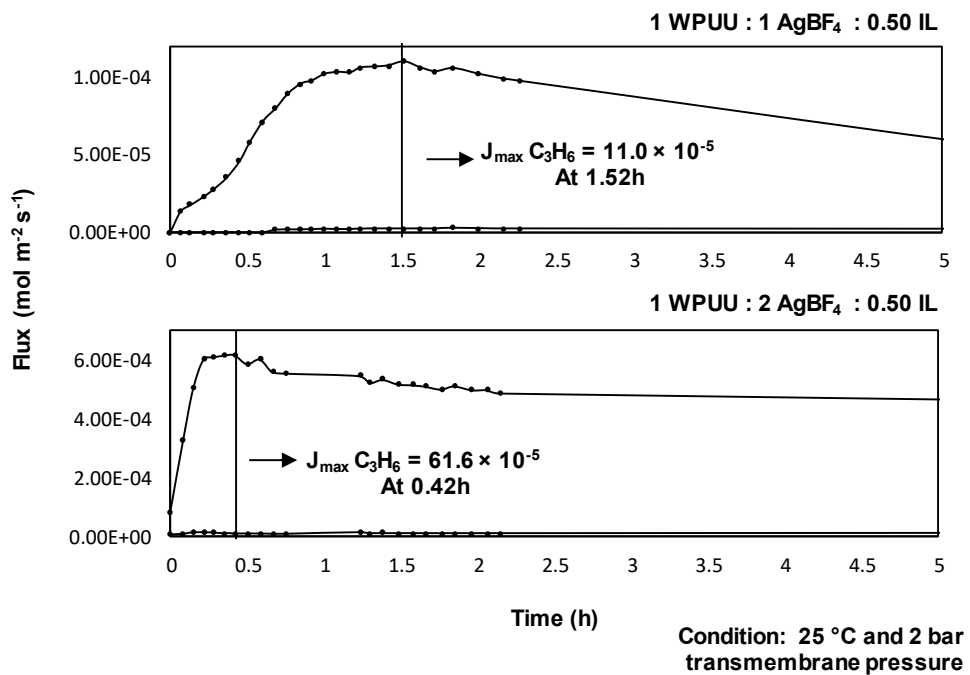


Figure 31. Flux of propylene, propane, and selectivity vs. permeation time for membrane with high $AgBF_4$ content in the initial time of the experiments.

To check the carrier properties of the membrane after the decline of olefin flux in the first hours of permeation, the permeation cell was opened (protected from light) and closed after 15 min. The permeation test was restarted to observe the olefin flux behavior (**Figure 32**). The membrane used for this test was with the weight ratio of 1WPUU : 1 AgBF₄ : 0.25 IL. Initially, the membrane achieved the olefin J_{\max} of $4.94 \cdot 10^{-5} \text{ mol m}^{-2} \text{ s}^{-1}$, afterward, the flux decline started until attain the olefin flux of $1.06 \cdot 10^{-5} \text{ mol m}^{-2} \text{ s}^{-1}$ at 20.3 h of experiment. At this point, the cell was opened and closed after 15 min. Olefin flux was recovery at $4.15 \cdot 10^{-5} \text{ mol m}^{-2} \text{ s}^{-1}$ (recovery of 84%), but, after 27.2 h the olefin flux attain the value of $1.01 \cdot 10^{-5} \text{ mol m}^{-2} \text{ s}^{-1}$. This result shows that the initial olefin flux decline in WPUU/AgBF₄/IL membranes is mainly caused by moisture loss during experiments with dried gases. The recovery of olefin flux took place when the membrane was in contact with atmospheric air during 15 min., which repairs the moisture level inside the membrane. However, when the dried gases started to cross the membrane, again, the moisture level decreases and the Ag⁺ cation becomes tightly attached to ether groups leading to metal unfeasibility for olefin interaction. If any critical Ag⁺ reduction problem related to Ag⁺/ether interaction takes place, probably, it should occur in larger long-term permeation tests.

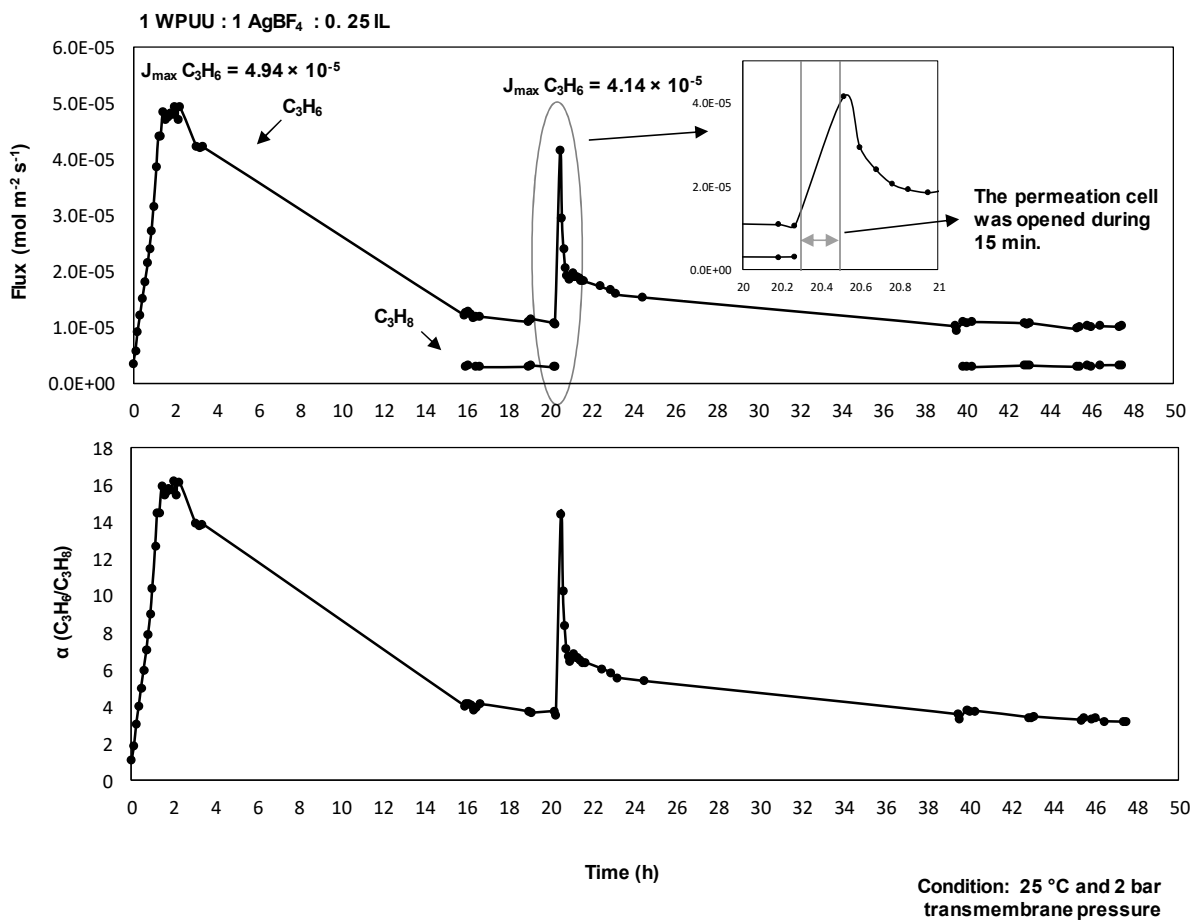


Figure 32. Flux of propylene and propane vs. permeation for 1 WPUU: 1 AgBF₄: 0.25 IL membrane. In this experiment, the permeation cell was opened and closed to restart the run.

Table 21. Results for the WPUU/AgBF₄ membranes at the end of gas permeation experiments.

Membrane (weight ratio based on 0.750g of WPUU)	J C ₃ H ₆ (10 ⁻⁵ mol m ⁻² s ⁻¹)	α (C ₃ H ₆ /C ₃ H ₈)	Permeance (GPU)		Time of experiments values (h)
			C ₃ H ₈	C ₃ H ₆	
1 WPUU	5.15	1.80	0.59	1.06	28.8
1 WPUU : 0.25 IL	4.35	1.95	0.45	0.86	45.6
1 WPUU : 1 AgBF ₄	1.63	1.12	0.29	0.33	63.1
1 WPUU : 1 AgBF ₄ : 0.25 IL	1.02	3.20	0.06	0.20	47.5
1 WPUU : 1 AgBF ₄ : 0.50 IL	1.65	4.07	0.08	0.33	46.9
1 WPUU : 2 AgBF ₄ : 0.50 IL	8.98	2.42	0.75	1.85	62.7

Condition: 25 °C and 2 bar transmembrane pressure.

Final performance values at the end of long-term permeation experiments are present in **Table 21**. Compared to WPUU membrane, 1 WPUU: 0.25 IL membrane presented lower values of olefin and paraffin permeance (permeance drop: paraffin 24% and olefin 19%). The FTIR analysis suggests a smooth imidazolium/ether group interaction and probably it could be the cause of olefin and paraffin permeance drops. In less extent, this interaction decreased the chain mobility of polymer matrix influencing on gas transport properties of the membrane. In 1 WPUU: 1 AgBF₄ membrane, the intensive Ag⁺/ether interaction was responsible for reduce the polymer chain mobility; thus, the permeances of both gases decreased (permeance drop: paraffin 51% and olefin 69%) with selectivity nearly to 1. However, when IL was added the final selectivity of the membranes increased. In 1 WPUU: 1 AgBF₄: 0.25 IL membrane was 3.20 and in 1 WPUU: 1 AgBF₄: 0.5 IL membrane was 4.07. Compared to 1 WPUU: 1 AgBF₄ membrane, the main difference was the low paraffin flux found in the membrane with IL. Probably, the IL could protect the Ag⁺ cation against the initial reduction process that produces Ag⁰. Over the time, the Ag⁰ growth and agglomeration cause the formation of some defects or holes at the interface between the metal particle and the polymer chains. Without discrimination, the gases can easily pass through this pathway with lower mass transport resistance that leads to selectivity loss in long-term permeation experiments.⁵¹ In the membrane without IL, the selectivity nearly to 1 and the higher paraffin flux may be indicate the initial process of Ag⁰ formation and growth. When IL is present this process seems to be under control to some extent. The intensive Ag⁺/ether interaction was smoothed by the addition of IL, as shown in FTIR analysis. This is the reason for the protection against the silver reduction inside the polymer matrix.

In 1 WPUU: 2 AgBF₄: 0.5 IL membrane (**Table 21**), the high content of AgBF₄ indeed could provide a higher olefin flux compared to all membranes. However, paraffin flux also followed this behavior, and was the higher among the membranes. The result was a selectivity of 2.42. In this case, the high amount of silver salt maybe was forming some small silver nanoparticles aggregates inside the polymer matrix during the permeation process, leading to the selectivity loss. Other possibility is the weight ratio of 2 AgBF₄: 0.5 IL used that was not enough to ensure the IL protection against the initial reduction process of Ag⁺ cation. The FTIR analysis showed that the most intense Ag⁺/ether interaction was found in this membrane. Thus, the IL added could not weaken the interaction between the Ag⁺ cations and the ether groups avoiding the reduction process.⁵¹

4.4. Conclusions

WPUU/Ag NP membranes up to 50 wt% of silver content could not reach the facilitated transport of olefin, even with an interaction Ag NP/ether group inside polymer matrix, which could polarize the Ag NP surface. In attempt to provide activation to Ag NP, it was added BMImBF₄ or p-Bq to the membranes. The presence of these activator agents improved discreetly the selectivity of the membranes (from 1.84 in 1 WPUU(2) membrane to 2.92 in 1 WPUU(2) : 1 Ag NP : 1 IL : 0.85 p-Bq membrane); however, the facilitated transport was not observed.

WPUU/AgBF₄ membranes with more than 50 wt% of AgBF₄ (weight ration of 1WPUU: 1 AgBF₄) provided a facilitated transport of olefin. However, the olefin flux decreased during the permeation experiment due to the intensive Ag⁺/ether interaction in WPUU matrix. As an effort to solve this problem, IL (BMImBF₄) was introduced to the electrolyte composite membranes prepared. IL was able to smooth Ag⁺/ether interaction leading to an increase of the final selectivity when compared with membrane without IL. The higher selectivity (4.07) was found in 1 WPUU: 1 AgBF₄: 0.5 IL membrane. Before the olefin flux drop, the maximum olefin permeance (13.94 GPU) and selectivity (97.5) was observed in 1 WPUU: 2 AgBF₄: 0.5 IL membrane.

The main cause of initial olefin flux decline was the moisture loss during experiments with dried gases. For the 1 WPUU: 1 AgBF₄: 0.25 IL membrane, it was possible to recovery (84%) of olefin flux when the permeation cell was opened, and the membrane was in contact with atmospheric air during 15 min., repairing the moisture level of the material. This result suggests that the initial source of olefin flux decline was not the Ag⁺ reduction problem, but the moisture loss, which leads to Ag⁺ cations unfeasibility for olefin interaction.

Chapter 5

5. CONCLUSIONS AND CHALLENGES FOR FUTURE RESEARCHES

5.1. Conclusions

In an attempt to save energy in the naphtha steam cracking process, some alternatives have been proposed to replace or integrate with the current cryogenic distillation separation of olefins and paraffins. Among several technologies, facilitated transport membranes have stood out owing to the combination of high selectivity and permeance. However, to be used in the industrial separation, some instability issues should be considered. The Ag^+ cation, the main carrier for the facilitated transport membrane, suffers deactivation by poisonous agents from gaseous stream or by the contact with the polymer matrix of the membrane, which can reduce the Ag^+ cation. Therefore, the current arduous task is to maintain the selectivity in long-term separation process avoiding these deactivation problems. To attain this goal, the following clever alternatives have been proposed to overcome the hurdle: (i) the use of silver nanoparticles, (ii) the use of ionic liquids for the stabilization of Ag^+ , (iii) *in situ* regeneration of electrolyte polymeric membrane by using oxidizing agents, and (iv) the use of highly fluorinated polymers.

The most prominent result of these alternatives was achieved by $\text{AgBF}_4/\text{BMImBF}_4/\text{PVDF-HFP}$ membrane. The mixture selectivity of 700 and propylene permeability of 6630 Barrer (*ca.* 55 GPU) were stable for 10 days. Among alternatives, the use of Ag NP revealed high resistance against reduction agents and silver acetylide formation. However, required use of Ag NP polarizing agents like p-BQ, TCNQ and tetrathiafulvalene (TTF) can be another source of instability for the separation due to the inherent instability of these electron acceptors. Although, most of the results reported in the literature did not consider the presence of poisonous agents in the permeation experiments, the Compact Membrane Systems Company claims resistance against common poisonous agents for its commercial separation system called OptiperTM.

Among alternatives, Ag NP/activator and $\text{AgBF}_4/\text{BMImBF}_4$ systems were chosen to be tested in waterborne poly(urethane urea) (WPUU) matrix in order to evaluate the maintenance of selectivity in long-term separation tests. To prepare Ag NP/WPUU composite membranes, the method adopted for the synthesis *in situ* of Ag NP, using WPUU aqueous dispersion as stabilizing agent, was able to overcome the challenges to control the suitable dispersion and low polydispersity of Ag NP in aqueous medium. The WPUU/Ag NP dispersions were employed to prepare WPUU/Ag NP membranes with silver content up to 50wt%. and free of synthesis residue. TEM, SAXS and XRD results demonstrated that synthesized Ag NP were in nanometric scale, with less than 20 nm.

WPUU/Ag NP membranes up to 50 wt% of silver content could not reach the facilitated transport of olefin, even with an interaction Ag NP/ether group inside polymer matrix, which could polarize the Ag NP surface. In attempt to provide activation to Ag NP, it was added BMImBF₄ or p-Bq to the membranes. However, the facilitated transport was not observed probably because of low electron acceptor feature of BMImBF₄ and by the poor stability of p-Bq. The best result was achieved using the 1 WPUU(2) : 1 Ag NP : 1 IL : 0.85 membrane that showed a mixture selectivity of 2.92 and propylene permeance of 0.7 GPU. On the other hand, the facilitated transport of olefins was reached in AgBF₄/BMImBF₄/WPUU membranes. However, the olefin flux decreased during the permeation experiment. The main cause of initial olefin flux decline was the moisture loss during experiments with dried gases. Therefore, the initial source of olefin flux decline was not the Ag⁺ reduction problem, but the moisture loss, which leads to Ag⁺ cations unfeasibility for olefin interaction. The best result after olefin flux decline was found in 1 WPUU: 1 AgBF₄: 0.5 IL membrane, mixture selectivity of 4.0 and propylene permeance of 0.33 GPU after 45 h of experiment. Before the olefin flux drop, the maximum olefin permeance of 13.94 GPU and selectivity of 97.5 was observed in 1 WPUU: 2 AgBF₄: 0.5 IL membrane.

This Thesis reviews the main problems related to the membrane instabilities in olefin/paraffin separations pointing out some perspective of solutions to solve the drawbacks. Among solutions, the use of Ag NP/activator and AgBF₄/BMImBF₄ systems were selected to be applied in WPUU membranes. The systems present problems for the use in WPUU matrix. The activating agents for Ag NP, BMImBF₄ and p-Bq, were not able to provide the facilitated transport of olefins due to: (i) low electron acceptor feature of BMImBF₄ and (ii) poor stability of p-Bq. The AgBF₄/BMImBF₄ /WPUU membranes reached the facilitated transport of olefin; however, the initial olefin flux decreased during the tests due to humidification requirement to flux maintenance. Although all efforts in this work, it is not an easy task to achieve or keep the facilitated transport even with promising alternatives highlighted during the Thesis review (Chapter 1). Therefore, the search for other alternatives a new material to be applied in facilitated transport membrane for olefin separation remains as a challenge.

5.2. Challenges for future researches

Regarding the experience accumulated during the development of this Thesis, it is possible to point out some challenges for future researches.

Most of the results reported in the literature did not perform permeation test with the presence of poisonous agents. Thus, for future experiments, poisonous agents should be considered in the test to have access to more realistic data of operational conditions. With the development of some solutions highlighted in Chapter 1, probably, the future efforts will be dedicated to understand deeply the problems regarding the poisonous agents, trying to figure out more robust solutions.

The olefin flux decrease during the initial hours of permeation, reported by many authors as consequence of silver deactivation by reduction, maybe it can be moisture loss caused by the passage of dried gases through the membrane. If any deactivation by reduction occurs, the effect of olefin flux decline should be isolated from the moisture loss to clarify the data. Thus, for a fair judgment, future works should present data with dried and humidified feed gases.

There is a clear tendency of using fluorinated polymers for facilitated transport membranes for olefin/paraffin separation (Chapter 1). Therefore, there is a huge gap to study various fluorinated polymer classes or other kind of inert polymer applied to facilitated transport of olefins.²⁴⁴

Related to Ag NP, some future works could ask the following question. Could the shape of silver Ag NP influence in the gas transport? In a material where Ag NP can act properly as olefin carrier, may be very interesting to change the shape of Ag NP with different synthesis conditions and after checking the influence in the olefin transport. Other step more audacious may be the orientation control of these Ag NP inside the polymer matrix. For instance, a orientation of flat Ag NP in the flux direction could maximize the olefin flux.

Finally, to avoid the use of polarizing agents for Ag NP activation, some polymers could act like a polarizing agent. Polymer applied in organic solar cell are photovoltaic materials. Normally, these polymers are formed by conjugated double bond structures like in current polarizing molecules (p-Bq, TCNQ, TTF). One possible work to be proposed is the use of photovoltaic polymer in preparation of membranes with Ag NP for olefin/paraffin separation. This membrane also could be a blend of photovoltaic polymer with usual polymer matrix has already been applied for this separation.

REFERENCES

- (1) Petrochemicals Europe. *Petrochemicals Make Things Happen*; 2017.
- (2) Hyde, B. *Light Olefins Market Review*; IHS Inc., 2012.
- (3) Rappaport, H. Ethylene and Polyethylene Global Overview; Plastics Industry Trade Association (SPI) Film and Bag Conference: Chicago, 2011.
- (4) Nakayama, N. Global Supply and Demand of Petrochemical Products Relied on LPG as Feedstock; International LP Gas Seminar: Tokyo, 2017.
- (5) Sattler, J. J. H. B.; Ruiz-Martinez, J.; Santillan-Jimenez, E.; Weckhuysen, B. M. Catalytic Dehydrogenation of Light Alkanes on Metals and Metal Oxides. *Chem. Rev.* **2014**, *114* (20), 10613–10653.
- (6) Galadima, A.; Muraza, O. Revisiting the Oxidative Coupling of Methane to Ethylene in the Golden Period of Shale Gas: A Review. *J. Ind. Eng. Chem.* **2016**, *37*, 1–13.
- (7) Tian, P.; Wei, Y.; Ye, M.; Liu, Z. Methanol to Olefins (MTO): From Fundamentals to Commercialization. *ACS Catal.* **2015**, *5* (3), 1922–1938.
- (8) Amghizar, I.; Vandewalle, L. A.; Van Geem, K. M.; Marin, G. B. New Trends in Olefin Production. *Engineering* **2017**, *3* (2), 171–178.
- (9) Brooks, R. E. Modeling the North American Market for Natural Gas Liquids; 32nd US Association of Energy and Economics (USAEE) Conference: Anchorage, 2013.
- (10) Foster, J. Can Shale Gas Save the Naphtha Crackers ? *Platts special report: Petrochemicals*. 2013, p 3.
- (11) Akah, A.; Al-Ghrami, M. Maximizing Propylene Production via FCC Technology. *Appl. Petrochemical Res.* **2015**, 1–16.
- (12) Ren, T.; Patel, M.; Blok, K. Olefins from Conventional and Heavy Feedstocks: Energy Use in Steam Cracking and Alternative Processes. *Energy* **2006**, *31* (4), 425–451.
- (13) Chuapet, W.; Limphitakphong, N.; Tantisattayakul, T.; Kanchanapiya, P.; Chavalparit, O. A Study of Energy Intensity and Carbon Intensity from Olefin Plants in Thailand. *MATEC Web Conf.* **2016**, *68*, 6–10.
- (14) Zimmermann, H.; Walzl, R. Ethylene. In *Ullmann's Encyclopedia of Industrial Chemistry*; Wiley-VCH: Weinheim, 2012; Vol. 13, pp 465–529.
- (15) Falqi, F. H. *The Miracle of Petrochemicals. Olefins Industry: An in-Depth Look at Steam-Crackers*; Universal-Publishers Boca Raton, Ed.; Florida, 2009.
- (16) European Commission. Reference Document on Best Available Techniques in the

- Large Volume Organic Chemical Industry February 2003. *Integr. Pollut. Prev. Control* **2003**, *1* (February), 267–289.
- (17) Xu, L.; Rungta, M.; Brayden, M. K.; Martinez, M. V.; Stears, B. A.; Barbay, G. A.; Koros, W. J. Olefins-Selective Asymmetric Carbon Molecular Sieve Hollow Fiber Membranes for Hybrid Membrane-Distillation Processes for Olefin/paraffin Separations. *J. Memb. Sci.* **2012**, *423–424*, 314–323.
- (18) Baker, R. W.; Low, B. T. Gas Separation Membrane Materials: A Perspective. *Macromolecules* **2014**, *47* (20), 6999–7013.
- (19) Park, J.; Kim, K.; Shin, J.-W.; Tak, K.; Park, Y.-K. Performance Study of Multistage Membrane and Hybrid Distillation Processes for Propylene/propane Separation. *Can. J. Chem. Eng.* **2017**, *95* (12), 2390–2397.
- (20) Safarik, D. J.; Eldridge, R. B. Olefin/Paraffin Separations by Reactive Absorption: A Review. *Ind. Eng. Chem. Res.* **1998**, *37* (7), 2571–2581.
- (21) Huang, H. Y.; Padin, J.; Yang, R. T. Comparison of π -Complexations of Ethylene and Carbon Monoxide with Cu^+ and Ag^+ . *Ind. Eng. Chem. Res.* **1999**, *38* (7), 2720–2725.
- (22) Tian, Y.; Zhou, H.; Qiao, Y.; Tang, R.; Zhao, G.; Leng, G. In-Situ Reduction of $\text{Cu}(\text{CH}_3\text{COO})_2$ to Prepare π -Complexation Adsorbent for Propylene/propane Separation by Slurry Bed. *Sep. Sci. Technol.* **2017**, *52* (12), 1959–1966.
- (23) Anson, A.; Wang, Y.; Lin, C. C. H.; Kuznicki, T. M.; Kuznicki, S. M. Adsorption of Ethane and Ethylene on Modified ETS-10. *Chem. Eng. Sci.* **2008**, *63* (16), 4171–4175.
- (24) Rege, S. U.; Padin, J.; Yang, R. T. Olefin/paraffin Separations by Adsorption: π -Complexation vs. Kinetic Separation. *AIChE J.* **1998**, *44* (4), 799–809.
- (25) Aguado, S.; Bergeret, G.; Daniel, C.; Farrusseng, D. Absolute Molecular Sieve Separation of Ethylene/Ethane Mixtures with Silver Zeolite A. *J. Am. Chem. Soc.* **2012**, *134* (36), 14635–14637.
- (26) Bao, Z.; Chang, G.; Xing, H.; Krishna, R.; Ren, Q.; Chen, B. Potential of Microporous Metal–organic Frameworks for Separation of Hydrocarbon Mixtures. *Energy Environ. Sci.* **2016**, *9* (12), 3612–3641.
- (27) Li, P.; He, Y.; Arman, H. D.; Krishna, R.; Wang, H.; Weng, L.; Chen, B. A Microporous Six-Fold Interpenetrated Hydrogen-Bonded Organic Framework for Highly Selective Separation of $\text{C}_2\text{H}_4/\text{C}_2\text{H}_6$. *Chem. Commun.* **2014**, *50* (86), 13081–13084.
- (28) Huang, L.; Cao, D. Selective Adsorption of Olefin–paraffin on Diamond-like Frameworks: Diamondyne and PAF-302. *J. Mater. Chem. A* **2013**, *1* (33), 9433.

- (29) Luna-Triguero, A.; Vicent-Luna, J. M.; Becker, T. M.; Vlugt, T. J. H.; Dubbeldam, D.; Gómez-Álvarez, P.; Calero, S. Effective Model for Olefin/Paraffin Separation Using (Co, Fe, Mn, Ni)-MOF-74. *ChemistrySelect* **2017**, *2* (2), 665–672.
- (30) Peng, J.; Wang, H.; Olson, D. H.; Li, Z.; Li, J. Efficient Kinetic Separation of Propene and Propane Using Two Microporous Metal Organic Frameworks. *Chem. Commun.* **2017**.
- (31) Wang, Y.; Hu, Z.; Cheng, Y.; Zhao, D. Silver-Decorated Hafnium Metal-Organic Framework for Ethylene/Ethane Separation. *Ind. Eng. Chem. Res.* **2017**, *56* (15), 4508–4516.
- (32) Bernardo, P.; Drioli, E.; Golemme, G. Membrane Gas Separation: A Review/state of the Art. *Ind. Eng. Chem. Res.* **2009**, *48* (10), 4638–4663.
- (33) Pozun, Z. D.; Henkelman, G. A Model to Optimize the Selectivity of Gas Separation in Membranes. *J. Memb. Sci.* **2010**, *364* (1–2), 9–16.
- (34) Gajbhiye, S. B. Membranes of Poly(phenylene Oxide) and Its Copolymers: Synthesis, Characterization, and Application in Recovery of Propylene from a Refinery off-Gas Mixture. *J. Appl. Polym. Sci.* **2013**, *127* (4), 2497–2507.
- (35) Staudt-Bickel, C.; Koros, W. J. Olefin/paraffin Gas Separations with 6FDA-Based Polyimide Membranes. *J. Memb. Sci.* **2000**, *170* (2), 205–214.
- (36) Lee, U.; Kim, J.; Chae, I. S.; Han, C. Techno-Economic Feasibility Study of Membrane Based Propane/propylene Separation Process. *Chem. Eng. Process. Process Intensif.* **2017**, *119*, 62–72.
- (37) Tang, Z.; Lu, B.; Hu, X.; Pham, T.; Li, L. F. Mixed Matrix Membranes for Olefin/paraffin Separation and Method of Making Thereof. U.S. Patent 2017/291147 A1, 2017.
- (38) Zhang, C.; Dai, Y.; Johnson, J. R.; Karvan, O.; Koros, W. J. High Performance ZIF-8/6FDA-DAM Mixed Matrix Membrane for Propylene/propane Separations. *J. Memb. Sci.* **2012**, *389*, 34–42.
- (39) Antonio, M. R.; Tsou, D. T. Silver Ion Coordination in Membranes for Facilitated Olefin Transport. *Ind. Eng. Chem. Res.* **1993**, *32* (2), 273–278.
- (40) Li, Y.; Wang, S.; He, G.; Wu, H.; Pan, F.; Jiang, Z. Facilitated Transport of Small Molecules and Ions for Energy-Efficient Membranes. *Chem. Soc. Rev.* **2015**, *44* (1), 103–118.
- (41) Ho, W. S.; Dalrymple, D. C. Facilitated Transport of Olefins in Ag⁺-Containing Polymer Membranes. *J. Memb. Sci.* **1994**, *91* (1–2), 13–25.

- (42) Pollo, L. D.; Duarte, L. T.; Anacleto, M.; Habert, A. C.; Borges, C. P. Polymeric Membranes Containing Silver Salts for Propylene/propane Separation. *Brazilian J. Chem. Eng.* **2012**, *29* (2), 307–314.
- (43) Liu, J.; Goss, J. M.; Calverley, E. M.; Beyer, D. E. Separation of Gases via Carbonized Vinylidene Chloride Copolymer Gas Separation Membranes and Process for the Preparation of the Membranes. W.O. Patent 2017/160815 A1, 2017.
- (44) Liu, J.; Calverley, E. M.; McAdon, M. H.; Goss, J. M.; Liu, Y.; Andrews, K. C.; Wolford, T. D.; Beyer, D. E.; Han, C. S.; Anaya, D. A.; et al. New Carbon Molecular Sieves for Propylene/propane Separation with High Working Capacity and Separation Factor. *Carbon N. Y.* **2017**, *123*, 273–282.
- (45) Fallanza, M.; Ortiz, A.; Gorri, D.; Ortiz, I. Polymer-Ionic Liquid Composite Membranes for Propane/propylene Separation by Facilitated Transport. *J. Memb. Sci.* **2013**, *444*, 164–172.
- (46) Majumdar, S.; Koizumi, Y.; Shangguan, N.; Feirring, A. E. Thin Film Composite Membranes for Separation of Alkenes from Alkanes. W.O. Patent 2016/182887 A1, 2016.
- (47) Kim, Y. R.; Lee, J. H.; Choi, H.; Cho, W.; Kang, Y. S. Chemical Stability of Olefin Carrier Based on Silver Cations and Metallic Silver Nanoparticles against the Formation of Silver Acetylide for Facilitated Transport Membranes. *J. Memb. Sci.* **2014**, *463*, 11–16.
- (48) Shen, X.; Abro, R.; Alhumaydhi, I. A.; Abdeltawab, A. A.; Al-Enizi, A. M.; Chen, X.; Yu, G. Separation of Propylene and Propane by Functional Mixture of Imidazolium Chloride Ionic Liquid – Organic Solvent – Cuprous Salt. *Sep. Purif. Technol.* **2017**, *175*, 177–184.
- (49) GESTIS Substance Database. Institute for Occupational Safety and Health of the German Social Accident Insurance www.dguv.de/ifa/gestis-database (accessed Mar 1, 2018).
- (50) Sholl, D. S.; Lively, R. P. Seven Chemical Separations to Change the World. *Nature* **2016**, *532*, 435–437.
- (51) Park, Y. S.; Chun, S.; Kang, Y. S.; Kang, S. W. Durable Poly(vinyl alcohol)/AgBF₄/Al(NO₃)₃ Complex Membrane with High Permeance for Propylene/propane Separation. *Sep. Purif. Technol.* **2017**, *174* (3), 39–43.
- (52) Faiz, R.; Li, K. Olefin/paraffin Separation Using Membrane Based Facilitated Transport/chemical Absorption Techniques. *Chem. Eng. Sci.* **2012**, *73*, 261–284.

- (53) Merkel, T. C.; Blanc, R.; Ciobanu, I.; Firat, B.; Suwarlim, A.; Zeid, J. Silver Salt Facilitated Transport Membranes for Olefin/paraffin Separations: Carrier Instability and a Novel Regeneration Method. *J. Memb. Sci.* **2013**, *447*, 177–189.
- (54) Giannakopoulos, I. G.; Nikolakis, V. Separation of Propylene/Propane Mixtures Using Faujasite-Type Zeolite Membranes. *Ind. Eng. Chem. Res.* **2005**, *44* (1), 226–230.
- (55) Nikolakis, V.; Xomeritakis, G.; Abibi, A.; Dickson, M.; Tsapatsis, M.; Vlachos, D. G. Growth of a Faujasite-Type Zeolite Membrane and Its Application in the Separation of Saturated/unsaturated Hydrocarbon Mixtures. *J. Memb. Sci.* **2001**, *184* (2), 209–219.
- (56) Liu, D.; Ma, X.; Xi, H.; Lin, Y. S. Gas Transport Properties and Propylene/propane Separation Characteristics of ZIF-8 Membranes. *J. Memb. Sci.* **2014**, *451*, 85–93.
- (57) Zhang, C.; Lively, R. P.; Zhang, K.; Johnson, J. R.; Karvan, O.; Koros, W. J. Unexpected Molecular Sieving Properties of Zeolitic Imidazolate Framework-8. *J. Phys. Chem. Lett.* **2012**, *3* (16), 2130–2134.
- (58) Kwon, H. T.; Jeong, H.-K. *In Situ* Synthesis of Thin Zeolitic–Imidazolate Framework ZIF-8 Membranes Exhibiting Exceptionally High Propylene/Propane Separation. *J. Am. Chem. Soc.* **2013**, *135* (29), 10763–10768.
- (59) Kwon, H. T.; Jeong, H.-K. Highly Propylene-Selective Supported Zeolite-Imidazolate Framework (ZIF-8) Membranes Synthesized by Rapid Microwave-Assisted Seeding and Secondary Growth. *Chem. Commun.* **2013**, *49* (37), 3854.
- (60) Pan, Y.; Li, T.; Lestari, G.; Lai, Z. Effective Separation of Propylene/propane Binary Mixtures by ZIF-8 Membranes. *J. Memb. Sci.* **2012**, *390–391*, 93–98.
- (61) Kim, J. H.; Lee, D. H.; Won, J.; Jinnai, H.; Kang, Y. S. The Structural Transitions of Pi-Complexes of Poly(styrene-*B*-Butadiene-*B*-Styrene) Block Copolymers with Silver Salts and Their Relation to Facilitated Olefin Transport. *J. Memb. Sci.* **2006**, *281*, 369–376.
- (62) Baker, R. W. *Membrane Technology and Applications*, 3rd ed.; John Wiley and Sons, Ed.; Chichester, 2012.
- (63) Merkel, T.; Blanc, R.; Zeid, J.; Suwarlim, A.; Firat, B.; Wijmans, H.; Asaro, M.; Greene, M. *Separation of Olefin / Paraffin Mixtures with Carrier Facilitated Membranes*; Report DE-FC36-04GO14151, U.S. Department of Energy, 2007.
- (64) Liskey, C. W.; Liu, C.; Tran, H. Q. Polyimide Membranes with Very High Separation Performance for Olefin/paraffin Separation. U.S. Patent 2015/0328594 A1, 2015.
- (65) Chevron Phillips Chemical Company LP <http://www.cpchem.com/en-us/Pages/default.aspx> (accessed Jul 12, 2017).

- (66) Baker, R. W. Future Directions of Membrane Gas Separation Technology. *Ind. Eng. Chem. Res.* **2002**, *41* (6), 1393–1411.
- (67) Das, M. Membranes for Olefin/paraffin Separations, Georgia Institute of Technology, 2009.
- (68) HABERT, A. C.; BORGES, C. P.; NOBREGA, R. *Processo de Separação Por Membranas*; E-papers: Rio de Janeiro, 2006.
- (69) Baker, R. W. Gas Separation. In *Membrane Technology and Applications*; Baker, R. W., Ed.; John Wiley & Sons, Ltd: Chichester, 2004; pp 301–353.
- (70) Lin, H.; Freeman, B. D. Gas Solubility, Diffusivity and Permeability in Poly(ethylene Oxide). *J. Memb. Sci.* **2004**, *239* (1), 105–117.
- (71) Ghosal, K.; Chern, R. T.; Freeman, B. D. Effect of Basic Substituents on Gas Sorption and Permeation in Polysulfone. *Macromolecules* **1996**, *29* (12), 4360–4369.
- (72) MULDER, M. *Basic Principles of Membrane Technology*, 2. ed.; Kluwer Academic Publishers: Dordrecht, 1996.
- (73) Ning, L.; De-ning, W.; Sheng-kang, Y.; Luo; Wang; Ying. Hydrogen-Bonding Properties of Segmented Polyether Poly(urethane Urea) Copolymer. *Macromolecules* **1997**, *30* (15), 4405–4409.
- (74) WOLINSKA-GRABCZYK, A. Effect of the Hard Segment Domains on the Permeation and Separation Ability of the Polyurethane-Based Membranes in Benzene/cyclohexane Separation by Pervaporation. *J. Memb. Sci.* **2006**, *282* (1–2), 225–236.
- (75) Wang, Y.; Goh, T. Y.; Goodrich, P.; Atilhan, M.; Khraisheh, M.; Rooney, D.; Thompson, J.; Jacquemin, J. Impact of Ionic Liquids on Silver Thermoplastic Polyurethane Composite Membranes for Propane/propylene Separation. *Arab. J. Chem.* **2017**, in press.
- (76) Faiz, R.; Li, K. Polymeric Membranes for Light Olefin/paraffin Separation. *Desalination* **2012**, *287*, 82–97.
- (77) Delpech, M. C.; Coutinho, F. M. B. Waterborne Anionic Polyurethanes and Poly(urethane-Urea)s: Influence of the Chain Extender on Mechanical and Adhesive Properties. *Polym. Test.* **2000**, *19* (8), 939–952.
- (78) Coutinho, F. M. B.; Delpech, M. C.; Garcia, M. E. F. Evaluation of Gas Permeability of Membranes Obtained from Poly(urethane-Urea)s Aqueous Dispersions Based on Hydroxyl-Terminated Polybutadiene. *Polym. Test.* **2002**, *21* (6), 719–723.
- (79) Li, H.; Freeman, B. D.; Ekiner, O. M. Gas Permeation Properties of Poly(urethane-

- Urea)s Containing Different Polyethers. *J. Memb. Sci.* **2011**, *369* (1–2), 49–58.
- (80) Reis, R. A.; Pereira, J. H. C.; Campos, A. C. C.; Barboza, E. M.; Delpech, M. C.; Cesar, D. V.; Dahmouche, K.; Bandeira, C. F.; Dahmoucheb, K.; Bandeira, C. F. Waterborne Poly(urethane-Urea)s Gas Permeation Membranes for CO₂/CH₄ Separation. *J. Appl. Polym. Sci.* **2018**, *135* (11), 46003.
- (81) Surya Murali, R.; Yamuna Rani, K.; Sankarshana, T.; Ismail, A. F.; Sridhar, S. Separation of Binary Mixtures of Propylene and Propane by Facilitated Transport through Silver Incorporated Poly(Ether-Block-Amide) Membranes. *Oil Gas Sci. Technol. – Rev. d'IFP Energies Nouv.* **2015**, *70* (2), 381–390.
- (82) Isanejad, M.; Azizi, N.; Mohammadi, T. Pebax Membrane for CO₂/CH₄ Separation: Effects of Various Solvents on Morphology and Performance. *J. Appl. Polym. Sci.* **2017**, *134* (9), 1–9.
- (83) Wang, Y.; Ren, J.; Deng, M. Ultrathin Solid Polymer Electrolyte PEI/Pebax2533/AgBF₄ Composite Membrane for Propylene/propane Separation. *Sep. Purif. Technol.* **2011**, *77* (1), 46–52.
- (84) Armstrong, S.; Freeman, B.; Hiltner, A.; Baer, E. Gas Permeability of Melt-Processed Poly(ether Block Amide) Copolymers and the Effects of Orientation. *Polymer (Guildf).* **2012**, *53* (6), 1383–1392.
- (85) Bai, S.; Sridhar, S.; Khan, A. . Metal-Ion Mediated Separation of Propylene from Propane Using PPO Membranes. *J. Memb. Sci.* **1998**, *147* (1), 131–139.
- (86) Krol, J. J.; Boerrigter, M.; Koops, G. H. Polyimide Hollow Fiber Gas Separation Membranes: Preparation and the Suppression of Plasticization in Propane/propylene Environments. *J. Memb. Sci.* **2001**, *184* (2), 275–286.
- (87) Okamoto, K.; Noborio, K.; Hao, J.; Tanaka, K.; Kita, H. Permeation and Separation Properties of Polyimide Membranes to 1,3-Butadiene and N-Butane. *J. Memb. Sci.* **1997**, *134* (2), 171–179.
- (88) Burns, R. L.; Koros, W. J. Defining the Challenges for C₃H₆/C₃H₈ Separation Using Polymeric Membranes. *J. Memb. Sci.* **2003**, *211* (2), 299–309.
- (89) Kang, S. W.; Hong, J.; Park, J. H.; Mun, S. H.; Kim, J. H.; Cho, J.; Char, K.; Kang, Y. S. Nanocomposite Membranes Containing Positively Polarized Gold Nanoparticles for Facilitated Olefin Transport. *J. Memb. Sci.* **2008**, *321* (1), 90–93.
- (90) Kim, J. H.; Min, B. R.; Won, J.; Joo, S. H.; Kim, H. S.; Kang, Y. S. Role of Polymer Matrix in Polymer/silver Complexes for Structure, Interactions, and Facilitated Olefin Transport. *Macromolecules* **2003**, *36* (16), 6183–6188.

- (91) Kang, S. W.; Kang, Y. S. Silver Nanoparticles Stabilized by Crosslinked Poly(vinyl Pyrrolidone) and Its Application for Facilitated Olefin Transport. *J. Colloid Interface Sci.* **2011**, *353* (1), 83–86.
- (92) Kang, Y. S.; Kang, S. W.; Kim, H.; Kim, J. H.; Won, J.; Kim, C. K.; Char, K. Interaction with Olefins of the Partially Polarized Surface of Silver Nanoparticles Activated by P-Benzoquinone and Its Implications for Facilitated Olefin Transport. *Adv. Mater.* **2007**, *19* (3), 475–479.
- (93) Cussler, E. L.; Aris, R.; Bhowan, A. On the Limits of Facilitated Diffusion. *J. Memb. Sci.* **1989**, *43* (2–3), 149–164.
- (94) Dewar, M. J. S. A Review of the P-Complex Theory. *Bull. la Socie'te' Chim.* **1951**, *18*, C71-9.
- (95) Chatt, J., Duncanson, L. A. Olefin Co-Ordination Compounds. Part III. Infrared Spectra and Structure: Attempted Preparation of Acetylene Complexes. *J. Chem. Soc.* **1953**, 2939.
- (96) Miessler, G. L.; Fischer, P. J.; Tarr, D. A. *Inorganic Chemistry*, 5th ed.; Pearson: Upper Saddle Rive, NJ, 2014.
- (97) Cotton, F. A.; Wilkinson, G.; Murillo, C. A.; Bochmann, M. *Advanced Inorganic Chemistry*, 6th ed.; Wiley-Interscience, Ed.; New York, 1999.
- (98) Scholander, P. F. Oxygen Transport through Hemoglobin Solutions. *Science* **1960**, *131*, 585.
- (99) Kim, J. H.; Kang, Y. S.; Won, J. Silver Polymer Electrolyte Membranes for Facilitated Olefint Transport: Carrier Properties, Transport Mechanism and Separation Performance. *Macromol. Res.* **2004**, *12* (2), 145–155.
- (100) E.F. Steigelmann; R.D. Hughes. Process for Separation of Unsaturated Hydrocarbons. U.S. Patent 3,758,603, 1973.
- (101) Hughes, R. D.; Mahoney, J. A.; Steigelmann, E. F. Olefin Separation by Facilitated Transport Membranes. In *Recent Developments in Separation Science*; Li, N. N., Calo, J. M., Eds.; CRC Press: Boca Raton, 1986; pp 173–196.
- (102) Duan, S.; Ito, A.; Ohkawa, A. Separation of Propylene/propane Mixture by a Supported Liquid Membrane Containing Triethylene Glycol and a Silver Salt. *J. Memb. Sci.* **2003**, *215* (1–2), 53–60.
- (103) Fallanza, M.; Ortiz, A.; Gorri, D.; Ortiz, I. Experimental Study of the Separation of Propane/propylene Mixtures by Supported Ionic Liquid Membranes Containing Ag⁺–RTILs as Carrier. *Sep. Purif. Technol.* **2012**, *97*, 83–89.

- (104) Pitsch, F.; Krull, F. F.; Agel, F.; Schulz, P.; Wasserscheid, P.; Melin, T.; Wessling, M. An Adaptive Self-Healing Ionic Liquid Nanocomposite Membrane for Olefin-Paraffin Separations. *Adv. Mater.* **2012**, *24* (31), 4306–4310.
- (105) Kárászová, M.; Kacirková, M.; Friess, K.; Izák, P. Progress in Separation of Gases by Permeation and Liquids by Pervaporation Using Ionic Liquids: A Review. *Sep. Purif. Technol.* **2014**, *132*, 93–101.
- (106) Teramoto, M.; Matsuyama, H.; Yamashiro, T.; Katayama, Y. Separation of Ethylene from Ethane by Supported Liquid Membranes Containing Silver Nitrate as a Carrier. *J. Chem. Eng. Japan* **1986**, *19* (5), 419–424.
- (107) Ravanchi, M. T.; Kaghazchi, T.; Kargari, A. Facilitated Transport Separation of Propylene-Propane: Experimental and Modeling Study. *Chem. Eng. Process. Process Intensif.* **2010**, *49* (3), 235–244.
- (108) Ravanchi, M. T.; Kaghazchi, T.; Kargari, A. Supported Liquid Membrane Separation of Propylene-Propane Mixtures Using a Metal Ion Carrier. *Desalination* **2010**, *250* (1), 130–135.
- (109) Oliver H. Leblanc; William J. Ward; Stephen L. Matson; Shiro G. Kimura. Facilitated Transport in Ion-Exchange Membranes. *J. Memb. Sci.* **1980**, *6*, 339–343.
- (110) Eriksen, O. I.; Aksnes, E.; Dahl, I. M. Facilitated Transport of Ethene through Nafion Membranes. Part II. Glycerine Treated, Water Swollen Membranes. *J. Memb. Sci.* **1993**, *85* (1), 99–106.
- (111) Eriksen, O. I.; Aksnes, E.; Dahl, I. M. Facilitated Transport of Ethene through Nafion Membranes. Part I. Water Swollen Membranes. *J. Memb. Sci.* **1993**, *85* (1), 89–97.
- (112) Rabago, R.; Noble, R. D.; Koval, C. A. Effects of Incorporation of Fluorocarbon and Hydrocarbon Surfactants into Perfluorosulfonic Acid (Nafion) Membranes. *Chem. Mater.* **1994**, *6* (7), 947–951.
- (113) Sungpet, A.; Way, J. D.; Thoen, P. M.; Dorgan, J. R. Reactive Polymer Membranes for Ethylene/ethane Separation. *J. Memb. Sci.* **1997**, *136* (1–2), 111–120.
- (114) Yamaguchi, T.; Baertsch, C.; Koval, C. A.; Noble, R. D.; Bowman, C. N. Olefin Separation Using Silver Impregnated Ion-Exchange Membranes and Silver Salt/polymer Blend Membranes. *J. Memb. Sci.* **1996**, *117* (1–2), 151–161.
- (115) Thoen, P. M.; Noble, R. D.; Koval, C. A. Unexpectedly Large Selectivities for Olefin Separations Utilizing Silver Ion in Ion-Exchange Membranes. *J. Phys. Chem.* **1994**, *98* (4), 1262–1269.
- (116) Koval, C.; Bryant, D.; Engelhardt, H.; Manley, D.; Rabago, R.; Thoen, P.; Noble, R.

- Facilitated Transport of Unsaturated Hydrocarbons in Perfluorosulfonic Acid (Nafion) Membranes. In *Chemical Separations with Liquid Membranes*; Bartsch, R.; Way, J. D., Ed.; ACS Symposium Series; American Chemical Society: Washington, DC, 1996; Vol. 642, pp 286–302.
- (117) Liu, L.; Feng, X.; Chakma, A. Unusual Behavior of Poly(ethylene oxide)/AgBF₄ Polymer Electrolyte Membranes for Olefin-Paraffin Separation. *Sep. Purif. Technol.* **2004**, *38* (3), 255–263.
- (118) Pinnau, I.; Toy, L. G. Solid Polymer Electrolyte Composite Membranes for Olefin/paraffin Separation. *J. Memb. Sci.* **2001**, *184* (1), 39–48.
- (119) Kim, J. H.; Min, B. R.; Kim, C. K.; Won, J. New Insights into the Coordination Mode of Silver Ions Dissolved in Poly (2-Ethyl-2-Oxazoline) and Its Relation to Facilitated Olefin. *Macromolecules* **2002**, *35*, 5250–5255.
- (120) Sunderrajan, S.; Freeman, B. D.; Hall, C. K.; Pinnau, I. Propane and Propylene Sorption in Solid Polymer Electrolytes Based on Poly(ethylene Oxide) and Silver Salts. *J. Memb. Sci.* **2001**, *182* (1–2), 1–12.
- (121) Morisato, A.; He, Z.; Pinnau, I.; Merkel, T. C. Transport Properties of PA12-PTMO/AgBF₄ Solid Polymer Electrolyte Membranes for Olefin/paraffin Separation. *Desalination* **2002**, *145* (1), 347–351.
- (122) Merkel, T. C.; He, Z.; Morisato, A.; Pinnau, I. Olefin/paraffin Solubility in a Solid Polymer Electrolyte Membrane. *Chem. Commun.* **2003**, *37* (13), 1596.
- (123) Kim, J. H.; Kang, S. W.; Kang, Y. S. Threshold Silver Concentration for Facilitated Olefin Transport in Polymer/silver Salt Membranes. *J. Polym. Res.* **2012**, *19* (1), 9753.
- (124) Kim, J. H.; Min, B. R.; Kim, H. S.; Won, J.; Kang, Y. S. Facilitated Transport of Ethylene across Polymer Membranes Containing Silver Salt: Effect of HBF₄ on the Photoreduction of Silver Ions. *J. Memb. Sci.* **2003**, *212* (1), 283–288.
- (125) Kim, J. H.; Won, J.; Kang, Y. S. Olefin-Induced Dissolution of Silver Salts Physically Dispersed in Inert Polymers and Their Application to Olefin/paraffin Separation. *J. Memb. Sci.* **2004**, *241* (2), 403–407.
- (126) Kang, Y. S.; Kim, J. H.; Won, J.; Kim, H. S. Solid-State Facilitated Transport Membranes for Separation of Olefins / Paraffins and Oxygen / Nitrogen. In *Materials Science of Membranes for Gas and Vapor Separation*; Yampolskii, Y., Pinnau, I., Freeman, B., Eds.; John Wiley & Sons, Ltd.: Chichester, 2006; pp 391–410.
- (127) Kim, J. H.; Won, J.; Kang, Y. S. Silver Polymer Electrolytes by π -Complexation of Silver Ions with Polymer Containing C=C Bond and Their Application to Facilitated

- Olefin Transport Membranes. *J. Memb. Sci.* **2004**, *237* (1–2), 199–202.
- (128) Kim, J. H.; Min, B. R.; Won, J.; Kang, Y. S. Revelation of Facilitated Olefin Transport through Silver-Polymer Complex Membranes Using Anion Complexation. *Macromolecules* **2003**, *36* (12), 4577–4581.
- (129) Kim, J. H.; Min, B. R.; Won, J.; Kang, Y. S. Complexation Mechanism of Olefin with Silver Ions Dissolved in a Polymer Matrix and Its Effect on Facilitated Olefin Transport. *Chem. Eur. J.* **2002**, *8* (3), 650–654.
- (130) Kim, J. H.; Min, B. R.; Kim, C. K.; Won, J.; Kang, Y. S. Spectroscopic Interpretation of Silver Ion Complexation with Propylene in Silver Polymer Electrolytes. *J. Phys. Chem. B* **2002**, *106* (10), 2786–2790.
- (131) Kang, S. W.; Char, K.; Kim, J. H.; Kim, C. K.; Kang, Y. S. Control of Ionic Interactions in Silver Salt-Polymer Complexes with Ionic Liquids: Implications for Facilitated Olefin Transport. *Chem. Mater.* **2006**, *18* (7), 1789–1794.
- (132) Duarte, L. T.; Habert, A. C.; Borges, C. P. Preparation and Morphological Characterization of Polyurethane/polyethersulfone Composite Membranes. *Desalination* **2002**, *145* (1–3), 53–59.
- (133) Ferraz, H. C.; Duarte, L. T.; Alves, M. D. L.; Habert, A. C.; Borges, C. P. Recent Achievements in Facilitated Transport Membranes for Separation Processes. *Brazilian J. Chem. Eng.* **2007**, *24* (1), 101–118.
- (134) Kang, S.; Kim, J.; Won, J. Enhancement of Facilitated Olefin Transport by Amino Acid in Silver-Polymer Complex Membranes. *Chem. Commun.* **2003**, *2* (3), 768–769.
- (135) Kim, J. H.; Park, S. M.; Won, J.; Kang, Y. S. Unusual Separation Property of Propylene/propane Mixtures through Polymer/silver Complex Membranes Containing Mixed Salts. *J. Memb. Sci.* **2005**, *248* (1–2), 171–176.
- (136) Preechatiwong, W.; Schultz, J. M. Electrical Conductivity of Poly(ethylene Oxide)-Alkali Metal Salt Systems and Effects of Mixed Salts and Mixed Molecular Weights. *Polymer (Guildf)*. **1996**, *37* (23), 5109–5116.
- (137) Jose, B.; Ryu, J. H.; Lee, B. G.; Lee, H.; Kang, Y. S.; Kim, H. S. Effect of Phthalates on the Stability and Performance of AgBF₄-PVP Membranes for Olefin/paraffin Separation. *Chem. Commun.* **2001**, 2046–2047.
- (138) Hun Park, H.; Won, J.; Oh, S. G.; Kang, Y. S. Effect of Nonionic N-Octyl β -D-Glucopyranoside Surfactant on the Stability Improvement of Silver Polymer Electrolyte Membranes for Olefin/paraffin Separation. *J. Memb. Sci.* **2003**, *217* (1–2), 285–293.

- (139) Pastoriza-Santos, I.; Liz-Marzán, L. M. Formation and Stabilization of Silver Nanoparticles through Reduction by *N,N*-Dimethylformamide. *Langmuir* **1999**, *15* (4), 948–951.
- (140) Wistrand, L. Silver Tetrafluoroborate. In *e-EROS Encyclopedia of Reagents for Organic Synthesis*; John Wiley & Sons, 2005; pp 1–8.
- (141) Kang, S. W.; Kim, J. H.; Won, J.; Kang, Y. S. Suppression of Silver Ion Reduction by $\text{Al}(\text{NO}_3)_3$ Complex and Its Application to Highly Stabilized Olefin Transport Membranes. *J. Memb. Sci.* **2013**, *445* (3), 156–159.
- (142) Kang, S. W.; Kim, J. H.; Char, K.; Kang, Y. S. Chemical Activation of AgNO_3 to Form Olefin Complexes Induced by Strong Coordinative Interactions with Phthalate Oxygens of Poly(ethylene Phthalate). *Ind. Eng. Chem. Res.* **2006**, *45* (11), 4011–4014.
- (143) Song, D.; Kang, Y. S.; Kang, S. W. Highly Permeable and Stabilized Olefin Transport Membranes Based on a Poly(ethylene Oxide) Matrix and $\text{Al}(\text{NO}_3)_3$. *J. Memb. Sci.* **2015**, *474* (0), 273–276.
- (144) Sung Park, Y.; Soo Kang, Y.; Wook Kang, S. Cost-Effective Facilitated Olefin Transport Membranes Consisting of polymer/ $\text{AgCF}_3\text{SO}_3/\text{Al}(\text{NO}_3)_3$ with Long-Term Stability. *J. Memb. Sci.* **2015**, *495* (3), 61–64.
- (145) Park, Y. S.; Kang, S. W. Role of Ionic Liquids in Enhancing the Performance of the polymer/ $\text{AgCF}_3\text{SO}_3/\text{Al}(\text{NO}_3)_3$ Complex for Separation of Propylene/propane Mixture. *Chem. Eng. J.* **2016**, *306*, 973–977.
- (146) Arcella, V.; Troglia, C.; Ghielmi, A. Hyflon Ion Membranes for Fuel Cells. *Ind. Eng. Chem. Res.* **2005**, *44* (20), 7646–7651.
- (147) Huang, Y.; Merkel, T. C.; Baker, R. W. Pressure Ratio and Its Impact on Membrane Gas Separation Processes. *J. Memb. Sci.* **2014**, *463*, 33–40.
- (148) Pozun, Z. D.; Tran, K.; Shi, A.; Smith, R. H.; Henkelman, G. Why Silver Nanoparticles Are Effective for Olefin / Paraffin Separations. *J. Phys. Chem. C* **2011**, *115*, 1811–1818.
- (149) Chae, I. S.; Kang, S. W.; Park, J. Y.; Lee, Y. G.; Lee, J. H.; Won, J.; Kang, Y. S. Surface Energy-Level Tuning of Silver Nanoparticles for Facilitated Olefin Transport. *Angew. Chemie - Int. Ed.* **2011**, *50* (13), 2982–2985.
- (150) Choi, H.; Lee, J. H.; Kim, Y. R.; Song, D.; Kang, S. W.; Lee, S. S.; Kang, Y. S. Tetrathiafulvalene as an Electron Acceptor for Positive Charge Induction on the Surface of Silver Nanoparticles for Facilitated Olefin Transport. *Chem. Commun.* **2014**, *50* (24), 3194–3196.

- (151) Kang, S. W.; Char, K.; Kang, Y. S. Novel Application of Partially Positively Charged Silver Nanoparticles for Facilitated Transport in Olefin/Paraffin Separation Membranes. *Chem. Mater.* **2008**, *20* (4), 1308–1311.
- (152) Lee, J. H.; Kang, S. W.; Yeom, M. S.; Kim, Y. R.; Choi, H.; Song, D.; Won, J.; Kang, Y. S. A Strong Linear Correlation between the Surface Charge Density on Ag Nanoparticles and the Amount of Propylene Adsorbed. *J. Mater. Chem. A* **2014**, *2* (19), 6987.
- (153) Shin, H. S.; Yang, H. J.; Kim, S. Bin; Lee, M. S. Mechanism of Growth of Colloidal Silver Nanoparticles Stabilized by Polyvinyl Pyrrolidone in γ -Irradiated Silver Nitrate Solution. *J. Colloid Interface Sci.* **2004**, *274* (1), 89–94.
- (154) Hong, G. H.; Song, D.; Chae, I. S.; Oh, J. H.; Kang, S. W. Highly Permeable Poly(ethylene Oxide) with Silver Nanoparticles for Facilitated Olefin Transport. *RSC Adv.* **2014**, *4* (10), 4905.
- (155) Rezende, C. G. F.; Borges, C. P.; Habert, A. C. Sorption of Propylene and Propane in Polyurethane Membranes Containing Silver Nanoparticles. *J. Appl. Polym. Sci.* **2016**, *133* (4), 6–11.
- (156) Kang, S. W.; Char, K.; Kim, J. H.; Kang, Y. S. Ionic Liquid as a Solvent and the Long-Term Separation Performance in a Polymer/silver Salt Complex Membrane. *Macromol. Res.* **2007**, *15* (2), 167–172.
- (157) Shalu; Chaurasia, S. K.; Singh, R. K.; Chandra, S. Thermal Stability, Complexing Behavior, and Ionic Transport of Polymeric Gel Membranes Based on Polymer PVdF-HFP and Ionic Liquid, [BMIM][BF₄]. *J. Phys. Chem. B* **2013**, *117* (3), 897–906.
- (158) Zarca, R.; Ortiz, A.; Gorri, D.; Ortiz, I. Generalized Predictive Modeling for Facilitated Transport Membranes Accounting for Fixed and Mobile Carriers. *J. Memb. Sci.* **2017**, *542*, 168–176.
- (159) Zarca, G.; Horne, W. J.; Ortiz, I.; Urtiaga, A.; Bara, J. E. Synthesis and Gas Separation Properties of Poly(ionic Liquid)-Ionic Liquid Composite Membranes Containing a Copper Salt. *J. Memb. Sci.* **2016**, *515*, 109–114.
- (160) Zarca, R.; Ortiz, A.; Gorri, D.; Ortiz, I. Facilitated Transport of Propylene Through Composite Polymer-Ionic Liquid Membranes. Mass Transfer Analysis. *Chem. Prod. Process Model.* **2016**, *11* (1), 77–81.
- (161) Zarca, R.; Ortiz, A.; Gorri, D.; Ortiz, I. A Practical Approach to Fixed-Site-Carrier Facilitated Transport Modeling for the Separation of Propylene/propane Mixtures through Silver-Containing Polymeric Membranes. *Sep. Purif. Technol.* **2017**, *180*, 82–

- 89.
- (162) Fallanza, M.; Ortiz, A.; Gorri, D.; Ortiz, I. Propylene and Propane Solubility in Imidazolium, Pyridinium, and Tetralkylammonium Based Ionic Liquids Containing a Silver Salt. *J. Chem. Eng. Data* **2013**, *58* (8), 2147–2153.
- (163) Ortiz, A.; María, L.; Gorri, D.; Haan, A. B.; Ortiz, I. Reactive Ionic Liquid Media for the Separation of Propylene / Propane Gaseous Mixtures. *Ind. Eng. Chem. Res.* **2010**, *49* (16), 7227–7233.
- (164) Guo, C. G.; Wang, Q. G.; Zhou, G. D.; Mak, T. C. W. Synthesis and Characterization of $\text{Ag}_2\text{C}_2 \cdot 2\text{AgClO}_4 \cdot 2\text{H}_2\text{O}$: A Novel Layer-Type Structure with the Acetylide Dianion Functioning in a μ_6 - $\eta_1, \eta_1 : \eta_2, \eta_2 : \eta_2, \eta_2$ Bonding Mode inside an Octahedral Silver Cage. *Chem. Commun.* **1998**, No. 3, 339–340.
- (165) Compact Membrane Systems Company <https://compactmembrane.com/> (accessed Dec 20, 2017).
- (166) Delaware Company Is Overall Winner of Petrochemical Innovation Awards. *The Global Delaware Blog*. Wilmington March 11, 2016.
- (167) Kattula, M.; Ponnuru, K.; Zhu, L.; Jia, W.; Lin, H.; Furlani, E. P. Designing Ultrathin Film Composite Membranes: The Impact of a Gutter Layer. *Sci. Rep.* **2015**, *5*, 1–9.
- (168) Galizia, M.; Chi, W. S.; Smith, Z. P.; Merkel, T. C.; Baker, R. W.; Freeman, B. D. 50th Anniversary Perspective: Polymers and Mixed Matrix Membranes for Gas and Vapor Separation: A Review and Prospective Opportunities. *Macromolecules* **2017**, *50* (20), 7809–7843.
- (169) Ramon, G. Z.; Wong, M. C. Y.; Hoek, E. M. V. Transport through Composite Membrane, Part 1: Is There an Optimal Support Membrane? *J. Memb. Sci.* **2012**, *415–416*, 298–305.
- (170) Lundy, K. A.; Cabasso, I. Analysis and Construction of Multilayer Composite Membranes for the Separation of Gas Mixtures. *Ind. Eng. Chem. Res.* **1989**, *28* (6), 742–756.
- (171) Eriksen, O. I.; Aksnes, E.; Dahl, I. M.; Lee, F. M. Use of Silver-Exchanged Ionomer Membranes for Gas Separation. US Patent 5,191,151 A, 1993.
- (172) Feiring, A. E.; Lazzeri, J.; Majumdar, S. Membrane Separation of Olefin and Paraffin Mixtures. US Patent 2015/0025293 A1, 2015.
- (173) Justice, R. S. University of Cincinnati, UNIVERSITY OF CINCINNATI, 2007.
- (174) Porod, G. X-Ray Low Angle Scattering of Dense Colloid Systems. Part I. *Kolloid-Z* **1951**, 83–114.

- (175) Schaefer, D. Polymers, Fractals, and Ceramic Materials. *Science* (80-.). **1989**, No. 243, 1023–1027.
- (176) DW Schaefer, M. A. Ultra-Small-Angle Neutron Scattering: A New Tool for Materials Research. *Curr. Opin. Solid State Mater. Sci.* **2004**, 39–47.
- (177) Beaucage, G. Approximations Leading to a Unified Exponential Power-Law Approach to Small-Angle Scattering. *J. Appl. Crystallogr.* **1995**, No. 29, 717–728.
- (178) G Beaucage, D. S. Structural Studies of Complex-Systems Using Small-Angle Scattering - a Unified Guinier Power-Law Approach. **1994**, No. 172, 797–805.
- (179) Beaucage, G.; Ulibarri, T. A.; Black, E. P.; Schaefer, D. W. Multiple Size Scale Structures in Silica—Siloxane Composites Studied by Small-Angle Scattering. In *Hybrid Organic-Inorganic Composites*; ACS Publications, 1995; pp 97–111.
- (180) Beaucage, G.; Kammler, H. K.; Pratsinis, S. E. Particle Size Distributions from Small-Angle Scattering Using Global Scattering Functions. *J. Appl. Crystallogr.* **2004**, 37 (4), 523–535.
- (181) Das, R.; Nath, S. S.; Chakdar, D.; Gope, G.; Bhattacharjee, R. Preparation of Silver Nanoparticles and Their. **2009**, 1–6.
- (182) Lanje, A. S.; Sharma, S. J.; Pode, R. B. Synthesis of Silver Nanoparticles: A Safer Alternative to Conventional Antimicrobial and Antibacterial Agents. *J. Chem. Pharm. Res.* **2010**, 2 (3), 478–483.
- (183) Delpech, M. C.; Miranda, G. S. Waterborne Polyurethanes: Influence of Chain Extender in Ftir Spectra Profiles. *Cent. Eur. J. Eng.* **2011**, 2 (2), 231–238.
- (184) De Oliveira Patricio, P. S.; Pereira, I. M.; Da Silva, N. C. F.; Ayres, E.; Pereira, F. V.; Oréface, R. L. Tailoring the Morphology and Properties of Waterborne Polyurethanes by the Procedure of Cellulose Nanocrystal Incorporation. *Eur. Polym. J.* **2013**, 49 (12), 3761–3769.
- (185) Campos, A. C. C. Universidade Do Estado Do Rio de Janeiro Centro de Tecnologia E Ciências Instituto de Química Antoniel Carlos Carolino Campos Síntese E Caracterização de Filmes de Nanopartículas de Prata Dispersas Em Poli (Uretano-Ureia) Para Separação de Gases Petroqu. **2013**.
- (186) Coutinho, F. M. B.; Delpech, M. C.; Alves, T. L.; Ferreira, A. A. Degradation Profiles of Cast Films of Polyurethane and Poly(urethane-Urea) Aqueous Dispersions Based on Hydroxy-Terminated Polybutadiene and Different Diisocyanates. *Polym. Degrad. Stab.* **2003**, 81 (1), 19–27.
- (187) Coutinho, F. M. B.; Delpech, M. C. Degradation Profile of Films Cast from Aqueous

- Polyurethane Dispersions. *Polym. Degrad. Stab.* **2000**, *70* (1), 49–57.
- (188) He, Y.; Xie, D.; Zhang, X. The Structure, Microphase-Separated Morphology, and Property of Polyurethanes and Polyureas. *J. Mater. Sci.* **2014**, *49* (21), 7339–7352.
- (189) Rolph, M. S.; Markowska, A. L. J.; Warriner, C. N.; O'Reilly, R. K. Blocked Isocyanates: From Analytical and Experimental Considerations to Non-Polyurethane Applications. *Polym. Chem.* **2016**, *7* (48), 7351–7364.
- (190) Madbouly, S. A.; Otaigbe, J. U. Recent Advances in Synthesis, Characterization and Rheological Properties of Polyurethanes and POSS/polyurethane Nanocomposites Dispersions and Films. *Prog. Polym. Sci.* **2009**, *34* (12), 1283–1332.
- (191) Queiroz, D. P.; Norberta de Pinho, M. Structural Characteristics and Gas Permeation Properties of Polydimethylsiloxane/poly(propylene Oxide) Urethane/urea Bi-Soft Segment Membranes. *Polymer (Guildf)*. **2005**, *46* (7), 2346–2353.
- (192) Król, P. Synthesis Methods, Chemical Structures and Phase Structures of Linear Polyurethanes. Properties and Applications of Linear Polyurethanes in Polyurethane Elastomers, Copolymers and Ionomers. *Prog. Mater. Sci.* **2007**, *52* (6), 915–1015.
- (193) Mattia, J.; Painter, P. A Comparison of Hydrogen Bonding and Order in a Polyurethane and Poly(urethane-urea) and Their Blends with Poly(ethylene Glycol). *Macromolecules* **2007**, *40* (5), 1546–1554.
- (194) Sheth, J. P.; Aneja, A.; Wilkes, G. L.; Yilgor, E.; Atilla, G. E.; Yilgor, I.; Beyer, F. L. Influence of System Variables on the Morphological and Dynamic Mechanical Behavior of Polydimethylsiloxane Based Segmented Polyurethane and Polyurea Copolymers: A Comparative Perspective. *Polymer (Guildf)*. **2004**, *45* (20), 6919–6932.
- (195) Hicks, E. M.; Ultee, A. J.; Drougas, J. Spandex Elastic Fibers: Development of a New Type of Elastic Fiber Stimulates Further Work in the Growing Field of Stretch Fabrics. *Science* **1965**, *147* (3656), 373–379.
- (196) Coutinho, F. M. B.; Delpech, M. C.; Santos, C. C.; Almeida, R. B. L. Síntese E Caracterização de Dispersões Aquosas de Poliuretanos À Base de Copolímeros Em Bloco de Poli(glicol Etilênico) E Poli(glicol Propilênico). *Quim. Nova* **2008**, *31* (6), 1437–1443.
- (197) Mishra, A. K.; Jena, K. K.; Raju, K. V. S. N. Synthesis and Characterization of Hyperbranched Polyester-Urethane-urea/K10-Clay Hybrid Coatings. *Prog. Org. Coatings* **2009**, *64*, 47–56.
- (198) Barboza, E. M.; Delpech, M. C.; Garcia, M. E. F. Avaliação Das Propriedades de Barreira de Membranas Obtidas a Partir de Dispersões Aquosas À Base de Poliuretanos

- E Argila Evaluation of Carbon Dioxide Gas Barrier Properties of Membranes Obtained from. **2014**, *24*, 94–100.
- (199) BARBOSA, E. M. Avaliação Das Propriedades de Barreira a Gases de Membranas Obtidas a Partir de Dispersões Aquosas À Base de Poliuretanos E Argila, Instituto de Química, Universidade do Estado do Rio de Janeiro, 2011.
- (200) Coutinho, F. M. B.; Delpech, M. C.; Garcia, M. E. F. Terminated Polybutadiene. **2002**, *21*, 719–723.
- (201) Coutinho, F. M. B.; Delpech, M. C.; Garcia, M. E. F. Avaliação Das Propriedades Mecânicas E Da Permeabilidade a Gases de Membranas Obtidas a Partir de Dispersões Aquosas de Poliuretanos À Base de Polibutadieno Líquido Hidroxilado. *Polímeros* **2004**, *14* (4), 230–234.
- (202) Henriques, J.; Pereira, C. Juliana Henriques Costa Pereira Caracterização de Filmes Formados Por Dispersões Aquosas de Poli (Uretano-Uréia) S Para Aplicação Em Membranas Para Permeação de Gases Rio de Janeiro 2012, Instituto de Química, Universidade do Estado do Rio de Janeiro, 2012.
- (203) Baker, R. W. CARRIER FACILITATED TRANSPORT. In *Membrane Technology and Applications*; John Wiley & Sons, Ltd, 2004; pp 425–463.
- (204) Lau, C. H.; Li, P.; Li, F.; Chung, T.-S.; Paul, D. R. Reverse-Selective Polymeric Membranes for Gas Separations. *Prog. Polym. Sci.* **2013**, *38* (5), 740–766.
- (205) Raveendran, P.; Wallen, S. L. Cooperative C-H...O Hydrogen Bonding in CO₂-Lewis Base Complexes: Implications for Solvation in Supercritical CO₂. *J. Am. Chem. Soc.* **2002**, *124* (42), 12590–12599.
- (206) Peponi, L.; Puglia, D.; Torre, L.; Valentini, L.; Kenny, J. M. Processing of Nanostructured Polymers and Advanced Polymeric Based Nanocomposites. *Mater. Sci. Eng. R Reports* **2014**, *85* (1), 1–46.
- (207) Griffith, M.; Udekwu, K. I.; Gkotzis, S.; Mah, T.; Alarcon, E. I. *Silver Nanoparticle Applications*; 2015.
- (208) Hornyak, G. L.; Tibbals, H. F.; Dutta, J.; Moore, J. J. *Introduction to Nanosciences*; Group, T. & F., Ed.; CRC Press: Boca Raton, 2008.
- (209) Pachfule, P.; Balan, B. K.; Kurungot, S.; Banerjee, R.; Taberna, L.; Mitra, S.; Poizot, P.; Simon, P.; Tarascon, J. M.; Hagrman, P. J.; et al. One-Dimensional Confinement of a Nanosized Metal Organic Framework in Carbon Nanofibers for Improved Gas Adsorption. *Chem. Commun.* **2012**, *48* (14), 2009.
- (210) Sih, B. C.; Wolf, M. O.; Rao, C. N. R.; Cheetham, A. K.; Daniel, M.-C.; Astruc, D.;

- Schmid, G.; Bäuml, M.; Geerkens, M.; Heim, I.; et al. Metal Nanoparticle—conjugated Polymer Nanocomposites. *Chem. Commun.* **2005**, *11* (27), 3375.
- (211) Wu, C.; Huang, J.; Wen, Y.; Wen, S.; Shen, Y.; Yeh, M. Preparation of Antibacterial Waterborne Polyurethane/silver Nanocomposite. *J. Chinese Chem. Soc.* **2009**, *56*, 1231–1235.
- (212) Dallas, P.; Sharma, V. K.; Zboril, R. Silver Polymeric Nanocomposites as Advanced Antimicrobial Agents: Classification, Synthetic Paths, Applications, and Perspectives. *Adv. Colloid Interface Sci.* **2011**, *166* (1), 119–135.
- (213) Wilson, J. L.; Poddar, P.; Frey, N. A.; Srikanth, H.; Mohamed, K.; Harmon, J. P.; Kotha, S.; Wachsmuth, J. Synthesis and Magnetic Properties of Polymer Nanocomposites with Embedded Iron Nanoparticles. *J. Appl. Phys.* **2004**, *95* (3), 1439.
- (214) Richard M. Crooks, *; Mingqi Zhao; Li Sun; Victor Chechik, and; Yeung, L. K. Dendrimer-Encapsulated Metal Nanoparticles: Synthesis, Characterization, and Applications to Catalysis. **2000**.
- (215) Tan, K. S.; Cheong, K. Y. Advances of Ag, Cu, and Ag-Cu Alloy Nanoparticles Synthesized via Chemical Reduction Route. *J. Nanoparticle Res.* **2013**, *15* (4).
- (216) Tolaymat, T. M.; El Badawy, A. M.; Genaidy, A.; Scheckel, K. G.; Luxton, T. P.; Suidan, M. An Evidence-Based Environmental Perspective of Manufactured Silver Nanoparticle in Syntheses and Applications: A Systematic Review and Critical Appraisal of Peer-Reviewed Scientific Papers. *Sci. Total Environ.* **2010**, *408* (5), 999–1006.
- (217) Creighton, J. A.; Blatchford, C. G.; Albrecht, M. G. Plasma Resonance Enhancement of Raman Scattering by Pyridine Adsorbed on Silver or Gold Sol Particles of Size Comparable to the Excitation Wavelength. *J. Chem. Soc. Faraday Trans. 2* **1979**, *75* (0), 790.
- (218) Zhang, R.; Khalizov, A.; Wang, L.; Hu, M.; Xu, W. Nucleation and Growth of Nanoparticles in the Atmosphere. *Chem. Rev.* **2012**, *112* (3), 1957–2011.
- (219) Gittins, D. I.; Caruso, F. Spontaneous Phase Transfer of Nanoparticulate Metals from Organic to Aqueous Media **. **2001**, 3001–3004.
- (220) Kumar, A.; Joshi, H.; Pasricha, R.; Mandale, A. B.; Sastry, M. Phase Transfer of Silver Nanoparticles from Aqueous to Organic Solutions Using Fatty Amine Molecules. *J. Colloid Interface Sci.* **2003**, *264* (2), 396–401.
- (221) Liu, Y. C.; Lin, L. H. New Pathway for the Synthesis of Ultrafine Silver Nanoparticles from Bulk Silver Substrates in Aqueous Solutions by Sonoelectrochemical Methods.

- Electrochem. commun.* **2004**, 6 (11), 1163–1168.
- (222) Pinto, V. V.; Ferreira, M. J.; Silva, R.; Santos, H. A.; Silva, F.; Pereira, C. M. Long Time Effect on the Stability of Silver Nanoparticles in Aqueous Medium: Effect of the Synthesis and Storage Conditions. *Colloids Surfaces A Physicochem. Eng. Asp.* **2010**, 364 (1–3), 19–25.
- (223) Solomon, S. D.; Bahadory, M.; Jeyarajasingam, A. V; Rutkowsky, S. A.; Boritz, C. Synthesis and Study of Silver Nanoparticles. **2007**, 84 (2), 322–325.
- (224) Van Dong, P.; Ha, C.; Binh, L.; Kasbohm, J. Chemical Synthesis and Antibacterial Activity of Novel-Shaped Silver Nanoparticles. *Int. Nano Lett.* **2012**, 2 (1), 9.
- (225) Mavani, K.; Shah, M. Synthesis of Silver Nanoparticles by Using Sodium Borohydride as a Reducing Agent. *Int. J. Eng. Res. Technol.* **2013**, 2 (3), 1–5.
- (226) Bonsak, J.; Thesis. CHEMICAL SYNTHESIS OF SILVER NANOPARTICLES FOR LIGHT TRAPPING by Jack Bonsak, University of Oslo, 2010.
- (227) ASTM E2550 - 07. Standard Test Method for Thermal Stability by Thermogravimetry. *ASTM International*. West Conshohocken 2007.
- (228) LAFUENTE, B.; DOWNS R. T.; YANG, H.; STONE, N. The Power of Databases: The RRUFF Project. In *Highlights in Mineralogical Crystallography*; Danisi, T. A. and R. M., Ed.; W. De Gruyter: Berlin, 2015; pp 1–30.
- (229) Theivasanthi, T.; Alagar, M. Electrolytic Synthesis and Characterization of Silver Nanopowder. *eprint arXiv:1111.0260* **2011**.
- (230) Konwar, U.; Karak, N.; Mandal, M. Vegetable Oil Based Highly Branched Polyester/clay Silver Nanocomposites as Antimicrobial Surface Coating Materials. *Prog. Org. Coatings* **2010**, 68 (4), 265–273.
- (231) Sridhar, S.; Smitha, B.; Ramakrishna, M.; Aminabhavi, T. M. Modified Poly(phenylene Oxide) Membranes for the Separation of Carbon Dioxide from Methane. *J. Memb. Sci.* **2006**, 280 (1–2), 202–209.
- (232) Shahrooz, M.; Sadeghi, M.; Bagheri, R.; Laghaei, M. Elucidating the Significance of Segmental Mixing in Determining the Gas Transport Properties of Polyurethanes. *Macromolecules* **2016**, 49 (11), 4220–4228.
- (233) Ayres, E.; Oréface, R. L. Nanocompósitos Derivados de Dispersões Aquosas de Poliuretano E Argila: Influência Da Argila Na Morfologia E Propriedades Mecânicas. *Polímeros* **2007**, 17, 339–345.
- (234) Haynes, W. M. CRC Handbook of Chemistry and Physics, 93rd Edition - CRC Press Book <https://www.crcpress.com/CRC-Handbook-of-Chemistry-and-Physics-93rd>

- Edition/Haynes/9781439880494 (accessed Dec 5, 2015).
- (235) Santos, W. N.; F, R. G.; Mummery, P.; Wallwork, A. Propriedades Térmicas de Polímeros Por Métodos Transientes de Troca de Calor. **2003**, *13*, 265–269.
- (236) Cakic, S. M.; Stamenkovic, J. V.; Djordjevic, D. M.; Ristic, I. S. Synthesis and Degradation Profile of Cast Films of PPG-DMPA-IPDI Aqueous Polyurethane Dispersions Based on Selective Catalysts. *Polym. Degrad. Stab.* **2009**, *94* (11), 2015–2022.
- (237) Milanese, A. C.; Cioffi, M. O. H.; Voorwald, H. J. C. Flexural Behavior of Sisal/Castor Oil-Based Polyurethane and Sisal/Phenolic Composites. *Mater. Res.* **2012**, *15* (2), 191–197.
- (238) Kang, S. W.; Lee, D. H.; Park, J. H.; Char, K.; Kim, J. H.; Won, J.; Kang, Y. S. Effect of the Polarity of Silver Nanoparticles Induced by Ionic Liquids on Facilitated Transport for the Separation of Propylene/propane Mixtures. *J. Memb. Sci.* **2008**, *322* (3), 281–285.
- (239) Romero, A. I.; Parentis, M. L.; Habert, A. C.; Gonzo, E. E. Synthesis of Polyetherimide/silica Hybrid Membranes by the Sol–gel Process: Influence of the Reaction Conditions on the Membrane Properties. *J. Mater. Sci.* **2011**, *46* (13), 4701–4709.
- (240) Matteucci, S.; Yampolskii, Y.; Freeman, B. D.; Pinnau, I. Transport of Gases and Vapors in Glassy and Rubbery Polymers. In *Materials Science of Membranes for Gas and Vapor Separation*; Yampolskii, Y., Pinnau, I., Freeman, B., Eds.; John Wiley & Sons, Ltd.: Chichester, 2006; pp 1–47.
- (241) Padma, D. K. A Novel Synthetic Route for the Preparation of Silver Salts of Hexafluorophosphate, Tetrafluoroborate and Hexafluorosilicate. *Synth. React. Inorg. Met.-Org. Chem.* **1988**, *18* (4), 401–404.
- (242) Heimer, N. E.; Del Sesto, R. E.; Meng, Z.; Wilkes, J. S.; Carper, W. R. Vibrational Spectra of Imidazolium Tetrafluoroborate Ionic Liquids. *J. Mol. Liq.* **2006**, *124* (1–3), 84–95.
- (243) Mojet, B. L.; Ebbesen, S. D.; Lefferts, L. Light at the Interface: The Potential of Attenuated Total Reflection Infrared Spectroscopy for Understanding Heterogeneous Catalysis in Water. *Chem. Soc. Rev.* **2010**, *39* (12), 4643.
- (244) Okamoto, Y.; Du, Q.; Koike, K.; Mikeš, F.; Merkel, T. C.; He, Z.; Zhang, H.; Koike, Y. New Amorphous Perfluoro Polymers: Perfluorodioxolane Polymers for Use as Plastic Optical Fibers and Gas Separation Membranes. *Polym. Adv. Technol.* **2016**, *27*

(1), 33–41.